https://orcid.org/0000-0001-6801-3703

VILNIUS UNIVERSITY
CENTER FOR PHYSICAL SCIENCES AND TECHNOLOGY

Daria Pashneva

Atmospheric Black Carbon Aerosol Concentration Dynamics in an Urban Environment

DOCTORAL DISSERTATION

Natural Sciences,
Physics (N 002)

VILNIUS 2025

The dissertation was prepared between 2020 and 2024 at the SRI Center for Physical Sciences and Technology.

Academic supervisor – Dr. Steigvilė Byčenkienė (Center for Physical Sciences and Technology, Natural Sciences, Physics - N 002**)**

This doctoral dissertation will be defended in a public meeting of the Dissertation Defence Panel:

Chairman – Dr. Evaldas Maceika (Center for Physical Sciences and Technology, Natural Sciences, Physics - N 002).

Members:

Dr. Galina Lujanienė (Center for Physical Sciences and Technology, Natural Sciences, Physics - N 002),

Dr. Vaida Šerevičienė (Vilnius Gediminas Technical University, Technological Sciences, Environmental Engineering - T 004),

Dr. Vaida Vasiliauskienė (Vilnius Gediminas Technical University, Natural Sciences, Physics - N 002),

Dr. Arturs Viksna (University of Latvia, Natural Sciences, Chemistry - N 003).

The dissertation shall be defended at a public/closed meeting of the Dissertation Defence Panel at 1 p. m. on 4th February 2025 in meeting room D401 of the Center for Physical Sciences and Technology.

Address: Saulėtekio av. 3, Room No. D401, Vilnius, Lithuania

Tel.+37052648884; e-mail: office@ftmc.lt

The text of this dissertation can be accessed at the libraries of Center for Physical Sciences and Technology and Vilnius University, as well as on the website of Vilnius University: *www.vu.lt/lt/naujienos/ivykiu-kalendorius*

VILNIAUS UNIVERSITETAS
FIZINIŲ IR TECHNOLOGIJOS MOKSLŲ CENTRAS

Daria Pashneva

Atmosferos aerozolio juodosios anglies koncentracijos dinamikos tyrimai miesto aplinkoje

DAKTARO DISERTACIJA

Gamtos mokslai,
Fizika (N 002)

VILNIUS 2025

Disertacija rengta 2020-2024 metais VMTI Fizinių ir technologijos mokslų centre.

Mokslinis vadovas – dr. Steigvilė Byčenkienė (Fizinių ir technologijos mokslų centras, gamtos mokslai, fizika – N 002).

Gynimo taryba:

Pirmininkas – dr. Evaldas Maceika (Fizinių ir technologijos mokslų centras, gamtos mokslai, fizika – N 002).

Nariai:

dr. Galina Lujanienė (Fizinių ir technologijos mokslų centras, gamtos mokslai, fizika – N 002),

dr. Vaida Šerevičienė (Vilniaus Gedimino technikos universitetas, technologijos mokslai, aplinkos inžinerija – T 004),

dr. Vaida Vasiliauskienė (Vilniaus Gedimino technikos universitetas, gamtos mokslai, fizika – N 002),

dr. Arturs Viksna (Latvijos universitetas, gamtos mokslai, chemija – N 003).

Disertacija ginama viešame Gynimo tarybos posėdyje 2025 m. vasario mėn. 4 d. 13:00 val. Fizinių ir technologijos mokslų centro auditorijoje D401. Adresas: (Saulėtekio al. 3,Vilnius, Lietuva), tel. +37052648884 ; el. paštas office@ftmc.lt

Disertaciją galima peržiūrėti Fizinių ir technologijos mokslų centro bei VU bibliotekose ir VU interneto svetainėje adresu:
https://www.vu.lt/naujienos/ivykiu-kalendorius

ABBREVIATIONS

AAE	Absorption Ångström exponent
ATN	Attenuation
BC	Black carbon
BC_{BB}	Biomass burning related BC
BC_{FF}	Fossil fuel combustion
CPF	Conditional Probability Field analysis
E	East
ENE	East-Northeast
ESE	East-Southeast
F_{inf}	Infiltration factor
I/O	Indoor outdoor
KD	Kietosios dalelės (*in Lithuanian*)
N	North
NE	Northeast
NNE	North-Northeast
NNW	North-Northwest
NO_x	Nitrogen oxides
NW	Northwest
P	Pressure
PM	Particulate matter
PM_{10}	Particulate matter, where particles have an aerodynamic diameter equal to or less than 10 µm
$PM_{2.5}$	Particulate matter, where particles have an aerodynamic diameter equal to or less than 2.5 µm
RH	Relative humidity
S	South
SD	Standard deviation
SE	Southeast
SSE	South-Southeast
SSW	South-Southwest
SW	Southwest
T	Temperature
UFP	Ultrafine particles
VOC	Volatile organic compounds
W	West
WD	Wind direction
WNW	West

| WS | Wind speed |
| WSW | West-Southwestt |

CONTENTS

INTRODUCTION

Relevance

Atmospheric black carbon (BC) (or soot) is a component of particulate matter (PM), which is known to have adverse effects on air quality, climate change and human health, ranging from respiratory and cardiovascular disease to reduced cognitive function both locally and globally. Long-term exposure can lead to a worsening of these conditions, leading to chronic health problems and a higher risk of premature mortality.

Understanding the dynamics and source apportionment of atmospheric BC is essential for revealing regional variations in its mass concentration, assessing hourly and seasonal variations and determining the influence of meteorology, long-range transport and deposition patterns. Such studies are especially important in urban areas, where high population densities are exposed to elevated BC emissions from transport and residential heating, resulting in poor air quality and heightened health risks for residents. Furthermore, in urban settings, outdoor pollution directly affects indoor air quality, as BC particles can infiltrate indoor spaces, increasing indoor air pollution and associated health risks. Consequently, in urban environments, indoor air quality is often influenced by outdoor pollution levels, making it essential to assess BC dynamics both indoors and outdoors. Additionally, studying BC deposition on urban trees offers valuable insights into the role of vegetation in capturing particulate pollutants, presenting potential natural mitigation strategies to improve overall air quality. This underscores the importance of incorporating vegetation and green infrastructure into urban planning for pollution reduction.

Problem formulation

While biomass burning may be considered climate neutral in terms of CO_2 emissions, its impacts on air quality and public health can not be ignored. Black carbon is a potent short-lived climate pollutant with serious health implications. Accurately determining the contribution of BC from various biomass burning sources, such as transportation and residential wood combustion, remains a critical challenge. The key scientific problem is developing reliable methodologies for BC source apportionment to attribute emissions to specific sources and to evaluate their dynamics across different seasons and during extreme pollution events. This is essential for quantifying the environmental and health impacts and creating targeted policies to reduce BC emissions. Additionally, there is a significant gap in understanding how these pollutants infiltrated indoors, the factors influencing this infiltration, and the resultant indoor air quality and health outcomes. A holistic approach that

considers BC source apportionment, its dynamics, and the role of trees as deposition sinks is essential for tackling the complex challenges posed by BC pollution in urban environment.

This thesis outlines three distinct lines of research: (i) the urban background BC mass concentration sampling campaign; (ii) the investigation of the indoor-outdoor relationship of BC concentration and source apportionment; (iii) the investigation of the deposition of BC on urban trees (Norway spruce and silver birch). Three campaigns were conducted between September 2020 and May 2022 at the SRI Center for Physical Sciences and Technology (FTMC) located in Vilnius, the capital and largest city of Lithuania, to measure BC mass concentration.

The Main Aim

The aim of this study is to assess the dynamics of source-apportioned BC mass concentration in urban environments and to identify the principal factors that govern these concentrations.

Tasks

1. To identify the diurnal, weekly, and seasonal patterns in source-apportioned BC mass concentration and to determine the contribution of each source to BC mass concentration.
2. To investigate potential determinants influencing BC mass concentration during episodes of high pollution events for each season, identifying key contributors to elevated BC levels.
3. To assess the relationship between outdoor and indoor BC mass concentrations to understand how outdoor pollution influences indoor air quality.
4. To conduct an assessment of BC deposition on tree leaves as potential for air pollution reduction.

Scientific Novelty

This thesis provides new holistic insights into the sources and main drivers causes of black carbon pollution in Vilnius source-apportioned differentiating between fossil fuel combustion- and biomass-burning-related BC concentrations for all seasons, its impact on indoor air quality, and deposition on urban vegetation. So far, no detailed studies of BC levels have been reported in the capitals of Baltic countries to date.

Defensive Statements

1. A higher BC mass concentration, primarily attributed to the input of fossil fuel combustion-related BC, is observed during the heating season. Despite the observed increase in biomass burning contributions during the June-August months, fossil fuel combustion remains the primary factor contributing to the higher black carbon mass concentration during the non-heating season.
2. The highest BC concentrations are influenced by the dominant local source, with a remote source in autumn from the south at specific wind speeds. In contrast, the lower BC levels are influenced by distant sources.
3. The influence of grass burning on black carbon mass concentrations during extreme pollution events in spring exceeds that of meteorological phenomenon.
4. Black carbon originating from fossil fuel combustion is the source of about 80% of the total BC mass concentration in both indoor and outdoor air. On days with high air pollution, outdoor BC concentrations typically exhibit three- to fourfold increase, while indoor levels demonstrate a more moderate twofold increase.
5. The foliage of the silver birch and the needles of the Norway spruce have the potential to improve air quality in an urban environment by facilitating the removal of BC from the air.

Author Contribution

The author of the work was actively involved in the time-series analysis of BC mass concentration and the interpretation of the results. Additionally, the author designed graphical illustrations, co-authored manuscripts, and presented the findings at scientific conferences.

1. LITERATURE REVIEW

1.1. Atmospheric aerosol

Air pollution represents a significant and global concern, largely attributable to human activities. Atmospheric aerosols are by definition the particles suspended in the gas or liquid phase in the atmosphere (called aerosols or particulate matter). Given the significant impact of atmospheric aerosols on air quality, climate change, human health, ecosystems and visibility, these particles are currently of great scientific and political interest [1].

The physical and chemical properties of different types of aerosols determine the fate of these particles in the atmosphere and the effects they have on it. The typical size of aerosols is between 0.003 and 10 micrometers, with a residence time in the atmosphere of at least several hours [2,3]. Particles that have an aerodynamic diameter of less than 10 μm (PM$_{10}$) and 2.5 μm in size (PM$_{2.5}$) are key metrics in air pollution monitoring and legislative action is routinely taken to limit their respective concentrations (Figure 1) [4].
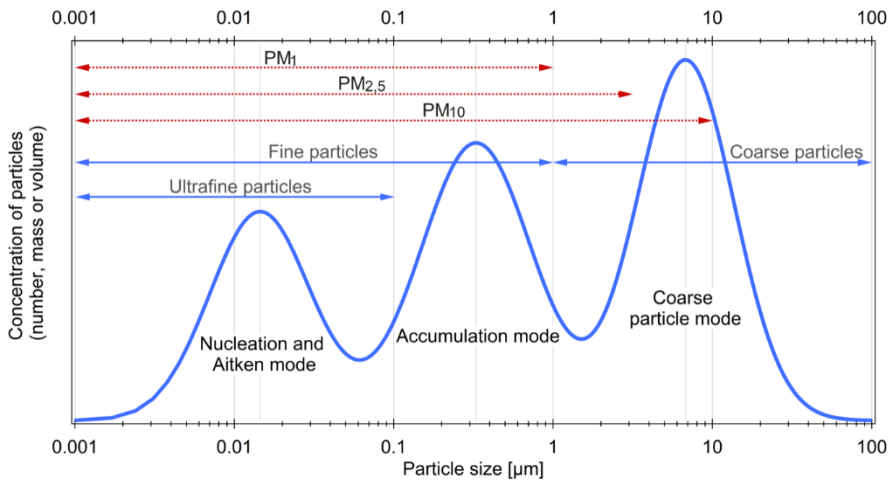
Figure 1. Idealized scheme of atmospheric aerosol size distribution. ICPF, CAS.

Particle size, along with the physical, chemical and optical properties, is strongly influenced by the source and the origin of PM can be either natural, such as volcanic eruptions [5] and sandstorms. Anthropogenic sources, however, are more persistent and pose greater challenges to air quality

management. These include fuel combustion [7], such as from transport, industrial processes, and power generation by fuel combustion [6]. Urban environments, in particular, are dominated by human-induced emissions of fine and ultrafine particles (Figure 1). Aerosol particles are further categorized based on how they are introduced into the atmosphere. "Primary" aerosol particles are directly emitted into the air as solid or liquid particles. On the other hand, "secondary" particles are not emitted directly but are formed through atmospheric chemical reactions, often involving precursor gases such as sulfur dioxide (SO_2), nitrogen oxides (NO_x), ammonia (NH_3), and volatile organic compounds (VOCs). These gases undergo complex transformations in the atmosphere, forming secondary aerosols like sulfates, nitrates, and organic aerosols. Aerosol processes that influence particle size are critical to understanding the behavior and effects of aerosols in the atmosphere. These processes include nucleation, condensation, coagulation, and atmospheric aging, all of which contribute to the formation, growth, and eventual removal of aerosol particles.

Major sources of primary fine particles include cars and trucks (especially those with diesel engines); open burning; wildfires; fireplaces, wood stoves, and outdoor wood boilers (also called hydronic heaters); cooking; dust from roads and construction; agricultural operations; and coal and oil-burning boilers (Figure 2). Major sources of secondary fine particles are power plants and some industrial processes, including oil refining and pulp and paper production [7].

Figure 2. The different sources of PM$_{2.5}$ in the environment (source: https://www.epa.gov/cmaq/overview-science-processes-cmaq)

The occurrence of episodic $PM_{2.5}$ pollution in urban areas appears to be more prevalent during the winter months in the Northern Hemisphere. This is attributed to a number of factors, including the decreased air temperature and the more frequent occurrence o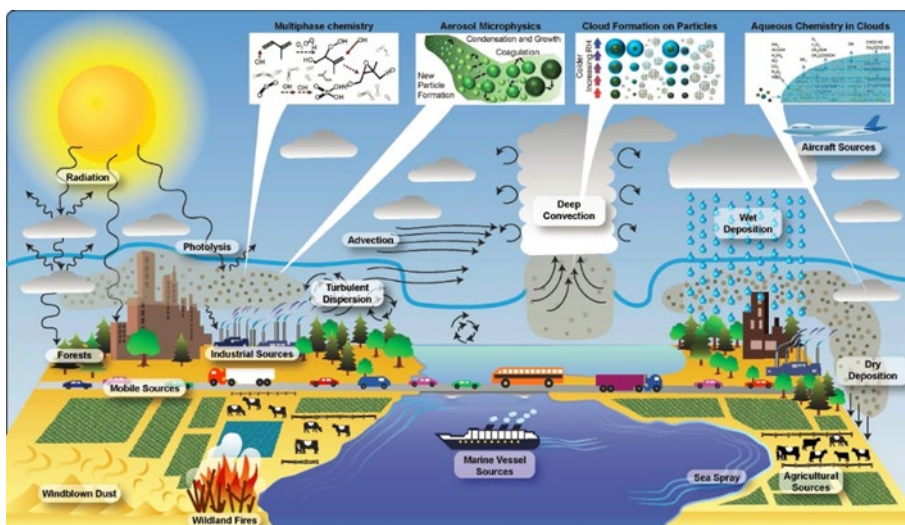f atmospheric inversions. These inversions are becoming more common due to global climate change, exacerbating wintertime air quality issues. Furthermore, summer episodes of increased $PM_{2.5}$ concentrations can be linked to other factors such as wildfires and active photochemistry leading to secondary particle formation. Wildfires, in particular, contribute significant amounts of fine particulate matter to the atmosphere during hot, dry conditions [8]. Activities such as transport and construction dust significantly contribute to elevated $PM_{2.5}$ levels during the summer months in cities.

Recent studies review indicates that 25% of the global urban ambient air pollution from $PM_{2.5}$ can be attributed to traffic, 15% to industrial activities, 20% to domestic fuel burning, 22% to sources of human origin that are currently unidentified, and 18% to natural dust and salt [7,8]. As indicated by S. Chansuebsri et al. (2024), in the context of Chiang Mai (Thailand), biomass burning and sea salt were the primary contributors of $PM_{2.5}$ during the smoke haze period, while traffic and dust were the predominant sources during the non-smoke haze period [9]. F. Pini et al. (2021) demonstrate that vehicles have a fundamental role in the atmospheric emission of PM_{10} polluting particles. The role of cars as the major source of PM_{10} pollution has undergone a significant transformation over the past five years [10]. L. Drudi et al. (2024) demonstrated how the composition of PM_{10} can change simultaneously in different locations and over time in the same location illustrating notable differences in the chemical composition of PM_{10}, and indicating variations in the sources and characteristics of aerosol particles [11].

1.2. Effects of particulate matter on environment and human health

In 2021, the number of premature deaths attributable to $PM_{2.5}$ in the EU was 253,000 [1]. This is despite the fact that the number of premature deaths in the EU linked to $PM_{2.5}$ has already fallen by 41% between 2005 and 2021. The highest mortality rates from $PM_{2.5}$ are observed in Central and Eastern Europe, with premature mortality rates at least 50% higher than the EU average. Conversely, the lowest rates (less than half the EU average) were observed in Ireland, Finland, Sweden, as well as Norway and Iceland (Figure 3). In Lithuania, this figure was slightly below the EU average.
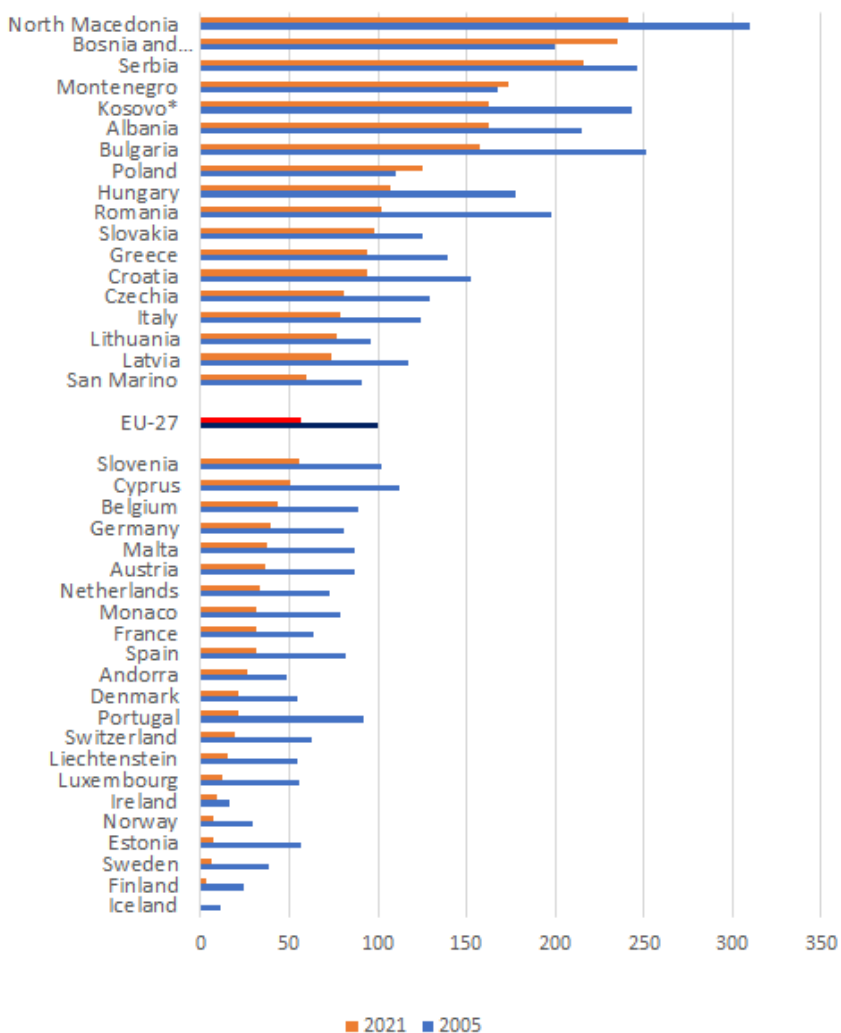
Figure 3. The figure shows for each country two bars, with the estimated number of premature deaths per 100,000 inhabitants attributable to exposure to annual $PM_{2.5}$ concentrations above 5 μg m^{-3} in both 2005 and 2021 (Source: Eionet report "Health risk assessment of air pollution: assessing the environmental burden of disease of air pollution in Europe in 2021").

The reduction in $PM_{2.5}$ concentrations and the subsequent decrease in the population's exposure to this air pollutant have resulted in this apparent reduction in premature deaths. In 2021, 97% of the urban population was still exposed to $PM_{2.5}$ at concentrations exceeding the new (2021) WHO recommended air quality level of 5 μg m^{-3}, according to the relevant EEA indicator. It should be noted that over 70% of the EU population currently resides in urban areas.

1.3. Black carbon aerosols and its sources

The term black carbon was first mentioned by T. Novakov in the 1970s [12]. Since then, it has been a subject of continued study due to its role in air pollution, which has become a significant issue particularly in the context of global urbanization [13]. Chemically, BC is a component of fine particulate matter (PM $\leq$ 2.5 µm in aerodynamic diameter) known for its strong light-absorbing properties and potential for warming, despite having a relatively short atmospheric lifetime. BC is formed during incomplete combustion processes and has a significant influence on regional and global air quality, public health, climate change, and ecosystems. Black carbon shortly after emission becomes mixed with other aerosol chemical species, including inorganics such as sulfate, nitrate and ammonium, and organic compounds. As a result, BC serves as an important indicator for assessing the adverse effects of particulates on human health, especially, in environments dominated by combustion sources. It is noteworthy for showing more robust associations with morbidity, mortality and life expectancy compared to $PM_{2.5}$ [14] (Figure 4).
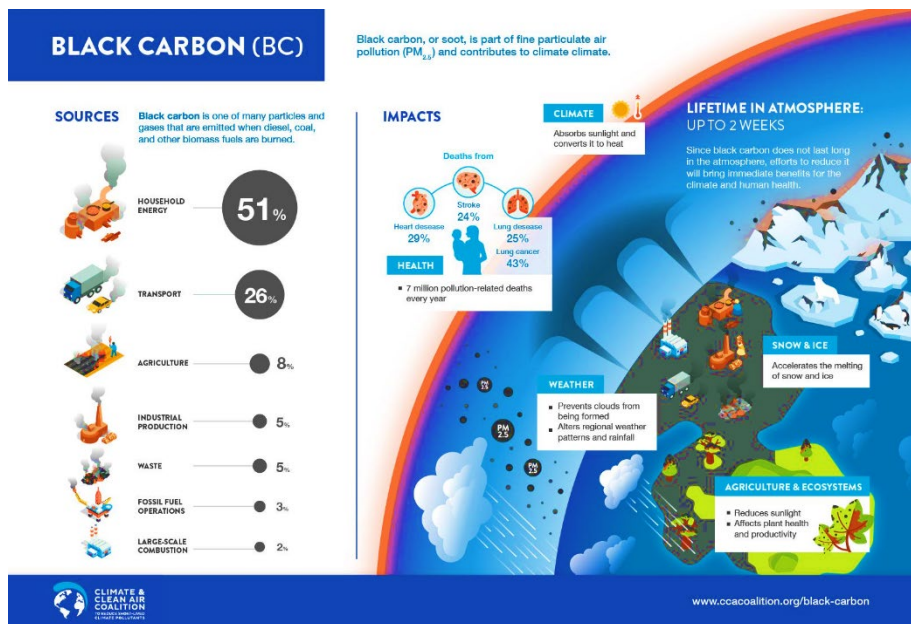
Figure 4. Source breakdown and impact overview of BC from the climate and clean air coalition (Climate & Clean Air Coalition 2018).

In urban areas, the primary sources of BC are typically transportation, residential combustion, and industry. In recent years, there has been a

noticeable decline in BC emissions from vehicular traffic, which can be attributed to technological advancements and legislative measures. However, the regulation of residential combustion emissions is still in its infancy in many European countries. This trend may result in a shift in the distribution of BC sources, with an increased contribution from residential combustion relative to the regulated sectors, namely engine and industrial emissions [5].

Atmospheric BC exhibits a pronounced spatial and temporal variability, attributable to the uneven distribution of its sources and the restricted atmospheric lifetime. In urban areas the largest BC concentrations are typically observed in close proximity to the source. However, BC can also be transported over long distances with air masses. In particular, the transport of BC to Arctic areas has been associated with a substantial impact on climate [5]. Table 1 gives further details of BC concentrations for different environments around the world, as studied by several previous authors.

Table 1. Mean BC values in different environments. Here UB is the urban background, RB - rural background, SUB - suburban background.

Place (environment)	Time period	Concentration ($\mu g\ m^{-3}$)	Reference
Vilnius, Lithuania (UB)	6/2021–5/2022	0.89	This study
Madrid, Spain (traffic urban site)	2014–2015	3.70	[15]
Madrid, Spain (UB)		2.33	
Madrid, Spain (RB)		2.61	
National Atmospheric Observatory Kosetice (NAOK), Czech Republic (RB)	2013	0.99	[16]
	2014	0.84	
	2015	0.64	
	2016	0.58	
	2017	0.65	
Zabrze, southern Poland (UB)	4/2019 - 3/2020	3.22	[17]
Amsterdam, (UB)	1–7/2013	1.09	[18]
Rotterdam, (UB) Netherlands	1–7/2013	1.10	
Jinan, China (UB)	9–11/2018	3.6	[19]

Place (environment)	Time period	Concentration ($\mu g\ m^{-3}$)	Reference
	12/2018–1/2019	5.8	
Wanzhou District, China (UB)	6/2013–2/2018	4.4	[20]
Sofia, Bulgaria (UB)	10/2020	2.4	[21]
	1/2021	3.6	
Burgas, Bulgaria (UB)	10/2020	1.63	
Burgas, Bulgaria (UB)	1/2021	1.75	
Helsinki, Finland (UB)	10/2015 - 5/2017	1.69	[22]
Helsinki, Finland (SUB)	12/2015 - 12/2016	0.88	
	1/2017 - 5/2017	1.04	
Paris, France (UB)	5/2012 - 12/2018		[23]
	Autumn	0.34	
	Winter	0.32	
	Spring	0.24	
	Summer	0.25	
San Francisco (near-highway)	7/2011–1/2018	1.43 (0.28–3.65)	[24]
San Francisco (SUB)		0.78 (0.09–2.61)	
Nairobi, (UB)	2014–2015	3.9	[25]
Hanoi, Vietnam (UB)	9/2016	S1 - 6.31 S2 - 4.0 S3 - 4.95 S4 - 4.29	[26]
Kadapa, India (RB)	9/2011–11/2012	2.20	[27]
Coruña, Spain (SUB)	2015–2016	0.85	[28]
Athens, Greece (SUB)	3/2013–2/2014	2.00	[29]
Klang Valley, Malaysia (SUB)	1–6/2020	1.90	[30]
Mahabaleshwar, India (RB)	3/2017–2/2019	1.56	[31]
Krakow, Poland (UB)	2/2020–3/2021	3.6	[32]

The results of different studies demonstrate the significant variability in temporal and spatial BC sources, which are closely tied to characteristics of

the measurement site, season, meteorological conditions, and time of day. The differences between cold and warm seasons indicate that the values of BC concentration in autumn and winter are significantly higher than those in spring and summer. The primary cause of this discrepancy is attributed to the practice of active wood combustion for heating during this period, in addition to the seasonal fluctuations in the boundary layer dynamics, which trap surface emissions in the colder months in a thinner layer than in summer. During the week, a decline in BC concentrations was observed on weekends, which is correlated with a reduction in emissions from transportation. During the day, BC concentrations are associated with enhanced vertical mixing, which results in a dilution of surface emitted pollutants. During daylight hours, BC concentrations are associated with enhanced vertical mixing, which results in a dilution of surface-emitted pollutants. The concentration of BC in the atmosphere is lowest during the middle of the day, as a result of the cycle of planetary boundary layer height. BC concentrations peak during rush hours, due to the emission of pollutants from road traffic, and the accumulation of emitted particles in a thinner boundary layer with reduced vertical mixing results in higher surface concentrations at night [22,23].

In the marine environment, most BC is transported over long-range from continental sources or has a local origin. For instance, this includes emissions from ships or activities on islands. BC from continental sources can be anthropogenic in origin (e.g. fossil fuel combustion) but can also originate from natural sources such as forest fires, which can result in marine BC increases from continental outflow [33].

1.4. Source apportionment of BC

Source apportionment of BC involves quantifying the contributions of various sources to BC concentrations in the atmosphere. The data presented in Table 2 illustrate the concentrations of BC_{FF} and BC_{BB} in a variety of environmental contexts.

Table 2. Mean BC_{FF} and BC_{BB} mass concentrations in different environments (UB is the urban background, RB - rural background, SUB - suburban background).

Place (environment)	Time period	Concentration, µg m⁻³		Reference
		BC_{FF}	BC_{BB}	
Madrid (traffic urban site)	12/20142/2020– 3/2021 12/2015	3.5	0.2	[15]
Madrid (UB)		2.1	0.2	
Madrid (RB)		0.9	1.7	
Athens, Greece (SUB)	3/2013–2/2014	1.7	0.3	[29]
Klang Valley, Malaysia (SUB)	1–6/2020	1.52	0.38	[30]
Xiamen, China (UB)	1–12/2014	2.9	1.3	[34]
Helsinki, Finland (UB)	10/2015– 5/2017	1.57	0.14	[22]
Helsinki, Finland (SUB)	12/2015– 12/2016	0.49	0.39	
	1/2017–5/2017	0.51	0.53	
Zabrze, southern Poland (UB)	4/2019–3/2020	2.33	0.93	[17]
Krakow, Poland (UB)	2/2020–3/2021	–	0.3	[32]
Mohanpur, eastern Indo-Gangetic Plain (RB)	Summer	3.5	0.7	[35]
	Monsoon	2.7	0.6	
	Post-monsoon	9.5	2.6	

1.5. Factors influencing BC dynamics

1.5.1. Surface meteorological conditions

Previous studies have reported that BC mass concentration correlates with meteorological conditions including planetary boundary layer, wind speed, wind direction, relative humidity, rainfall, barometric pressure, and air temperature. The results of numerous studies show that the increased BC aerosol concentration is associated with lower boundary layer height [23,36]. Liu et al (2022) [37] revealed that there was a strong negative correlation between wind speed (WS) and BC, while relative humidity (RH) showed a strong positive correlation (>0.7). While rainfall, barometric pressure, and air temperature (T) showed weak correlations with BC. This research highlights wind as a significant meteorological factor affecting the dispersion and transport of air masses. With higher WS, there would be a higher dispersion of BC in the atmosphere and a greater range of BC concentrations. Increased wind speed enhances ventilation effects, which consequently leads to the dispersion of aerosols and a decrease in BC concentration. Conversely, low wind speeds (up to 2.5 m s^{-1}) may indicate that the BC emissions originate from local sources rather than distant ones [38]. In a study by Raju et al. (2020) [31], a significant inverse correlation was observed between BC and wind speed, with a correlation coefficient of $r = -0.537$ (p-value of 0.0068). The concentration of BC at sites in closer proximity to the source was more strongly affected by wind speed. Furthermore, BC showed a stronger negative correlation with wind speed ($r = -0.64$), consistent with findings from numerous previous studies [20]. Helin et al. (2018) [22] observed a moderate negative correlation between air temperature and BC mass concentration at the suburban sites, whereas the correlation at urban site was negligible. This is attributed to the widespread use of wood for heating in Finland in private homes during the cold season. Similarly, Pani et al (2020) [39] reported that the increased BC mass concentrations were associated with regional biomass burning emissions and the accumulation of local urban pollution within the planetary boundary layer under favorable meteorological conditions such as lower temperature and wind speed, and a lack of rainfall, which reduces pollution removal.

The absence of a clear correlation between precipitation and the BC concentration may be explained by the hydrophobic nature of freshly emitted BC particles and the low intensity of precipitation. Fresh BC particles are typically resistant to scavenging due to their hydrophobic characteristics, while only aged BC particles, which have interacted with   hygroscopic

aerosols like sulphate or organic carbon, became more hydrophilic and thus susceptible to removal via precipitation [38]. However, Raju et al. (2020)] [31] reported an inverse correlation between BC and rainfall (r = − 0.75, p = 0.0001), attributing it to the efficient scavenging of BC particles by heavy rainfall in the Western Ghats (Mahabaleshwar). This emphasizes the crucial role of precipitation in the removal of particles, including BC, through the washing effect. Similarly, Huang et al. (2020) [20] found a significant negative correlation (r = – 0.74) between precipitation and BC concentration in the Wanzhou District. However, they observed a weaker correlation in another region of China., which they attributed to the higher precipitation frequency in southwest China compared to the northwest. Further studies, such as those by Liakakou et al. (2020) [40] and Tang et al. (2020) [41] demonstrate a nonlinear relationship between BC concentration, temperature and humidity, suggesting the existence of distinct mechanisms at varying RH and temperature levels that merit further investigation. Tang et al. (2020) [41] also noted in Yantai, that BC concentration increased with pressure below 1030 hPa but decreased once pressure exceeded 1030 hPa, indicating that atmospheric pressure plays a complex role in modulating BC levels.

1.5.2. Black carbon levels outdoors and indoors

Nowadays, individuals spend approximately 90% of their time indoors, whether at home, in offices, schools, or other enclosed spaces [42]. This underscores the critical importance of indoor air quality, as the majority of human exposure to air pollutants occurs indoors. Despite this, research on indoor particulate matter levels is relatively limited compared to studies on outdoor air quality. This is largely due to the broad range of indoor PM sources, such as printer emissions, dust resuspension, smoking, cleaning activities, and other behaviors, which contribute to the complexity of accurately assessing indoor air quality. Moreover, indoor environments are often comprised of multiple distinct microenvironments ranging from office spaces to industrial facilities and households – further complicating the determination of PM levels. Furthermore, indoor concentrations of certain pollutants have increased during the recent decades due to changes in building construction standards [43]. The relationship between indoor and outdoor varies depending on the type of pollutant specific characteristics of the home, such as proximity to roadways, building design (including construction and operational practices), ventilation systems, indoor pollution sources, and number of occupants [44–46]. Toxicological and epidemiological studies

suggest a clear association between both indoor and outdoor aerosol BC mass concentrations and potential health risks [47].

It is important to note that a key factor affecting indoor air quality is the level of ambient pollution and the building location. Variables such as local emissions, regional air quality, soil dust and atmospheric chemistry all contribute significantly to indoor air quality.

The geographical location of a building can significantly influences both the construction methods employed and its operational characteristics. In northern European countries, for instance, buildings tend to be more effectively isolated from the outdoor environment, and natural ventilation is less common. As a result, outdoor concentrations of PM and BC contribute relatively little to indoor air quality. In contrast, in southern European countries, where buildings are typically less isolated from the outdoor environment, indoor concentrations of PM and BC are more likely to be significantly affected by outdoor levels.

Ventilation systems in office and commercial buildings are generally classified into three categories. The first of these is natural ventilation, which occurs through openings such as windows and doors. The second type is mechanical ventilation, where temperature and humidity are controlled using heating, ventilation and air conditioning systems. The third type is mixed-mode ventilation, which integrates both natural and mechanical approaches. An example of this is the use of window air conditioners in conjunction with open windows and doors [46].

In modern buildings, natural ventilation is often replaced or at least partially provided by a mechanical ventilation/filtration system. In low energy buildings, outdoor PM enters the indoor environment mainly through the ventilation system and thus, the exposure to PM depends mainly on the filtration efficiency, air exchange rate, and the control of temperature and humidity [48]. The mechanisms of PM penetration indoors are well understood, and the impact of the ventilation operation has been thoroughly examined in several studies [49,50]. Mechanical ventilation and air filtration systems can significantly reduce infiltrating PM in residential and office buildings [51,52]. However, Zee et al. [53] pointed out that indoor fine dust (aerodynamic diameter <2.5 μm) filters (F8) near high traffic areas have only 30% removal efficiency for $PM_{2.5}$ and BC.

Nevertheless, it is clear that outdoor air quality has a substantial influence on indoor air quality. Previous studies have identified four potential sources of outdoor origin for PM_{10}. These are local traffic emissions, soil dust, biomass burning emissions, and regional coal combustion [44].

1.5.3. Relationship of BC with NO_x and PM

The relationship between BC, NO_x, and PM is complex and indicative of shared sources and combustion processes. Understanding these interconnections is crucial for addressing air quality and public health issues. Studies, such as Alfoldy et al. (2021) [54], have calculated BC/NO_x emission ratios to characterise the sources. The approaches provide insights into the relative contributions of different sources to air pollution. Diesel engines are a primary source of both pollutants compared to gasoline engines. Furthermore, in engines that do not comply with the Euro 5 standard, the BC emission is also significantly higher. However, both BC and NO_x emissions are highly influenced by engine specific characteristics and operational conditions, such as torque and crankshaft speed. The mechanisms by which BC and NO_x are produced within the engine differ considerably. BC is formed as a result of incomplete combustion, whereby fuel droplets injected into the combustion space are not fully oxidised. In contrast, nitrogen oxides are formed as a result of the oxidation of atmospheric nitrogen during the combustion process. In general, a high BC/NO_x ratio indicates a lack of air, resulting in incomplete combustion and a low combustion temperature. Conversely, a low BC/NO_x ratio suggests an excess of air and high-temperature combustion. Due to the circumstances of fuel injection and the elevated combustion temperature, diesel engines emit greater quantities of NO_x and considerably higher levels of BC than their gasoline counterparts. Consequently, the BC/NO_x emission ratio remains markedly higher in diesel engines than in gasoline engines. This makes the BC/NO_x emission ratio an effective tracer for differentiating between diesel and gasoline sources. Additionally, Alfoldy et al. (2021) [54] discuss the elevated BC/NO_x emission ratios observed within the study area in comparison to European road emissions. These ratios can be attributed to the combustion sources with insufficient air supply, such as oil and gas flares, which emit larger quantities of BC and lower quantities of NO_x in comparison to internal combustion engines. Liu et al (2022) [37] reported an increase in the positive correlation between BC and NO_x in the non-heating season compared to the heating season. This changes is partly due to the greater influence of mobile emissions on BC level during the non-heating season, leading to an increase in the correlation coefficient from 0.34 during the heating season to 0.69 in the non-heating season. In a study published in 2018, Helin et al. [22] observed a significant correlation between NO_x and BC concentration at street canyons (r = 0.87) and at detached house areas (r = 0.82-0.85). They found that residential heating contributes to the concentrations of NO_x and BC in the

detached house areas. However, NO_x levels observed in the street canyon site were significantly higher than those measured at the detached house areas, which suggests that traffic emissions are a primary contributor to these elevated levels. This finding also indicates that BC concentrations are influenced by the dispersion of these emissions across all sites. Additionally, Liu et al. (2022) [37] reported a strong positive correlation between BC concentrations and those of PM_{10} and $PM_{2.5}$, both during the heating and non-heating seasons. In 2018, Arif et al. (2018) demonstrated a significant correlation between the concentrations of particulate matter ($PM_{2.5}$ and PM_{10}) and BC (with a coefficient of determination of r = 0.5225 and a probability of p < 0.001). They proposed that natural sources, the transportation of aged pollutants, and windblown dust are the primary contributors to pollution [55].

1.5.4. Investigation of BC deposition (Green city concept)

Urbanization in Europe has already reached 75%, and this trend continues to rise. In the near future, over four-fifths of Europe's population will reside in cities [25]. Consequently, these urban areas will become the primary contributors to the majority of all emissions. The impacts of air and noise pollution, and climate change are increasingly evident, leading to a rapid decline in the quality of life within cities. Many cities worldwide have already recognised the benefits of urban greening. Urban trees can improve air quality by intercepting and removing particles from the surrounding air through dry deposition, which has a positive impact on human health [56]. Dry deposition refers to the process by which atmospheric particles and gases are deposited onto plant tissue, such as the surface of leaves, twigs, branches, and stems, as they pass near solid surfaces [57].

Empirical studies have demonstrated that $PM_{2.5}$ concentrations in Shanghai were reduced by 9% in wooded areas adjacent to urban environments [58]. Similarly, in Guangzhou, mean UFP level near the park were 41.8% lower than those found in the street canyon [59]. In Beijing, trees are estimated to remove 1,261 tons of pollutants annually, including 772 tons of PM_{10} [60]. Factors, such as air pollutant concentrations, meteorological conditions, building configuration and specific leaf characteristics – including canopy structure, growth stage, and leaf roughness significantly influence particle deposition [61–64]

For example, high rainfall combined with extreme winds mobilize and transport air pollution to the ground in throughfall, while exposed locations receive higher deposition rates due to reduced protection from adjacent slopes and tree canopy, which influence micrometeorological variations in wind

dynamics and particle availability for deposition [61,63] Research indicates that not all tree species possess equal capabilities for filtering air pollutants. Jin et al. (2021) [65] reported a more than sixfold difference in PM removal among ten different tree species. Notably, broad-leaved forests serve as the primary source of dry deposition in urban green spaces in China, accounting for 89.22% of the total dry deposition; additionally, the dry deposition on evergreen broad-leaved trees per unit area was twice that of deciduous broad-leaved trees. Moreover, a study by Min-Cheol Cho et al. (2021) [66] demonstrated that coniferous trees exhibits a higher rate of deposition of soot particles compared to broad-leaved trees. Comparative analyses of particle deposition on the front and back sides of broad leaves revealed that deposition rate is higher on the side with a more complex structure and surface roughness, even for the same leaf species. Consequently, the characteristics of particle deposition are significantly influenced by the structure and roughness of the leaf surface.

In a recent study, Elderbrock et al. (2023) [63] emphasized the importance of proximity to traffic-related emission sources in predicting the likelihood of high BC removal by trees. This finding aligns with previous studies on air pollutant concentration and deposition, reinforcing the potential of proximity as a predictor of atmospheric BC uptake. Their results suggest that the effective distance for pollution removal may extend up to 500 m from individual trees. Additionally, the study highlighted the significance of terrain characteristics, specifically the topographic position index and directional exposure, in influencing BC deposition in urban forest canopies. Elderbrock et al. (2023) [63] results suggested that the deciduous post oak should be prioritized in planting for BC removal over the evergreen live oak.

As Jõgiste et al. (2018) [67] notes, the Norway spruce (*Picea abies (L.) H.Karst*) and silver birch (*Betula pendula Roth*) rank among the most prevalent tree species in Lithuania. Their prevalence and naturalization across various regions underscore their suitability for study within the context of urban greening initiatives. The Norway spruce, in particular, serves as dominant species in Boreal and subalpine conifer forests across Central, Northern, and Eastern Europe, extending up to the Ural Mountains. Additionally, this species has been naturalised in many regions of Europe beyond its native habitat, including areas such as Britain and the Pyrenees Mountains. It has also been introduced to various countries outside Europe, including United States, Canada, and Japan, as well as in the southern hemisphere, including South Africa, Tasmania, and New Zealand. In contrast, Silver birch (*Betula pendula Roth*) is naturally distributed throughout most of Europe up to central Siberia, including southern regions such as the Iberian

Peninsula, southern Italy, and Greece. This species is particularly abundant in the boreal zone of northern Europe. The ability of both species to tolerate a wide range of site conditions presents an excellent opportunity to explore their potential within the conceptual framework of a green city.

Chapter 1 conclusions

Research demonstrates that BC levels exhibit significant temporal and spatial variability, largely driven by measurement location, seasonality, meteorological conditions, and time of day. These variations highlight the complex nature of BC emissions and the challenges in assessing their broader environmental and health impacts. Studies highlight the source apportionment; a critical analytical approach used to identify and quantify the contributions of various emission sources to the concentration of BC. This methodology is particularly relevant for understanding complex air quality issues, such as those associated with BC and PM.

One of the most critical insights is the substantial influence of outdoor air quality on indoor environments. Specifically, the quality of outdoor air impacts indoor air quality, with 85% of indoor BC concentrations originating from outdoor sources. The relationship between indoor and outdoor air quality is shaped by several factors, including the type of pollutant and the characteristics of the building. Key factors influencing this relationship include proximity to roadways, building design (which encompasses construction and operational practices), ventilation systems, the presence of indoor pollution sources, and the number of occupants). Understanding these dynamics is essential for developing effective strategies to improve indoor air quality and mitigate the health risks associated with air pollution.

High pollution events that exceed the 95th percentile highlight the need for effective regulation, and public health strategies. Understanding the causes and consequences of these events is crucial for developing interventions to protect public health and improve urban air quality. The co-existence of BC with NO_x and PM in urban areas suggests potential synergistic interactions among these pollutants. Their shared sources, particularly those associated with biomass burning- and transport-related activities underscore the importance of examining the dynamics between BC and NO_x in source apportionment studies. Therefore, understanding the dynamics between BC and NO_x is essential in the context of source apportionment, as it can significantly enhance our ability to identify and mitigate the sources.

The implementation of urban trees has the potential to enhance air quality by reducing the concentration of BC through the process of dry deposition on tree foliage, which in turn offers tangible benefits for human health. The efficacy of trees in filtering airborne particles varies considerably across species, influenced

by factors such as canopy structure, growth stage and leaf roughness can influence the deposition of particles in green spaces. In Lithuania, the Norway spruce (*Picea abies (L.*) *H.Karst*) and silver birch (*Betula pendula Roth*) are among the most commonly occurring tree species, providing a valuable opportunity to investigate their potential within the conceptual framework of a green city. Understanding the specific characteristics and benefits of these species can inform urban planning and management strategies aimed at optimizing the environmental and health outcomes associated with urban greening initiatives.

2.   MATERIALS AND METHODS

2.1.   Measurements site

Three campaigns to measure the dynamics of BC mass concentration were conducted at the SRI Center for Physical Sciences and Technology (FTMC), located at 54.72° N and 25.32° E in Vilnius, the capital and largest city of Lithuania (Figure 5).

1. The BC mass concentration sampling campaign was conducted over one year period, from 1 June 2021, to 31 May 2022.
2. The investigation of the indoor-outdoor relationship of BC concentration and source apportionment was conducted in October 2020–February 2021, during the heating season period.
3. The study to investigate the deposition of BC on urban trees (Norway spruce and silver birch) was conducted during September - October 2020, prior to the commencement of the residential heating season period.

Vilnius is situated in the Baltic region of Europe and covers a total area of 402 km^2. The Vilnius administrative zone is divided into 21 districts and has a population of approximately 601 952 inhabitants (Statistics Lithuania, 2024, https://osp.stat.gov.lt/gyventojai1).

The sampling site, characterized as residential area adjusted to forested areas, is located approximately 8 km northeast of the city center and about 600 m from a busy urban road. This location serves as a representative background environment for the wider area of the of Vilnius, allowing for the assessment of air quality influenced by both local and regional factors. The main sources are primarily local traffic and secondarily domestic heating, both of which contribute to local episodes of winter smog. Additionally, frequent local pollination events occur. Aerosols from other sources were also measured at the site, which can be attributed to long-range transport of biomass burning, mainly from Russia, Ukraine, and Belarus, as well as advection of mineral dust from African deserts into the free troposphere. [68].

To evaluate the contribution of outdoor to indoor BC mass concentration, measurements were carried out in a mechanically ventilated, unoccupied laboratory space in FTMC, which can be characterized as a typical office environment. The air supply system contained three-stage filtration (G4-F7-F9). The supply air is filtered at G4 to remove insects, sand, fly ash, spores, pollen, cement dust and other air pollutant particles larger than 10 µm. The DIN EN ISO 16890 standard specifies that pre-filter G4 has a filtration efficiency of 60-70% for coarse particles. In contrast, F7 and F9 filters are used to remove oil fumes, agglomerated soot, tobacco and other types of smoke particles from the air supply. F7 filters have an efficiency of 65-95% for $PM_{2.5}$ particles and 50-65% for PM_1 particles. The final filter (F9) achieves at least 80% efficiency for PM_1. It is important to note that indoor aerosol sources were kept to a minimum during the measurement campaign. Indoor activity was restricted, except for rare entrances by the sampling team. There is no food service located in the building, and windows and doors were kept closed. Therefore, any changes in indoor PM presence were due to the changes in outdoor PM and the air filtration system's performance.

Figure 5. Map of Lithuania highlighting the city of Vilnius and the specific sampling location at the SRI Center for Physical Sciences and Technology (FTMC).

The Aethalometer (See 2.2 Instrumentation and methods), was situated on the second floor of the building. The outdoor aerosol inlet was approximately 5 meters above the ground, while the indoor aerosol samples were taken at a height of approximately 1 meter above the floor of the room. Sampling between indoor and outdoor inlets was switched using an automatic valve control with a time resolution of 30 minutes.

2.2. Instrumentation and methods

2.2.1. Black carbon

A Magee Scientific Aethalometer, specifically models AE-31 and AE-33, was used to measure BC mass concentrations continuously in real-time. The optical transmission of carbonaceous aerosol particles was measured sequentially at seven wavelengths (λ= 370, 470, 520, 590, 660, 880, and 950 nm). The standard channel for BC measurements is 880 nm as it is considered to be the predominant absorber.

The Aethalometer measures the attenuation (ATN) of a light beam transmitted through a filter on which aerosols are continuously collected [69]:

$$ATN = 100 \cdot ln\frac{I_0}{I},\qquad [1]$$

where I_0 and I denote the intensity of a light beam through an empty and particle-laden spot of a filter tape, respectively.

The change in ATN over a certain time period (t, min) is proportional to the attenuation coefficient (b_{ATN}) given a known flow rate (Q, l/min) and spot size (A) onto which particles are collected:

$$b_{ATN} = \frac{A}{Q} \cdot \frac{\Delta ATN}{\Delta t},\qquad [2]$$

The source apportionment methodology employed for the measurement of BC mass concentration by Aethalometer is based on the Aethalometer Model proposed by Sandradewi et al. (2008) [70].

2.2.2. Black carbon source apportionment

The analysis of source apportionment data was conducted using specific aerosol absorption Ångström exponent (AAE) values for biomass burning (AAE_bb) of 2.2 and fossil fuel AAE_ff (0.9), which were determined for background urban in Vilnius in the papers (Drinovec et al., 2015; Minderytė et al., 2022; Sandradewi et al., 2008) [70–72].

Calculations can be made to determine the differences in aerosol particle light absorption across the 370-950 nm range. The AAE is a characteristic of carbonaceous aerosol particles that explains the dependence of particle light absorption on wavelength, as shown in Equation [3].

$$b_{abs}(\lambda) = b_0\lambda^{-AAE}\qquad [3]$$

where λ indicates wavelength, $b_{abs}(\lambda)$ the aerosol absorption coefficient for each wavelength, and b_0 is a wavelength-independent constant.

The absorption coefficients of BC attributable to each source (FF or BB) were determined using Equations [4,5]:

$$b_{abs\,FF} = \frac{b_{abs}(\lambda_1) - b_{abs}(\lambda_2) \times (\frac{\lambda_1}{\lambda_2})^{-AAE_{BB}}}{(\frac{\lambda_1}{\lambda_2})^{-AAE_{FF}} - (\frac{\lambda_1}{\lambda_2})^{-AAE_{BB}}} \,, \qquad [4]$$

$$b_{abs}(\lambda_1) = b_{abs\,FF}(\lambda_1) + b_{abs\,BB}(\lambda_1), \qquad [5]$$

$$AAE = -\frac{\ln\left(\frac{b_{abs}(\lambda_1)}{b_{abs}(\lambda_2)}\right)}{\ln\left(\frac{\lambda_1}{\lambda_2}\right)}, \qquad [6]$$

where $b_{abs}(\lambda_1)$ denotes total absorption at wavelength λ_1, $b_{abs}\,BB$ the absorption coefficient of biomass-burning-related BC, and $b_{abs}\,FF$ the absorption coefficient for BC from fossil fuel combustion at a wavelength λ_1. For our study, λ_1 was selected to be 470 nm, while λ_2 was 950 nm based on the most commonly used wavelength pair in the literature. The source-specific AAE values differ across regions based on commonly used fuels, fuel origin, and climate conditions [73]. Hourly mean BC mass concentration values were used for analysis.

The data for the concentrations of BC are presented as the mean value and ultrafine particles (SD). The time zone used in this study is UTC+2:00.

2.2.3. Foliage analysis

To investigate the potential influence of urban trees on BC removal, a typical area with a mix of conifer (spruce) and broadleaf (silver birch) tree species was selected for leaf and needle sampling, located in close proximity to the university campus and residential area, more than 0.35 km from busy roads and 3 km from industrial facilities, with a wooded area in between. Foliage sampling was carried out at three sites, each approximately 500 m from the BC sampling site. In Lithuania, the most commonly populated species are Norway spruce (*Picea abies (L.) H.Karst*) and silver birch (*Betula pendula Roth*), accounting for 24% and 19%, respectively [67]. This was the reason for choosing this location and these tree species for the measurements. This paper focuses solely on the dry deposition of pollutants on the surface of leaves and needles. It does not assess any subsequent processes, such as pollutant uptake or resuspension.

Transmission electron microscopy (Tecnai G2 F20 X-TWIN, resolution 0.25-0.102 nm) in combination with energy scattering X-ray spectroscopy (EDX) was used to characterize and obtain detailed information on the morphology, size, and elemental composition of individual aerosol particles deposited on the leaf of silver birch (*Betula pendula Roth*) and needle of Norway spruce (Picea abies (L.) H.Karst).

2.2.4. Air mass backward trajectories and MODIS satellite data

An analysis of the 72-hour backward trajectories of air masses arriving in Vilnius at 500 m, 1000 m and 1500 m above the ground was performed using the HYSPLIT4 (Hybrid Single-Particle Lagrangian Integrated Trajectory) model of the Air Resources Laboratory (ARL) to investigate the contribution of long-range transport of air masses to BC mass concentrations. This model is commonly used to study atmospheric trajectories, transport, and dispersion.

The fire data were obtained from the Resource Management System (FIRMS) of the NASA/GSFC Earth Science Data Information System (ESDIS) (https://firms. modaps.eosdis.nasa.gov/map). The data are derived from satellite observations that detect thermal anomalies associated with open fires reaching temperatures above 2000 K. The MODIS and Navy Aerosol Analysis and Prediction System (NAAPS) global aerosol model data were used to profile fire location maps over Lithuania. The presence of a smoke layer over Vilnius was confirmed by a combination of NAAPS model data and BC observations.

2.2.5. Meteorology

The hourly averages of temperature (T, °C), relative humidity (RH, %), wind speed (WS, m s^{-1}) and wind direction (WD, degrees), as well as the mass concentrations of air pollutants (NO_x and PM_{10}), were provided by the Environmental Protection Agency of Lithuania (www.gamta.lt).

The first campaign covered both heating and non-heating season periods. The heating season period, which runs from October to March, is characterised by lower ambient temperatures and the need for indoor heating. In contrast, the non-heating season period, which runs from April to September, is characterised by favourable weather conditions and does not require indoor heating (Table 3).

Table 3. Descriptive statistics of meteorological variables for heating and non-heating season periods.

	Heating season period		Non-heating season period	
	Mean (Min; Max)	SD	Mean (Min; Max)	SD
Temperature, °C	1.1 (-15.6; 17.7)	5.6	14.8 (-4.9; 35.5)	7.6
Relative Humidity, %	81.0 (20.0; 97.0)	17.0	70 (18.0; 97.0)	20.0
Barometric pressure, hPa	994.0 (960.0; 1026.0)	13.0	994.0 (962.0; 1011.0)	7.0
Wind speed, m s^{-1}	1.0 (0.11; 3.27)	0.50	0.64 (0.10; 3.13)	0.42

During the heating season period, the mean temperature was 1.1°C, with a range from -15.6°C to 17.7°C. In contrast, non-heating season period exhibited a significantly higher temperature of 14.8°C, ranging from -4.9°C to 35.5°C. The relative humidity levels also varied across periods, with averages of 81% during the heating season period (ranging from 20% to 97%), and 70% during the non-heating season period (ranging from 18% to 97%). Wind direction analysis revealed distinct patterns between the two periods. During the heating season period, the predominant wind direction was WNW accounting for 19.5% of the total observation, followed by S at 12.8% and NW at 10.5%. Conversely, the non-heating season period was characterized by NW winds, which represents 17% of the total, with WNW at 12.9%, NE at 9.0%, and ENE at 8.5%.

The seasons have been categorized into distinct monthly groups for analysis as follows: summer (June - August 2021), autumn (September - November 2021), winter (December 2021, January, - February 2022), and spring (March - May 2022). This classification facilitates a clearer understanding of seasonal variations in air quality parameters and their associated influences throughout the year. Table 4 provides a descriptive statistical overview of various meteorological variables across four seasons.

Table 4. Descriptive statistics of meteorological variables for all seasons.

	Summer	Autumn	Winter	Spring
	Mean (Min; Max)	Mean (Min; Max)	Mean (Min; Max)	Mean (Min; Max)
Temperature, °C	19.8 (6.0; 35.0)	6.9 (-7.2; 28.3)	-2.3 (-15.6; 6.0)	6.3 (-10.3; 25.3)
Relative Humidity, %	71 (25; 97)	82 (34; 97)	87 (33; 97)	61 (18; 96)
Barometric pressure, hPa	994 (979; 1007)	996 (965; 1019)	989 (960; 1026)	962 (996; 1026)
Wind speed, m s^{-1}	0.50 (0.10; 1.57)	0.82 (0.10; 2.7)	1.10 (0.18; 3.27)	0.93 (0.12; 3.19)

The data indicate that the average temperature during experiment in summer of 2022 was 19.8°C, with a peak of 35.0°C observed in June. This season is also characterised by the lowest average wind speed of 0.15 m s^{-1}, along with the lowest values for wind speed and air pressure compared to other seasons. Conversely, winter is characterized by the lowest average temperatures, recorded at -2.3°C and minimum temperature of -15.6°C. This season also experiences the highest average humidity at 87% and the highest average wind speeds of 1.1 m s^{-1}, exhibiting the most significant fluctuation range among the seasonal data.

All seasons exhibited temperature variation ranges exceeding 20°C, with autumn and spring demonstrating the most significant temperature fluctuations, which were notably similar between the two seasons. Spring also showed greatest fluctuations in humidity and air pressure, and had the lowest average humidity compared to other seasons.

2.2.6. Statistical analysis and Conditional Probability Field analysis

Air pollutants, including BC, PM_{10} and NO_x, as well as meteorological parameters such as wind speed and wind direction were analyzed using the statistical software Openair, R package version 4.3.1 for the Conditional Probability Function (CPF). Openair is a specialized R package developed primarily for the analysis of air pollution measurement data. The package includes many tools for importing and manipulating data, performing a wide range of analyses, and producing high-quality graphics and visualizations to improve understanding of air pollution data [74].

The CPF method is an effective approach for identifying major sources of air pollutants by calculating the probability of a species threshold value within a particular wind sector. This value is usually expressed as a high percentile, such as the 75th or 90th percentile, however, in this study, the 25th, 75th and 95th percentiles were utilized to assess both high concentrations (75th) and background (25th) concentrations. A comprehensive description of the CPF analysis can be found in Ashbaugh et al. (1985) [75].

The mathematical definition of the CPF is:

$$CPF_{\Delta\Theta} = \frac{m_{\Delta\Theta|C \geq x}}{n_{\Delta\Theta}} \qquad [7]$$

where $m\Delta\theta$ represents the count of samples in the wind sector θ with a concentration C greater than or equal to a threshold value x, while $n\Delta\theta$ denotes the total number of samples from the wind sector $\Delta\theta$.

3.   RESULTS AND DISCUSSION

3.1   BC mass concentration dynamics in urban environment

3.1.1. Overview of BC mass concentration measurement campaign

This study on BC analysis provides a comprehensive analytical approach, encompassing time series analysis across heating and non-heating season periods, as well as seasonal, daily and high pollution days. Throughout the annual measurement period, the concentrations of PM_{10} and NO_x and meteorological data were additionally analysed, which allows for a more comprehensive understanding of the relationship and behavior of BC during this period.

The annual mean concentration of BC was found to be 0.89 μg m^{-3}, with a standard deviation of 0.99 μg m^{-3}. This indicates high variability in the level of BC. The high variability of BC levels has been repeatedly observed in other studies [76,77]. The study revealed notable seasonal and monthly variations in BC mass concentrations, with the highest levels observed for all species, including source-apportioned BC, in March (Figure. 6). The mean monthly concentrations reached 1.96 μg m^{-3}, with BC from biomass burning (BC$_{BB}$) contributing 0.68 μg m^{-3}, and fossil fuel combustion (BC$_{FF}$) contributing 1.28 μg m^{-3}. Conversely, the lowest mass concentrations were observed in September for BC (0.5 μg m^{-3}) and BC$_{BB}$ (0.05 μg m^{-3}) indicating a period with minimal biomass burning activities and favorable atmospheric conditions for pollutant dispersion. For BC$_{FF}$, the lowest monthly concentration occurred

in July averaging 0.31 µg m⁻³, possibly reduced vehicular emission and increased mixing layer.
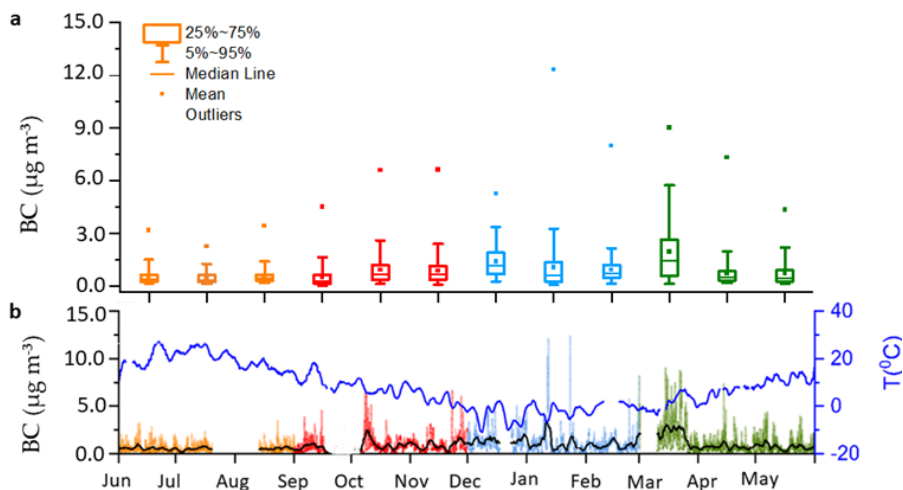

Figure 6. The time series of BC mass concentration and temperature (the black and blue lines represent the 72-h moving averages) (b) with box plots during the measurement period (a). The colours of the lines and boxes represent the seasons, with summer represented by orange, autumn by red, winter by blue, and spring by green.

The results demonstrate that BC mass concentration in Vilnius comparable to many sites in Europe during different periods, for example in Amsterdam and Rotterdam, Netherlands (1.09 and 1.10 µg m⁻³, respectively January–July 2013), Helsinki, Finland (0.88 µg m⁻³, December 2015–December 2016). Nevertheless, the concentration remains below that observed in most urban areas, for example the mean BC mass concentration at the neighboring territory of Zabrze, southern Poland (3.22 µg m⁻³, April 2019 – March 2020). The comparison between the values of BC detected in Vilnius and those reported for other European and non-European countries is presented in Table 2.

The source apportionment of BC revealed distinct contributions from fossil fuel combustion and biomass burning. The annual mean concentration of BC_{FF} and BC_{BB} were 0.63 µg m⁻³ (0.67) µg m⁻³ and 0.27 µg m⁻³ (0.35) µg m⁻³, respectively. Throughout the year, the contribution of BC_{BB} was 29.0% (11%) (Figure 7).
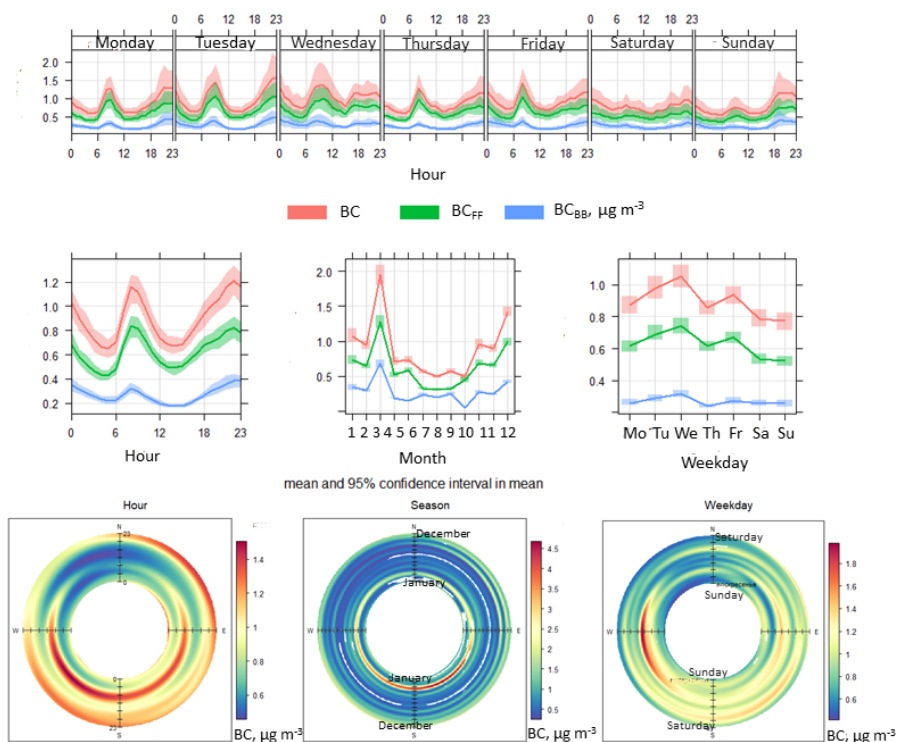
Figure 7. Time variation plots to show the mean pollutant concentrations with respect to their averaging times for BC, BC_{FF} and BC_{BB} by an hour of weekday, by hour, by month and by weekday Seasonal (mean concentrations displayed by time of year and wind direction), weekly (mean concentrations displayed by day of week and wind direction) and hourly (mean concentrations displayed by time of day and wind direction) Polar Annulus plots for BC, BC_{FF} and BC_{BB}.

This indicates that a significant portion of BC emissions originated from biomass burning, especially during colder months when residential heating is more prominent. Indeed, the highest mean mass concentration of BC (1.14 µg m^{-3}) was observed during the winter season. This is also attributable to a reduction in the lower boundary layer during the winter season and an increase in demand for residential heating and biomass burning [36]. In contrast, July exhibited the lowest monthly mean value (0.50 µg m^{-3}), which may be attributed to two primary factors: first, the consistently higher boundary layer observed during summer [36], and second, the vacation period, which resulted in reduced traffic activity within the city, further contributing to lower BC level.

The weekly BC mass concentrations demonstrated a notable increase across weekdays (Monday to Friday) and a pronounced decline during weekends (Saturday and Sunday). This trend was attributed to the influence of human activities, particularly a significant reduction in traffic levels. These findings were corroborated by other studies, including [30,41], which also documented a similar pattern. The diurnal variation of BC, BC_{FF} and BC_{BB} concentrations showed a typical urban pattern with a well-defined morning (from 7:00 and 9:00) and evening (from 18:00 to 23:00) emission peaks. The primary contributors to these peaks are the morning and evening rush hours. The annual morning peak concentrations for BC, BC_{FF} and BC_{BB} were 1.21 $\mu g\ m^{-3}$, 0.87 $\mu g\ m^{-3}$ and 0.34 $\mu g\ m^{-3}$, respectively. The annual evening peak concentrations for BC, BC_{FF} and BC_{BB} were 1.25 $\mu g\ m^{-3}$, 0.85 $\mu g\ m^{-3}$ and 0.41 $\mu g\ m^{-3}$, respectively.

The highest concentrations occurred from south-east, south and south-west directions during March. In the middle of the week, the highest concentrations come from the south-east, while the lowest concentrations come from the north-west during the whole week. Two peaks were associated with BC concentrations in the morning and evening from different directions, but most strongly associated with south-westerly winds from 7:00 to 11:00. BC showed a trend with two peaks in the morning and evening. The highest concentrations occurred from southeast, south and southwest directions in the morning (from 7:00 to 11:00) and from northeast directions in the evening (from 19:00 to 23:00).

Simultaneously, measurements were taken for other common urban pollutants. The annual mean mass concentration of PM_{10} was determined to be 19.68 $\mu g\ m^{-3}$ with standard deviation of 11.36 $\mu g\ m^{-3}$, while the annual mean NO_x concentration was found to be 21.62 $\mu g\ m^{-3}$ with a standard deviation of 23.10 $\mu g\ m^{-3}$. The annual mean concentration of PM_{10} is comparable to that observed in Latium Region, Italy (21.90 $\mu g\ m^{-3}$, 2006-2012) [78], Ciuc Basin, Romanian Carpathians (19.00 $\mu g\ m^{-3}$, 2008–2016) [79] and Germany (18.10 $\mu g\ m^{-3}$, 2015–2018) [80].

The results demonstrated a distinct monthly variation in pollutant concentrations, with the highest levels observed for PM_{10} and NO_x in March (a pattern also evident in BC concentration). The average monthly concentrations were 27.83 $\mu g\ m^{-3}$ and 35.43 $\mu g\ m^{-3}$, respectively. The lowest mass concentrations were observed in January for PM_{10} (0.5 $\mu g\ m^{-3}$) and in June/July for NO_x (0.31 $\mu g\ m^{-3}$). During the measurement period, PM_{10} and NO_x concentrations were consistently higher throughout the week, as shown in Figure 8. Weekdays (especially Thursday and Wednesday) showed higher concentrations compared to weekends (Saturday and Sunday). The reason for

this is probably due to the lower volume of traffic during the weekend. Concentrations were slightly lower on Mondays, which may be due to lower emissions from traffic during the weekend. The lowest concentrations of NO_x and PM_{10} were observed during the early morning hours (from 00:00 to 06:00 for NO_x and from 00:00 to 07:00 for PM_{10}). This is attributed to the absence of traffic at night and the dispersion of pollutants during the daytime. Thereafter, a progressive increase in NO_x concentrations was observed between 07:00 and 10:00, as well as between 08:00 and 11:00 in the case of PM_{10}. Subsequently, there was an increasing tendency of NO_x from 14:00 to 18:00 and plato from 19:00 to 22:00. This can be attributed to the evening traffic rush hour. A decreasing trend in PM_{10} is evident after 12:00.

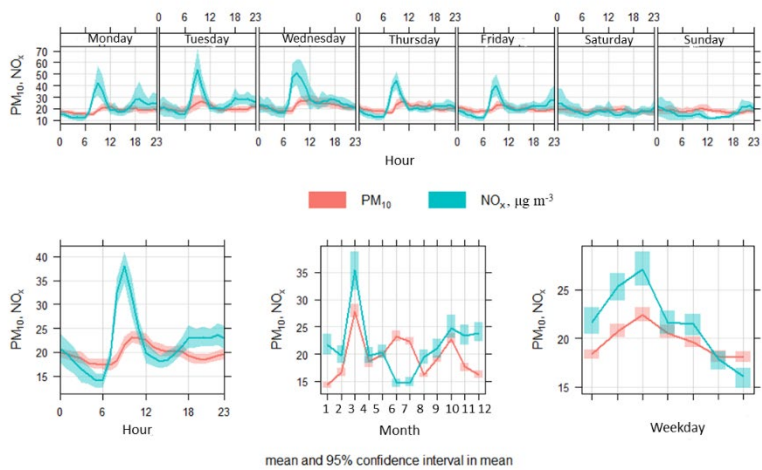Figure 8. Time variation plots to show the mean pollutant concentrations with respect to their averaging times for PM_{10} and NO_x by hour of weekday, by hour, by month, and by weekday.
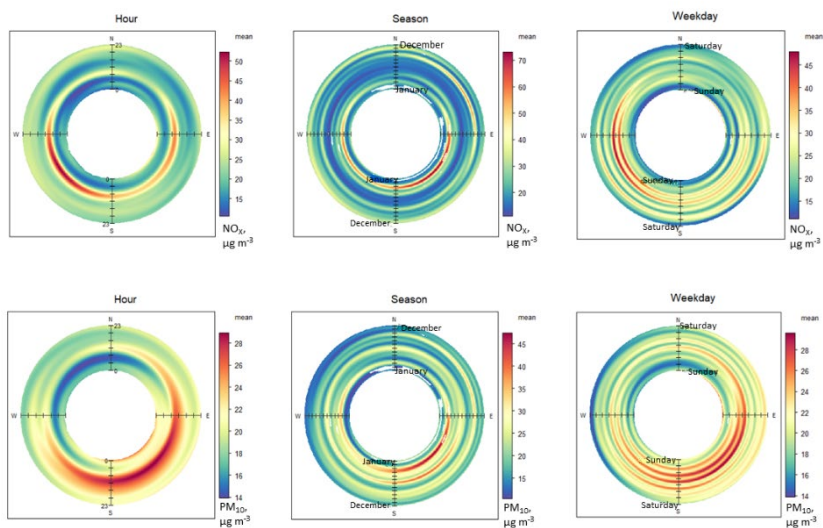
Figure 9. Seasonal (mean concentrations displayed by time of year and wind direction), weekly (mean concentrations displayed by day of week and wind direction) and hourly (mean concentrations displayed by time of day and wind direction) Polar Annulus plots for PM_{10} and NO_x.

The highest concentrations of NO_x and PM_{10} were observed in a south-easterly direction during March. The diurnal trends exhibited by each pollutant were distinctive. The highest concentrations of NO_x were observed from a south-west and west direction during the midweek period between 8:00 and 12:00. In contrast, the highest concentrations of PM_{10} were observed from a south-easterly direction during the working day, between the hours of 8:00 and 17:00. The highest concentration of pollutants in March can be attributed to grass burning and long-range transport from neighboring regions, particularly non-European countries [81–83]. This is validated by the presence of active fire detections in the FIRMS MODIS database and NAAPS model results, which indicate higher concentrations of smoke during March (discussed in greater detail in Section 3.1.5., entitled "Analysis of high BC mass concentration events").

3.1.2. Source-apportioned BC mass concentration during heating and non-heating season periods

The results showed that the mass concentrations of BC, BC_{FF} and BC_{BB} and NO_x were significantly different during the non-heating and heating season periods (Table 5). In particular, the average concentrations of BC, BC_{FF} and BC_{BB} were about 2 times higher during the heating period than during the

non-heating season period. Briefly, the mean concentrations for all pollutants of the non-heating and heating season periods were 0.61 (0.56) and 1.17 (1.22) μg m^{-3} for BC, 0.43 (0.44) and 0. 81 (0.80) for BC$_{FF}$, 0.17 (0.17) and 0.36 (0.44) μg m^{-3} for BC$_{BB}$, 20.02 (10.89) and 19.37 (11.78) μg m^{-3} for PM$_{10}$, 18.27 (16.47) and 24.92 (27.76) μg m^{-3} for NO$_x$. It is notable that there were no significant differences in PM$_{10}$ concentrations observed in Vilnius between the heating and non-heating season periods. During the heating season period, the concentration was 19.37 μg m^{-3}, while during the non-heating season period, it was 20.02 μg m^{-3}. Conversely, other urban areas exhibited a pronounced variation in PM$_{10}$ concentrations between the two periods. For comparison, in Italy, the concentration of PM$_{10}$ increased by an average of 9.36 μg m^{-3} during the winter months, which was attributed to increased household heating [54,79].

The highest mass concentrations during the non-heating season period were observed in May for BC (0.73 μg m^{-3}), BC$_{FF}$ (0.58 μg m^{-3}), and in August for BC$_{BB}$ (0.25 μg m^{-3}). The lowest mass concentrations were observed in September for BC (0.5 μg m^{-3}) and BC$_{BB}$ (0.05 μg m^{-3}), and in July for BC$_{FF}$ (0.31 μg m^{-3}).

Table 5. Descriptive statistics of BC, BC$_{FF}$, BC$_{BB}$, PM$_{10}$ and NO$_x$ (μg m^{-3}) for the heating and non-heating season periods.

	BC	BC$_{FF}$	BC$_{BB}$	PM$_{10}$	NO$_x$
Heating season period					
Mean (SD)	1.17 (1.22)	0.81 (0.80)	0.36 (0.44)	19.37 (11.78)	24.92 (27.76)
Mediana	0.23	0.59	0.22	16.48	16.63
Mode	0.26	0.23	0.03	10.0	14.34
Min; Max	0.04;12.33	0.03;8.48	0.01;5.64	0.07;88.09	4.40;347.03
Non-heating season period					
Mean (SD)	0.61 (0.56)	0.43 (0.44)	0.17 (0.17)	20.02 (10.89)	18.27 (16.47)
Mediana	0.43	0.29	0.12	17.77	13.00
Mode	0.16	0.05	0.01	14.0	9.56
Min; Max	0.01;7.32	0.01;6.07	0.01;1.51	1.00;174.51	3.44;247.99

During the heating season period, the concentrations of BC, BC_{FF}, BC_{BB} and NO_x were observed to be consistently higher throughout the week, as illustrated in Figure 10. Furthermore, these concentrations were found to be higher on weekdays in comparison to weekends (Saturday and Sunday). The lower volume of traffic on weekends is probably the cause of this phenomenon. Interestingly, the concentrations were observed to be slightly lower on Mondays, may be which attributed to a reduction in emissions from decreased traffic over the weekend traffic. In contrast, PM_{10} concentrations exhibited a decline from Wednesday to Saturday, suggesting potential variations in sources or atmospheric conditions influencing particulate matter levels throughout the week.

The observed pattern in both heating and non-heating season periods was similar; however, there was a notable disparity in the hourly variation of BC, BC_{FF}, and BC_{BB} averages between the two periods. The divergence in pattern can be attributed to variations in heating emissions and weather conditions. During the heating season period, the diurnal variation range of BC, BC_{FF} and BC_{BB} was considerable, reaching up to 0.76 µg m^{-3}, 0.52 µg m^{-3} and 0.27 µg m^{-3}, respectively (Figure 12). The diurnal variations in the concentrations of BC, BC_{FF} and BC_{BB} exhibited a distinctive urban trend, characterised by a discernible morning and evening emission peak. The morning peak was predominantly attributable to the morning rush hours, occurring between approximately 7:00 and 9:00 for both periods. During the heating season period, the peak concentrations of the three pollutants were as follows: 1.44 µg m^{-3} for BC, 1.05 µg m^{-3} for BC_{FF} and 0.39 µg m^{-3} for BC_{BB}. During the non-heating season period, morning peak concentrations of BC, BC_{FF}, and BC_{BB} were observed to be 0.90 µg m^{-3}, 0.65 µg m^{-3}, and 0.24 µg m^{-3}, respectively (Figure 10). The evening peak for the heating season period was observed between from 16:00 to 21:00. The primary contributors to this peak are the evening rush hour and residential heating. The peak concentrations for BC, BC_{FF} and BC_{BB} were 1.57 µg m^{-3}, 1.05 µg m^{-3} and 0.52 µg m^{-3}, respectively. For the non-heating season period, the evening peak was observed from 19:00 to 23:00 (peak concentrations of 0.90 µg m-3, 0.64 µg m^{-3} and 0.27 µg m^{-3} for BC, BC_{FF} and BC_{BB}, respectively. These patterns highlight the influence of traffic and heating on BC emissions, with distinct temporal variations between the heating and non-heating season periods.

A comparable diurnal fluctuation in BC mass concentrations has been demonstrated in various European cities, including Galicia, Barcelona, and Granada in Spain [28] and Ostrava in the Czech Republic [38]. Kucbel et al. (2017) [38] proposed that these differences may be attributed to a combination of anthropogenic emissions (from domestic heating and traffic),

44

meteorological conditions and boundary layer dynamics, which collectively favour the accumulation of pollutants.

An additional comparison of the PM_{10} and NO_x data from both periods reveals a strikingly similar pattern between 00:00 and 16:00 (Figure 14). However, it can be observed that the concentrations are higher during the heating season period. While the pattern of NO_x during both periods is almost identical, the daily variation of mean concentrations of NO_x during the heating season period was significantly higher than that observed during the non-heating season period. This is due to the variability of traffic emissions and prevailing meteorological conditions, such as a lower mixing layer height [84]. The lowest concentrations of NO_x were observed during two specific periods: from 01:00 to 06:00 for the heating season period and from 00:00 to 07:00 for the non-heating season period during the morning, and from 12:00 to 19:00 for the non-heating season period during the afternoon. These periods were identified based on the presence of very low or no traffic at night-time and the dispersion of pollutants during the daytime. Subsequently, there was an observable increase in NO_x levels from 07:00 to 11:00 for both periods, as well as from 17:00 to 21:00 for the heating season period (Figure 11,13). The initial peak can be attributed to the increase in morning traffic intensity, while the subsequent peak can be attributed to the evening traffic rush hour.

Figure 10. Time variation plots to show the mean pollutant concentrations with respect to their averaging times for BC, BC_{FF} and BC_{BB} by hour of weekday, by hour, by month and by weekday for the non-heating season period.

Figure 11. Time variation plots to show the mean pollutant concentrations with respect to their averaging times for PM_{10} and NO_x by hour of weekday, by hour, by month and by weekday for the non-heating season period.

Figure 12. Time variation plots to show the mean pollutant concentrations with respect to their averaging times for BC, BC_{FF} and BC_{BB} by hour of weekday, by hour, by month and by weekday for the heating season period.
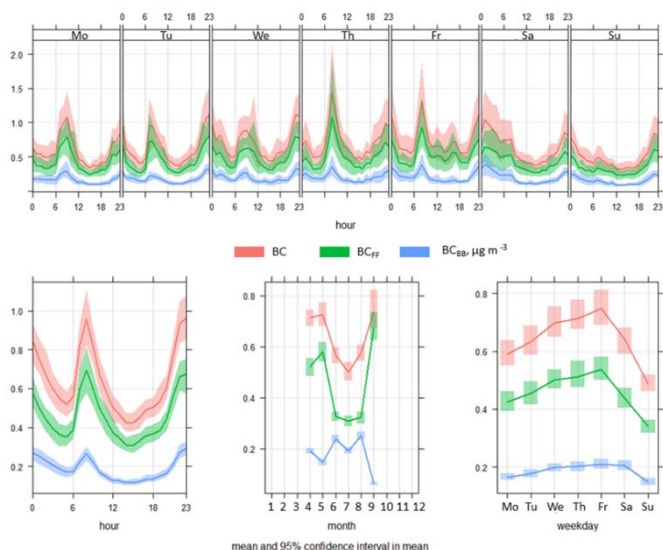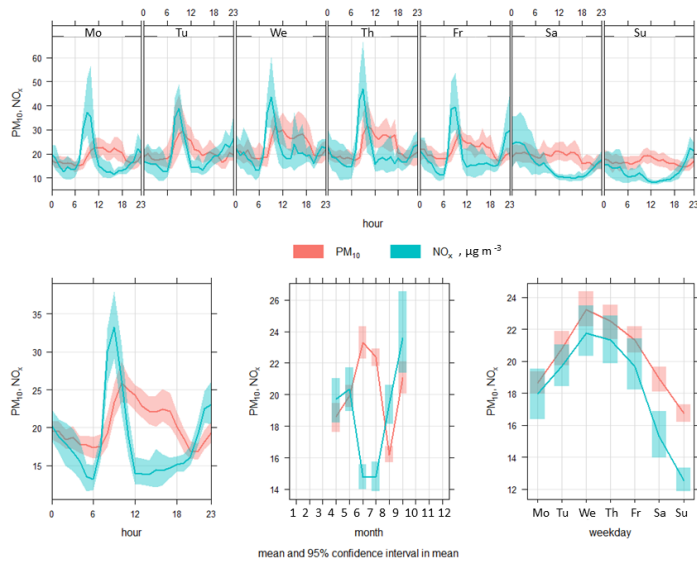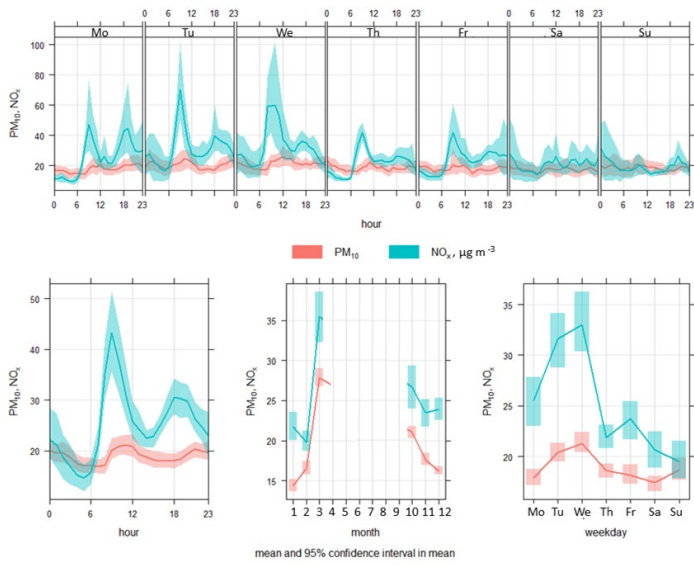
Figure 13. Time variation plots to show the mean pollutant concentrations with respect to their averaging times for PM_{10} and NO_x by hour of weekday, by hour, by month and by weekday for the heating season period.
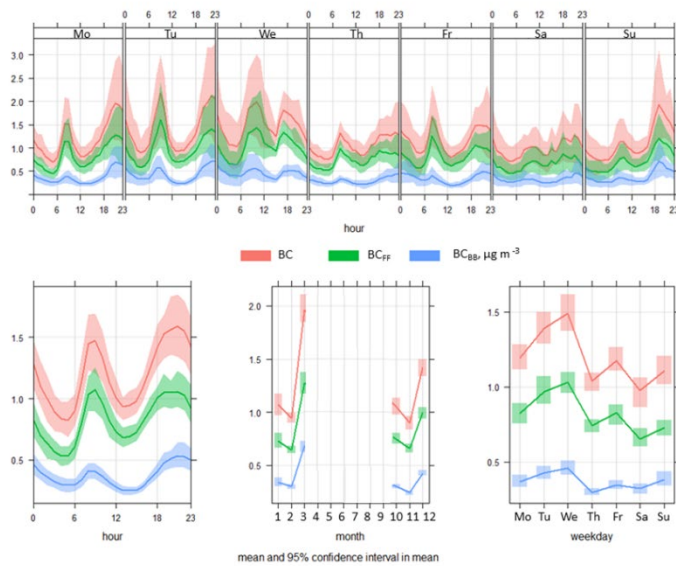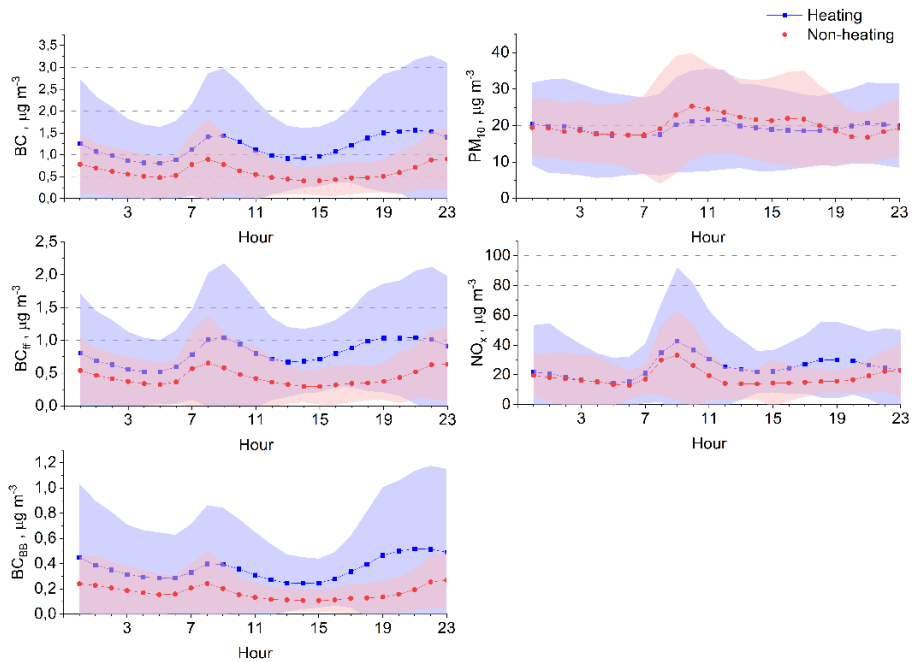

Figure 14. Diurnal variation of hourly mean concentrations of BC, BC_{FF}, BC_{BB}, PM_{10} and NO_x during the heating and non-heating season periods.

47

To evaluate the distribution and frequency of BC concentrations during the heating and non-heating season periods, histograms were analyzed. The typical patterns of BC mass concentrations during the heating and non-heating season periods, as illustrated in the histograms (Figure 15 and Table 5), indicated a lognormal distribution. The distribution of hourly concentrations across both heating and non-heating season periods was analysed using an interval of 0.25 μg m⁻³ for BC_{FF} and BC_{BB}, while 5.00 μg m⁻³ was used for PM_{10} and NO_x (Figure. 15). Fossil fuel combustion (BC_{FF}) and biomass combustion (BC_{BB}) dominated the lowest concentrations during non-heating season periods compared to heating season periods. There were more relatively clean days during the non-heating season period. This is indicated by the significantly higher frequency of low NO_x concentrations during the non-heating season period. PM_{10} concentrations show that only up to 15.00 μg m⁻³ there was a significantly higher frequency of heating season periods. As illustrated in Figure 15, the PM_{10} concentration outliers during the heating season period were observed to be below 90.00 μg m⁻³, while the outliers during the non-heating season period exhibited a concentration below 175.00 μg m⁻³.
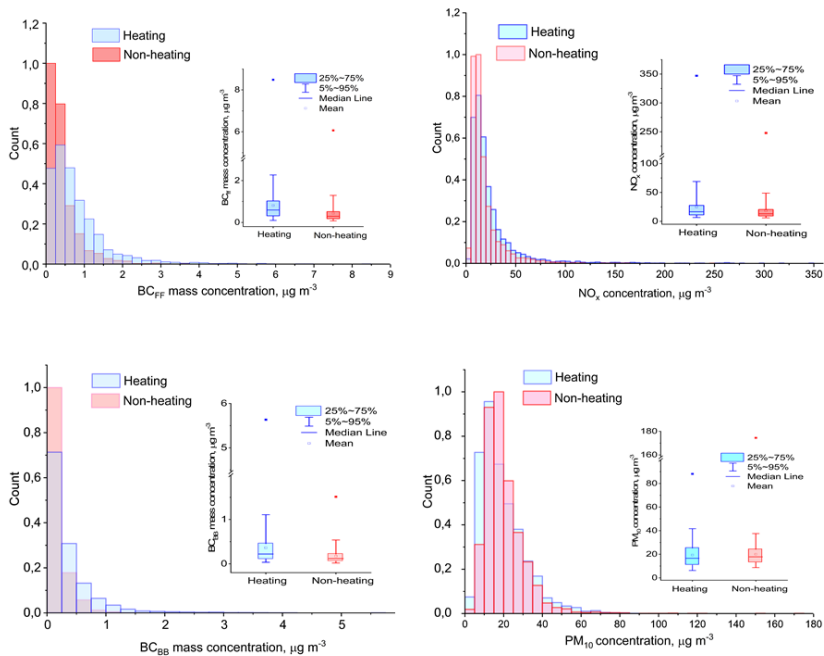
Figure 15. Histogram showing the distribution of concentrations and box plots of the hourly mean BC_{FF}, BC_{BB}, NO_x and PM_{10} concentrations during heating and non-heating season periods.

During the measurement period, three days were identified where the daily mean concentration of PM_{10} exceeded the EU air quality standard of 50.00 μg m^{-3} per 24 hours and a permitted exceedance of 35 days per year. Two of these days were observed during the heating period, while one day occurred during the non-heating period. More detailed analysis is provided in Section 3.1.5., entitled "Analysis of high BC mass concentration events".

The influence of meteorological factors must be taken into account in both heating and non-heating season periods. The descriptive statistics for the meteorological variables during the heating and non-heating season periods are presented in Table 1 of Section 2, entitled "Materials and Methods".
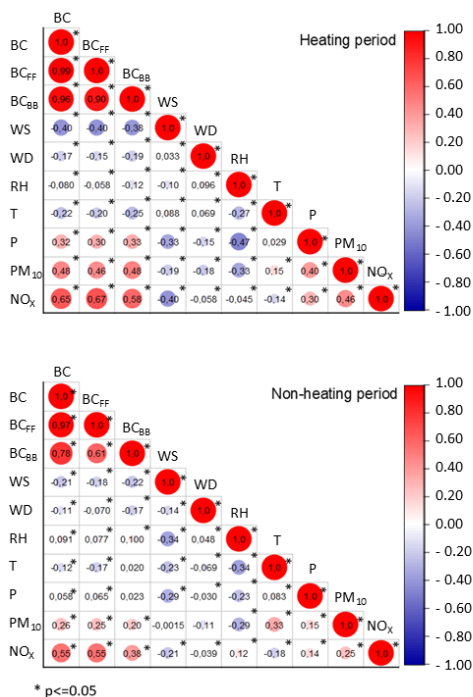
Figure 16. Correlation analysis of BC, BC_{FF}, BC_{BB}, NO_x and PM_{10} during the heating and non-heating season periods, * represent p <=0.05.

The heating season period showed a relatively strong positive correlation of BC (r=0.65) with NO_x and a moderate negative correlation between BC, BC_{FF}, BC_{BB}, NO_x and wind speed. In contrast, the non-heating season period showed a weak positive correlation between BC, BC_{FF}, BC_{BB} and PM_{10} concentrations and a moderate positive correlation between BC, BC_{FF}, BC_{BB} and NO_x concentrations. There was also a decrease in the negative correlation between BC, BC_{FF}, BC_{BB}, NO_x, PM_{10} and wind speed.

Despite the absence of a correlation between BC mass concentration and wind direction, the visualisation of mass concentration as a function of wind direction and speed using a polar plot can offer valuable insights into the spatial and temporal variability of air pollution, thereby facilitating a comprehensive understanding. Figure 17 illustrates the mean mass concentrations of BC, BC_{FF}, BC_{BB}, NO_x, and PM_{10} as a function of wind speed and direction for each period, with the use of a polar coordinate system. The colour scale indicates the mean concentration levels and intervals of wind speed (ws, m s^{-1}). During the heating season period, the polar plot for BC, BC_{FF}, BC_{BB}, NO_x and PM_{10} indicates that the sources (>2.0 µg m^{-3} for BC, >1.2 for BC_{FF}, >0.8 µg m^{-3} For BC_{BB}, 30.0 and 50.0 µg m^{-3} for PM_{10} and NO_x, a homogeneous distribution is observed around the sampling site for all wind directions and wind speeds up to 0.5 m s^{-1}. Nevertheless, it is probable that PM_{10} is emitted from additional sources in the NW direction at wind speed 3 m s^{-1} and in the SE direction at wind speed 2.5–3 m s^{-1}.

The polar plots for BC, BC_{FF}, BC_{BB}, and NO_x during the non-heating season period demonstrate that two sources exert the dominant influence. One source is local to the site, similar to that observed during the heating season period, while the other originates from a SW-SE direction. The highest concentrations of BC (exceeding 0.70 µg m^{-3}) were observed at the lowest wind speeds on calm days, indicating the presence of localised emissions distributed around the site and at wind speeds above 2.5 m s^{-1}. In contrast, the distribution of the PM_{10} source during the non-heating season period is not uniform around the site. In addition, a further source from the north-east is present, with a wind speed of between 3 and 3.5 m s^{-1}.
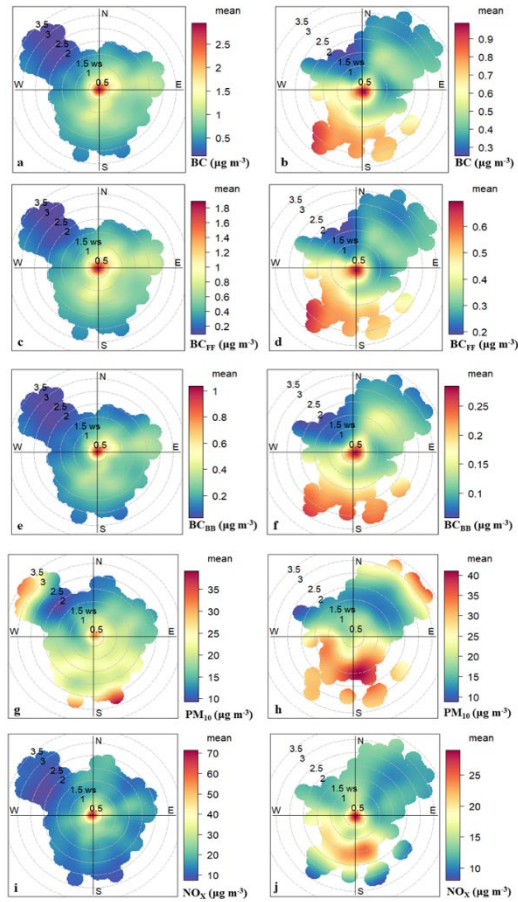
Figure 17. Polar plots of BC, BC_{FF}, BC_{BB}, PM_{10} and NO_x mass concentration as a function of wind speed and direction for heating (a, c, e, g, i) and non-heating season periods (b, d, f, h, j).

3.1.3. Temporal dynamics BC mass concentration throughout the seasons

The variability in BC mass concentrations underscores the intricate interconnections between emission sources, meteorological conditions, and human activities in urban settings. The concentration levels of BC tend to be higher during the winter months (1.14 µg m^{-3}) compared to the summer months (0.55 µg m^{-3}) (Table 6). This phenomenon can be attributed to increased biomass burning for the purpose of heating and the lower temperatures (Table 4, Figure 6). A comparable pattern was identified in Zhengzhou, China, and Madrid, Spain) [15,37].

Table 6. Descriptive statistics of BC, BC_{FF}, BC_{BB} (µg m⁻³) and BC_{BB}/BC ratio for the seasons and year.

Season		BC	BC_{FF}	BC_{BB}	BC_{BB}/BC, %	BC_{FF}/BC, %
Summer	Mean (SD)	0.55 (0.41)	0.32 (0.24)	0.23 (0.18)	41	59
	Median	0.42	0.25	0.17	41	59
	Min; Max	0.01; 3.43	0.01; 1.94	0.01; 1.51	6; 81	19; 94
Autumn	Mean (SD)	0.92 (0.83)	0.69 (0.61)	0.23(0.26)	23	77
	Median	0.71	0.54	0.15	25	75
	Min; Max	0.04; 6.62	0.03; 5.54	0.01; 2.40	2; 51	50; 100
Winter	Mean (SD)	1.14 (1.15)	0.78 (0.76)	0.35 (0.42)	30	70
	Median	0.84	0.59	0.23	29	71
	Min; Max	0.04; 12.33	0.03; 8.48	0.01; 5.64	3; 56	44; 97
Spring	Mean (SD)	1.05 (1.23)	0.75 (0.82)	0.31 (0.45)	26	74
	Median	0.60	0.46	0.14	24	76
	Min; Max	0.05; 9.01	0.04; 6.85	0.02; 3.84	5; 55	45; 95
Annual	Mean (SD)	0.89 (0.99)	0.63 (0.67)	0.27 (0.35)	29	71
	Median	0.58	0.41	0.15	28	69
	Min; Max	0.01; 12.33	0.01; 8.48	0.01; 5.64	2.00; 100.00	15; 97

This is reflected in the highest concentrations of biomass burning BC_{BB} being observed in winter (0.35 µg m^{-3}) and the lowest in autumn (0.23 µg m^{-3}). It is noteworthy that the concentration of BC_{FF} is also highest in winter (0.78 µg m^{-3}) in comparison to other seasons (Figure 18). In the spring season, particularly in March, grass burning can significantly contribute to elevated levels of air pollutants, including BC, by long-range transport from neighbouring regions, especially non-European countries [81–83]. This is corroborated by the presence of active fire detections in the FIRMS MODIS database and NAAPS model results, which indicate higher concentrations of smoke during March (see Section 4.1.5. Analysis of high BC mass concentration events). Across the seasons, the mean proportion of BC_{BB} in BC_{total} exhibited considerable variation, ranging from 23% to 41%. The highest contribution of BC_{BB} (41.0%) was observed in summer, while the lowest was observed in autumn (23%). Winter and spring levels were comparable, accounting for 30.0% and 27.0%, respectively.
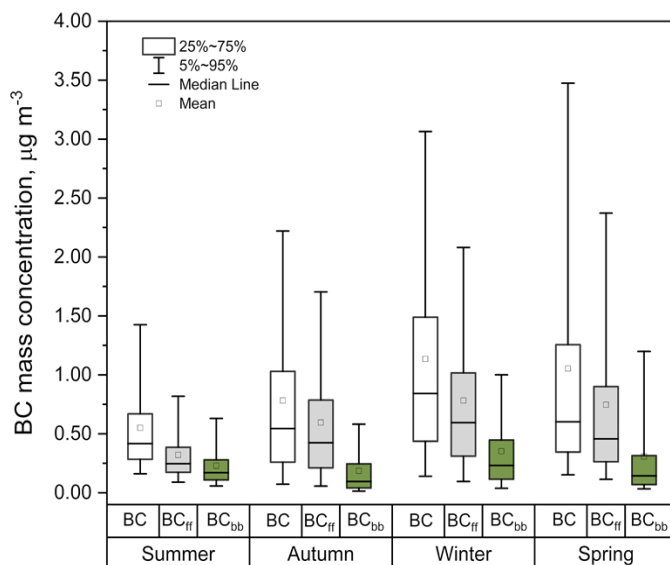
Figure 18. Seasonal mass concentrations of BC, BC_{FF} and BC_{BB} in µg m^{-3} in Vilnius during the study period. The range of the box depicts the bounds of the 25th and 75th percentiles of the data, while the whiskers extending from the box represent the bounds of the 5th and 95th percentiles, the colour of the box is white for BC, grey for BC_{FF} and green for BC_{BB}.

The highest levels of BC mass concentration were recorded on Friday for the summer and autumn seasons, reaching 0.66 and 0.88 µg m^{-3}, respectively,

on Wednesday in the winter season with a BC mass concentration of 1.66 µg m^{-3}, and on Tuesday in the spring season with a BC mass concentration of 1.33 µg m^{-3}. In contrast, the lowest level of BC mean mass concentration was observed on Sunday for the summer, autumn and spring seasons, with values of 0.41 µg m^{-3}, 0.70 µg m^{-3} and 0.81 µg m^{-3}, respectively. In the case of the winter season, the lowest concentration was observed on Saturday, with a value of 0.77 µg m^{-3}. The weekly BC mass concentrations exhibited a discernible increase over the course of weekdays (Monday to Friday), while showing a marked decline on weekends (Saturday and Sunday) attributable to human activities. Such patterns were also discernible in other studies [30,41].

In order to gain insight into the temporal variability of source-apportioned BC, the diurnal profile and frequency distribution of BC$_{FF}$ and BC$_{BB}$ mass concentrations during different seasons were analysed. As illustrated in Figure 5, the daily cycles of BC$_{FF}$ and BC$_{BB}$ in all four seasons exhibited comparable patterns of variation. The morning peaks were observed consistently between 07:00 and 09:00 during the spring and summer seasons, while those in the winter and autumn seasons occurred slightly later, between 08:00 and 11:00. Additionally, an evening peak was observed in all four seasons. It is noteworthy that the transition from winter to summer time has an impact on the timing of the peak occurrence.

Histograms were constructed to provide a quantitative representation of the variability in BC concentration values across the four seasons, thus offering insights into the fluctuations in emissions associated with biomass combustion and transportation (Figure 19). The summertime frequency distribution of BC$_{FF}$ mass concentration was relatively narrow, up to a maximum of 0.4 µg m^{-3}, with a typical single-peak distribution pattern when biomass burning activities are less prevalent. In contrast, the higher BC$_{FF}$ frequencies during autumn and winter are below 1 µg m^{-3}.
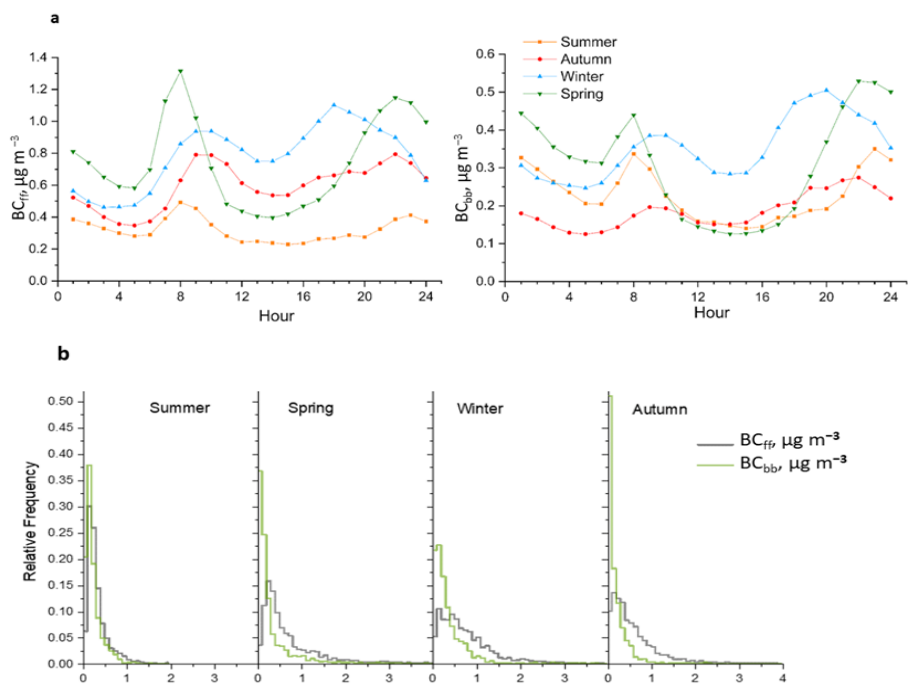
Figure 19. Diurnal variation (a) and histogram of relative frequency(b) BC_{FF} and BC_{BB} during the four seasons.

The behavior, transport and distribution of aerosol particles are subject to significant influence from weather conditions and atmospheric dynamics. The formation and subsequent growth, dispersal, transformation and deposition of aerosols are all influenced by meteorological factors including wind patterns, temperature, humidity and atmospheric stability. Subsequently, the potential influence of wind patterns on the concentration of BC will be discussed in greater detail. A combination of wind direction and polar CPF analysis can provide a more detailed understanding of source location and characteristics on a local scale. It is essential to consider the relationship between pollutants transported from other regions and those generated locally. The mean concentration of BC is higher in the autumn and winter seasons, as well as in instances where wind speeds are below 0.5 m s^{-1}.

In order to study the possible influence of near emission sources, data were represented as a percentile rose plot of BC concentrations. The percentile intervals are presented in colour according to the direction of the wind. The percentile rose of BC indicates the direction of origin of high concentrations at each season. The graph demonstrates high variability in the sources of these pollutants. The characteristics observed in the four seasons are similar. In

contrast to autumn, spring and summer, where high concentrations originate from multiple directions, winter shows a concentration of high concentrations from the SW, W, and NW. The situation for autumn and winter displays exhibits similarities with the 99th and 99.9th percentiles from north-west directions.

3.1.4. Multifaceted analysis of BC mass concentrations through conditional probability functions

A common approach to identifying the sources of atmospheric pollutants is through the application of the CPF. This approach provides directional information concerning the major sources of these pollutants, indicating which wind directions and wind speeds are associated with the highest concentrations. Additionally, the probability of these concentrations occurring can be determined. The highest concentrations (95th percentile BC concentration: 1.4 μg m^{-3}, 2.2 μg m^{-3}, 3.4 μg m^{-3}, and 3.5 μg m^{-3} for summer, autumn, winter, spring, respectively) demonstrate one local source exert the dominant influence (Figures 20-23e). It was found that the 75th percentile BC concentration in autumn demonstrated one additional source in the S direction at wind speeds of between 1 and 3 m s^{-1} (Figure 21e). The 25th percentile BC concentration (0.28 μg m^{-3}, 0.29 μg m^{-3}, 0.46 μg m^{-3}, and 0.34 μg m^{-3} for summer, autumn, winter, and spring, respectively) suggests the probability of low concentration locally and the presence of multiple sources in all directions (Figure 20-23d). The situation for autumn and winter displays commonalities, and the greatest probability is observed in the NE, E, SE, S and SW directions. An analysis of Figures 24-25 indicates that NO$_x$ has a local source in all seasons, while PM$_{10}$ can originate from the north-east and north-west directions in the spring (at wind speeds of 2.5 m s^{-1}) and from the south (at wind speeds of 1-1.5 m s^{-1}).

The pollution rose plot illustrates the wind directions that contribute the most to overall concentrations, as well as providing information on the varying concentration levels. The graph illustrates that, across all four seasons, the northwest direction consistently exhibits the greatest concentration of pollutions (BC, NO$_x$ and PM$_{10}$) (Figure 20-25c), with the northeast also demonstrating prominence during the summer months. In contrast, the south and southeast emerge as the dominant pollution sources during the autumn and winter seasons.
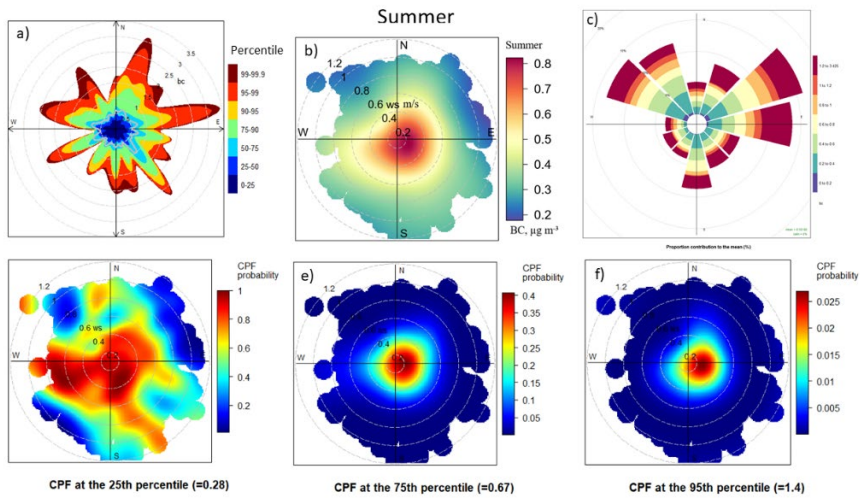
Figure 20. A percentile rose plot of BC mass (a), a polar plot of BC mass concentrations(b), pollution rose showing which wind directions contribute most to overall mean BC concentrations (c), conditional probability function of 25th percentile of BC (d), conditional probability function of 75th percentile of BC (e), conditional probability function of 95th percentile of BC (f) for summer season.
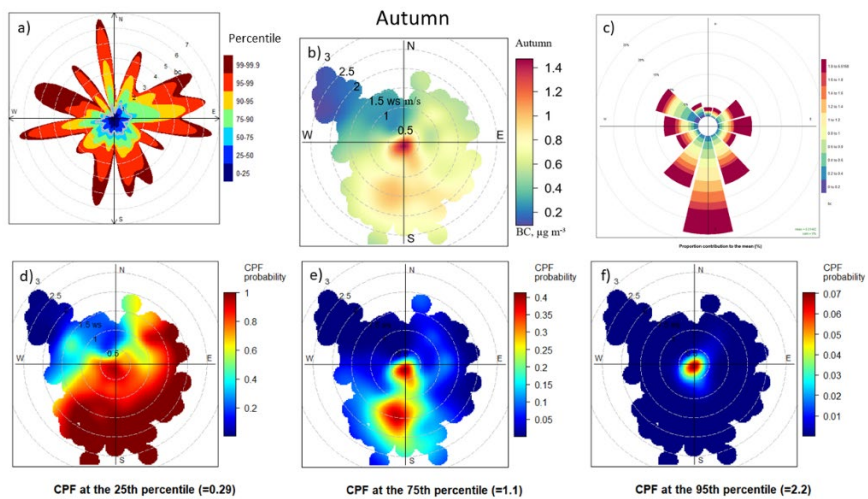
Figure 21. A percentile rose plot of BC mass concentrations (a), a polar plot of BC mass concentrations(b), pollution rose showing which wind directions contribute most to overall mean BC concentrations (c), conditional probability function of 25th percentile of BC (d), conditional probability function of 75th percentile of BC (e), conditional probability function of 95th percentile of BC (f) for autumn season.
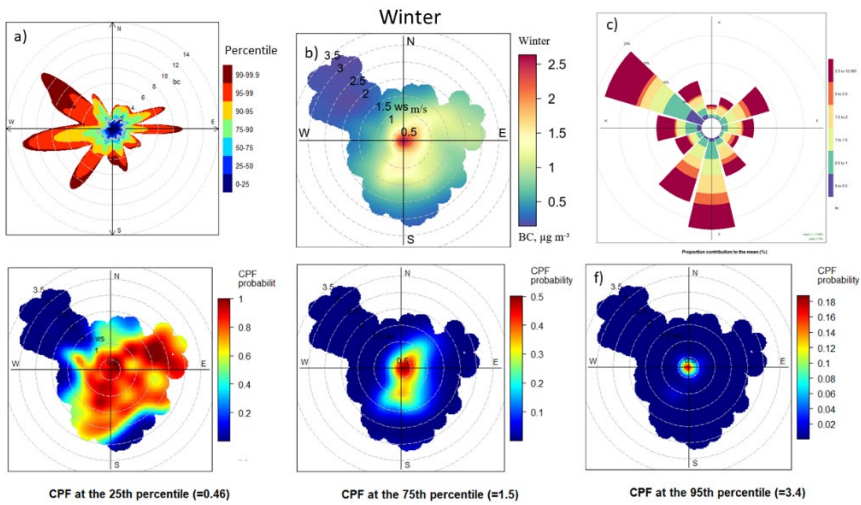
Figure 22. A percentile rose plot of BC mass concentrations (a), a polar plot of BC mass concentrations(b), pollution rose showing which wind directions contribute most to overall mean BC concentrations (c), conditional probability function of 25th percentile of BC (d), conditional probability function of 75th percentile of BC (e), conditional probability function of 95th percentile of BC (f) for winter season.
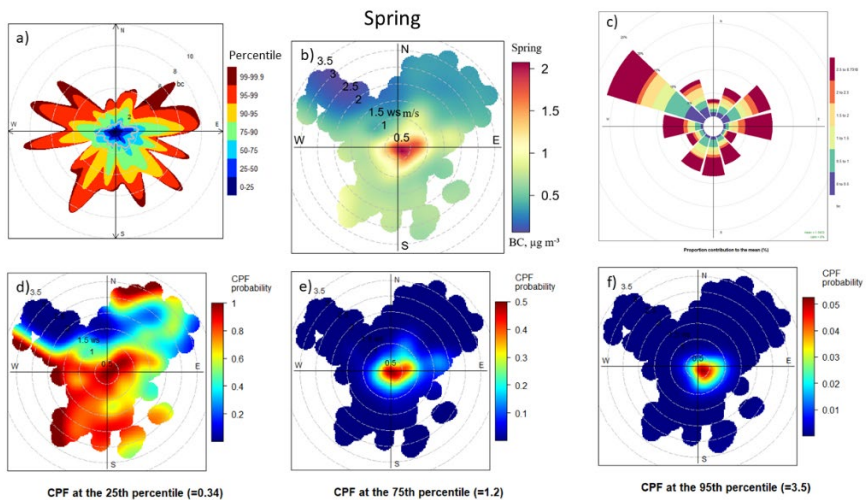
Figure 23. A percentile rose plot of BC mass (a), a polar plot of BC mass concentrations(b), pollution rose showing which wind directions contribute most to overall mean BC concentrations (c), conditional probability function of 25th percentile of BC (d), conditional probability function of 75th percentile of BC (e), conditional probability function of 95th percentile of BC (f) for spring season.
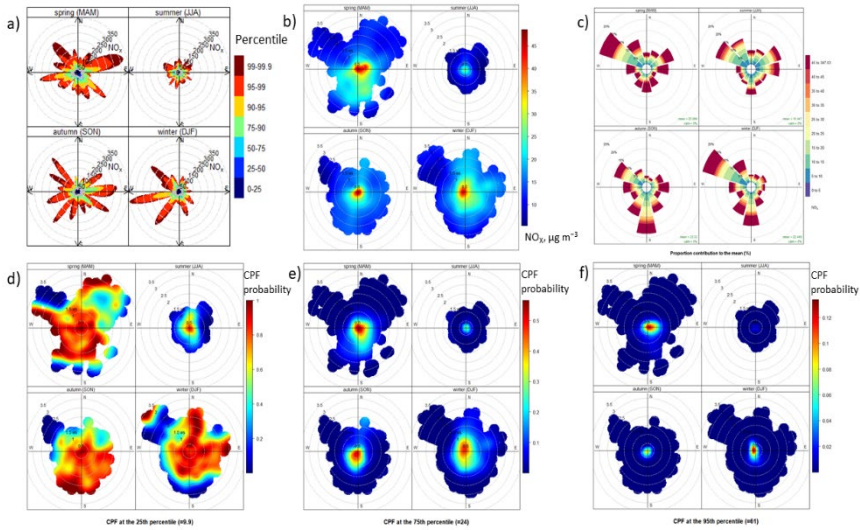
Figure 24. A percentile rose plot of BC mass concentrations(a), a polar plot of NO_x mass concentrations (b), pollution rose showing which wind directions contribute most to overall mean NO_x concentrations (c), conditional probability function of 25th percentile of NO_x (d), conditional probability function of 75th percentile of NO_x (e), conditional probability function of 95th percentile of NO_x (f) during the year.
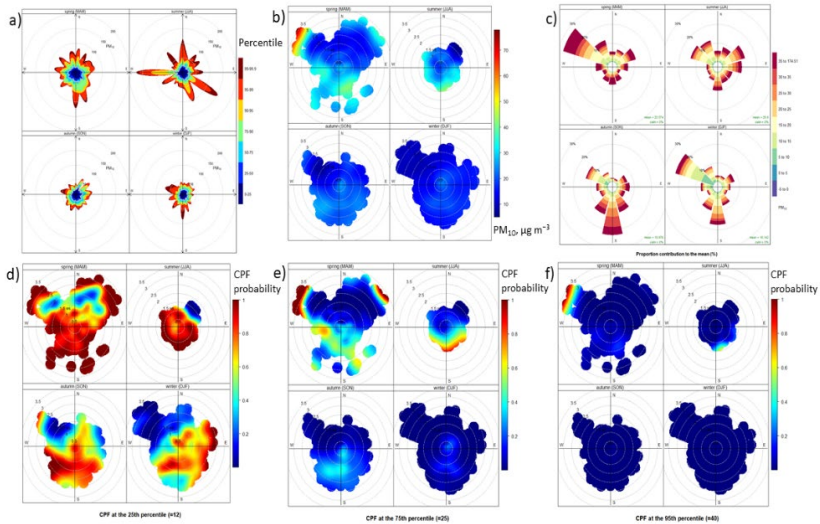
Figure 25. A percentile rose plot of BC mass concentrations(a), a polar plot of PM_{10} mass concentrations (b), pollution rose showing which wind directions contribute most to overall mean PM_{10} concentrations (c), conditional probability function of 25th percentile of PM_{10} (d), conditional

probability function of 75th percentile of PM_{10} (e), conditional probability function of 95th percentile of PM_{10} (f) during the year.

Matrices of the Pearson correlation coefficients and dendrogram between air pollutants, specifically BC, PM_{10} and NO_x, and meteorological parameters, namely WS, WD, RH, T and P, for the summer, autumn, winter and spring seasons are presented in Figure 26. It can be observed that the correlation between BC and other parameters varies depending on the season. The results demonstrate that BC, BC_{FF}, BC_{BB} and NO_x are consistently positioned within the same cluster, exhibiting moderate to strong correlation (ranging from r=0.48 to r=0.65). Conversely, PM_{10} in summer is situated in a disparate cluster and displays a markedly weak correlation with BC and its components. However, during other seasonal periods, the correlation varies from weak to moderate (ranging from r=0.38 to r=0.53).
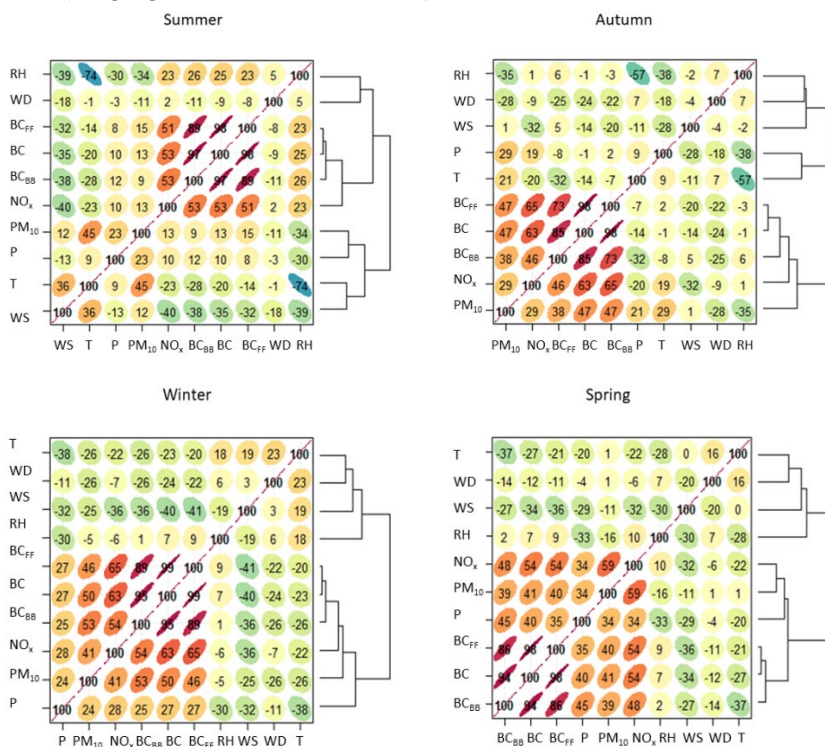
Figure 26. Correlation matrix plot and dendrogram representing associations between various air pollutants (BC, PM_{10}, NO_x) and meteorological parameters (WS, WD, RH, T, P) for summer, autumn, winter and spring. The colour, represents the strength of the relationship between each pair of parameters.

The dendrogram illustrates that, with the exception of pressure, all meteorological parameters are consistently grouped together. Pressure, however, is typically isolated and only during the autumn months is it observed to be included in the same cluster as the other meteorological parameters. A correlation matrix reveals the following patterns. In summer, BC is most strongly correlated with wind speed; in autumn, with wind direction and temperature, particularly for BC_{BB}; in winter, a correlation exists with all meteorological parameters, but the strongest is between wind speed and BC and BC_{FF}; in spring, the main correlation is with pressure, wind speed and temperature. Furthermore, temperature exhibits a stronger correlation with BC_{BB}, while wind speed shows a stronger correlation with BC and BC_{FF}.

3.1.5. Analysis of high BC mass concentration events

As evidenced in the preceding sections of this study, the seasonal variation can be discerned not only in meteorological conditions but also in the mean concentration of BC and in the ratio of source apportionment. As a consequence, the data from each season was subjected to separate analysis, resulting in the identification of 18 days with elevated levels of BC mass concentration exceeding the 95th percentile of concentrations recorded for the respective season. These are indicated in Figure 27. In particular, a total of five cases occurred during the summer months (June 12, June 23, June 30, July 16 and August 23), four cases in the autumn (October 8 to 10 and November 11), five in the winter (December 23, December 31, January 10, January 12 and January 23) and four in the spring (March 14 to 15 and March 22 to 23, which also could be regarded as two cases, each lasting for two consecutive days). Additionally, it was noted that these days frequently coincided with elevated concentrations of PM_{10} and NO_x. A comparison of the contribution of these days to annual concentrations with non-pollution days revealed increases of 9.9%, 10.5% and 12.5% for BC, BC_{FF} and BC_{BB} concentrations, respectively, and 3.5% and 6.9% for PM_{10} and NO_x. Figure 28 illustrates that the concentrations of BC, PM_{10} and NO_x on the high-pollution days were approximately twice as high as on days of minimal pollution. On the non-pollution days, the mean concentrations of BC, PM_{10} and NO_x were 0.81, 19.02 and 20.21 µg m^{-3}, respectively. In contrast, on the high-pollution days, these values increased to 2.38, 32.17 and 48.56 µg m^{-3}, representing a threefold increase in BC and a 2.4-fold increase in NO_x.
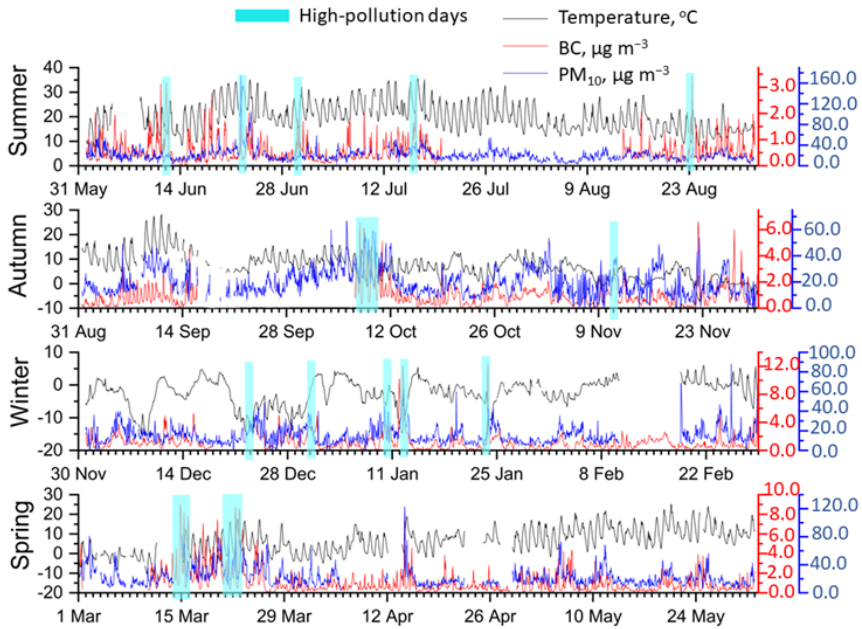
Figure 27. The time series of BC, PM$_{10}$ and air temperature during the four seasons with pronounced days of high air pollution (blue rectangles—periods with hourly BC mass concentration exceeding the 95th percentile of the BC concentration for the respective season).
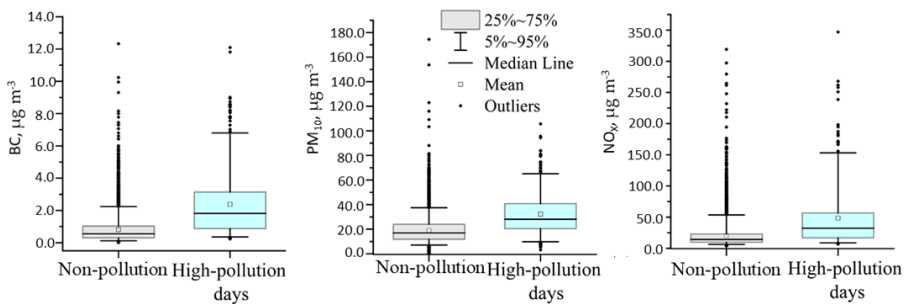
Figure 28. The comparison of BC, PM$_{10}$ and NO$_x$ concentrations on non-pollution and high-pollution days.

The underlying causes of increased concentrations and the occurrence of high-pollution days fluctuate depending on the season. The investigation of the interrelationship between BC concentrations, meteorological variables, NO$_x$ and PM$_{10}$ during high-pollution and non-pollution days provides valuable insights into the factors influencing the variability of air quality across all seasons.

A negative correlation (from −0.43 to −0.54) between WS and BC concentrations was observed during the high-pollution days, with the exception of the winter season. This indicates an inverse relationship between higher WS and lower BC levels. During the winter season, the data demonstrate a relationship between calm winds coming from the south and higher levels of BC (r = 0.56). In the winter season, a positive correlation was observed between BC and PM_{10} (ranging from 0.26 to 0.57) and NO_x (ranging from 0.60 to 0.87) on 80% of high-pollution days. Conversely, a negative correlation was noted between PM_{10} (ranging from -0.11) and NO_x (ranging from -0.29) on 20% of high-pollution days. During this period, there is also a difference in the correlation with WD, which ranges from negative (from -0.39 to -0.82) to positive (from 0.51 to 0.81). In the summer season, a weak positive correlation was observed in 60% of cases between BC and PM_{10} (ranging from 0.09 to 0.18), while in 40% of cases, a strong positive correlation was evident between PM_{10} and BC (ranging from 0.45 to 0.57). In the summer season, a distinction was also observed in the correlation with WD, with 80% exhibiting a negative correlation (ranging from -0.21 to -0.39) and 20% displaying a positive correlation (0.38).

Among the days with the highest levels of pollution during the summer months, one that recurs with regularity is 23–24 June. This date coincides with St. John's Day (Midsummer) in Lithuania, and is characterised by elevated concentrations of pollutants in the atmosphere. On this day, the air in Lithuania and some neighbouring countries becomes markedly polluted as a result of the burning of wood in open bonfires. In comparison to preceding and subsequent days, a twofold increase in both BC and BC_{BB} concentrations was observed on 23–24 June. A more detailed description can be found in the paper by Minderytė et al. (2023) [73]. The effects of relative humidity and temperature were significant only during the summer and spring periods, and their impact was more than twice as strong on days with high levels of pollution. However, their association with PM_{10} differed if they increased during the summer and decreased during the spring. In the autumn season, only 50% of the cases exhibited a strong correlation between BC and PM_{10} (0.64) and WD (−0.53). In the remaining 50% of cases, no correlation was observed between BC and PM_{10} (0.12) and WD (−0.19). Previously identified occurrences of spring season high-pollution days were found to be associated with illegal land clearing through grass burning in the Kaliningrad region, Ukraine and Belarus [82,83]. This hypothesis is supported by the presence of data indicating the occurrence of smog and active fires during this period. Figure 29 depicts a representative example of spring grass burning, which was observed on 22 March 2022. As evidenced by the smoke forecast from the

Navy Aerosol Analysis and Prediction System (NAAPS), plumes from the wildfires reached the study area (http://www.nrlmry.navy.mil/aerosol, accessed on 05/05/2024; see Figure 29c).
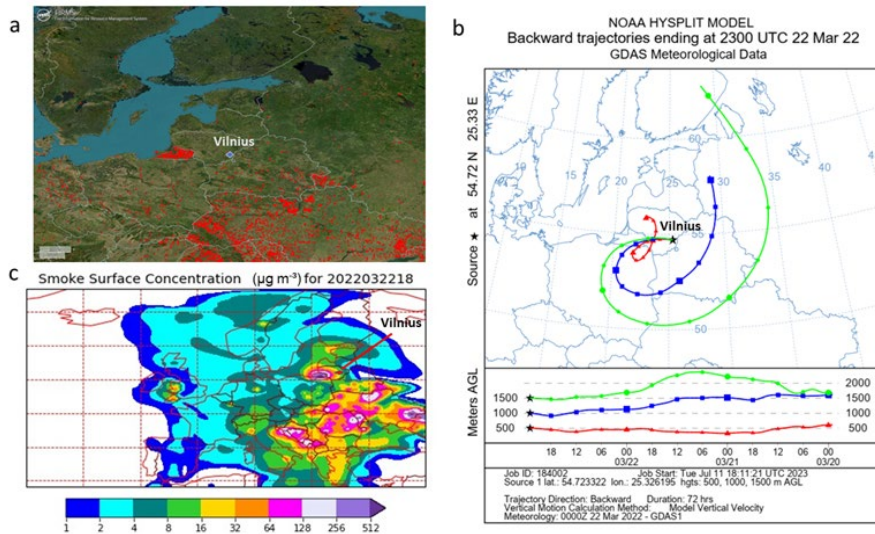
Figure 29. Case of spring grass burning observed on 22 March, 2022: (a) active fires (red dots) detected during March 2022 by the MODIS Rapid Response System (each red dot represents a single 1 km MODIS active fire pixel); (b) HYSPLIT back-trajectories of air masses arriving at Vilnius on 22 March 2022 at 500 m (red), 1000 m (blue) and 1500 m (green); (c) smoke surface concentration ($\mu g \, m^{-3}$).
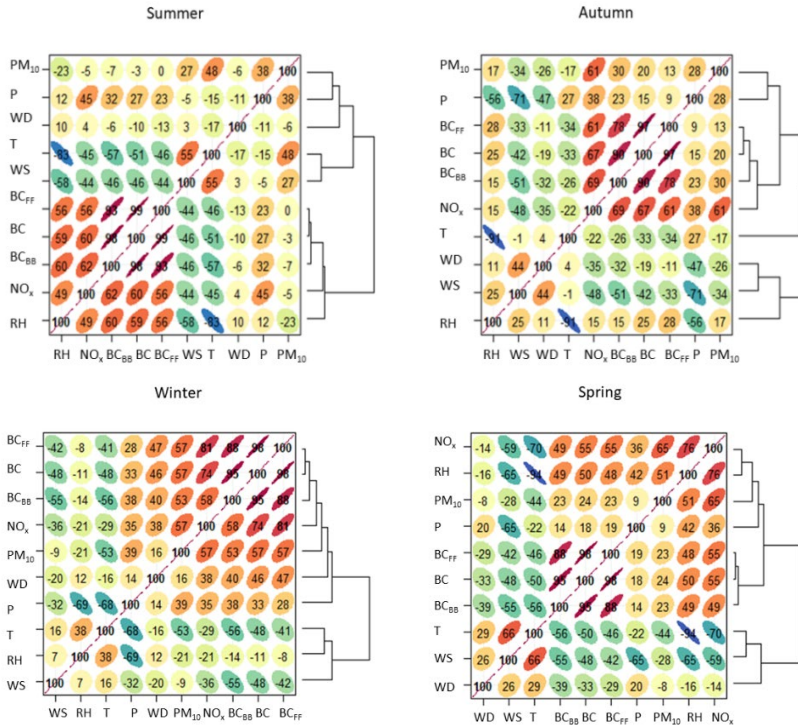
Figure 30. Correlation matrix plot and dendrogram representing associations between various air pollutants (BC, PM_{10}, NO_x) and meteorological parameters (WS, WD, RH, T, P) for high-pollution days. The colour, represents the strength of the relationship between each pair of parameters.

A comparison of the correlation matrix and the dendrogram of non-polluted (Figure 26) and polluted days (Figure 30) reveals a notable strengthening of correlations and a transformation in the clustering of the data. A stronger negative correlation was identified between BC and meteorological parameters, specifically wind speed and temperature, across all seasons. This finding implies an inverse relationship where higher WS is associated with lower BC levels and low air temperature is associated with higher BC levels. The correlation between BC and wind direction was stronger on special days in the winter and spring seasons. The spring season should be considered separately, as it exhibited an atypical pattern. In spring, the correlation between BC and NO_x remained the same, while that with PM_{10} decreased. It is also the only season where the correlation of BC with pressure on special days was significantly weaker than on usual days. Winter is the only season where the correlation with humidity shifted from weakly positive to weakly negative.

3.2 Indoor-Outdoor relationships of BC

To assess the impact of outdoor particulate pollution on indoor air quality, BC mass concentrations and source apportionment were studied indoors and outdoors. The infiltration factor (F_{inf}) was low (F_{inf}~0.03). The infiltration factor can be interpreted as the fraction of ambient particles that penetrate indoors and remain airborne [85]. This suggests that the three-stage building filter system (G4-F7-F9) offers effective protection against particle pollution from various sources and considerably decreases indoor exposure to PM_1. The mean BC mass concentration was 1.20 ± 0.97 µg m^{-3}. A relatively good correlation was found between the mass concentration of indoor and outdoor air r= 0.8, indicating a significant contribution of outdoor air pollution to indoor air. The average concentration of BC in indoor air is significantly lower, with values of 0.04 ± 0.03 µg m^{-3}. The measurement results indicate that indoor BC concentrations were $96 \pm 4\%$ lower than outdoor concentrations. To enhance comprehension of the association between BC and high pollution episodes, a comparison was made between the concentrations during the most polluted days ($PM_1 > 25$ µg m^{-3}) and the less polluted days ($PM_1 < 10$ µg m^{-3}). PM_1 concentration was determined by adding the concentrations of sulfate, nitrate, organic compounds, and BC. On polluted days, outdoor mass concentrations of BC increased by 3-4 times compared to clean days. However, indoor concentrations remained low and all PM_1 species showed only a small increase in absolute mass concentration (two-fold for BC). These results suggest that indoor BC peak concentrations are significantly lower than outdoor concentrations.

The indoor/outdoor concentration (I/O) ratio was used to investigate the relationship between indoor and outdoor BC concentration and the filtration efficiency of a mechanical ventilation system. When an indoor source is absent, the I/O ratio serves as a proxy for outdoor particle infiltration. However, this ratio may be influenced by both indoor emission sources and additional BC loss processes, including deposition and evaporation. The infiltration factor indicates the fraction of outdoor particles that penetrate indoors and remain in the air. The F_{inf} values were estimated using a linear regression method, with the slope corresponding to the infiltration coefficient and the intercept interpreted as an indicator of the source of indoor emissions [85]. The F_{inf} values in BC were 0.8, which is consistent with the results of a previous study by Singer et al. [86]. The BC intercept (0.01) was low, indicating that there were no indoor sources of these species. The median I/O ratios of BC (0.03) and F_{inf} are found to be within the same range (Table 7).

Table 7. Summary of concentrations (µg m^{-3}, SD), relative contributions (%, SD), and infiltration parameters of BC in indoor and outdoor environments.

	Outdoor		Indoor		I/O	F$_{inf}$
	Conc., µg m^{-3}	Contribution, %	Conc., µg m^{-3}	Contribution, %		
BC (SD)	1.20 (0.97)	8	0.04 (0.03)	5	0.03	0.027
BC$_{FF}$ (SD)	0.97 (0.79)	81	0.008 (0.008)	79	0.03	0.027
BC$_{BB}$ (SD)	0.23 (0.20)	19	0.030 (0.025)	21	0.03	0.032

For office buildings, a supply air filter with an efficiency of at least F7 (50-56% for PM$_1$) is generally recommended. However, a study by Singer et al. [86] found that a mechanical ventilation system without improved filtration (< F9) had capture efficiencies of 70%, 80% and 40% for PM$_{2.5}$, 6-100 nm and BC particles, respectively. In a modern office, the personal exposure of workers to outdoor particles is likely to be greater than that presented in this study, thus leading to the conclusion that a mechanical ventilation system with enhanced filtration (F9) represents the optimal solution for enhancing indoor air quality. Previous studies have demonstrated that higher temperature and lower relative humidity indoors during the winter period were significant contributors to the loss of PM mass [87]. The I/O ratios of BC demonstrate consistent performance along with gradients in T and RH, as illustrated in Figure 31.
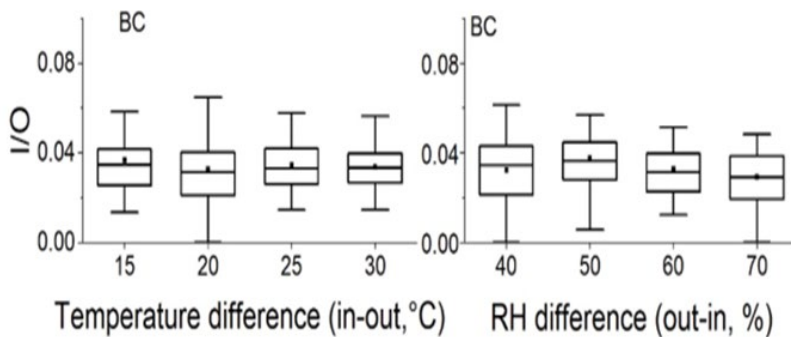
Figure 31. The impact of differences in temperature and relative humidity on I/O ratios of BC.

The statistical data on meteorological parameters for outdoor and indoor conditions can be found in Table 8. The outdoor air temperature during the measurement period ranged from -22.2 to 14.4^0C. Wind speed was recorded at a range of 0 to 12 m s^{-1}. The indoor temperature exhibited a narrow range of variation, from 21.4 to 25.5^0C. The RH differed significantly between the indoor and outdoor environments, with an average of 25.7% in the indoor environment and 91% in the outdoor environment.

Table 8. Descriptive statistics of meteorological parameters outdoors and indoors.

	Average	SD	Min	Max
Indoor temperature, ºC	22.5	0.3	21.4	25.5
Outdoor temperature, ºC	0.2	6.4	-22.2	14.4
Indoor relative humidity, %	25.7	7.0	8.0	45.0
Outdoor relative humidity, %	91.9	8.3	40.0	100.0

Figure 32 illustrates the fluctuations in the hourly averaged BC_{FF} and BC_{BB} mass concentrations, as well as the contribution of source-specific BC components, both outdoors and indoors. The concentration of BC_{FF} and BC_{BB} outdoors ranged from 0.03 to 7.25 µg m^{-3} (with an average of 0.97 ± 0.79 µg m^{-3}) and 0.03 to 2.13 µg m^{-3} (with an average of 0.23 ± 0.20 µg m^{-3}), respectively. The proportion of BC_{BB} in total BC was 19%. The concentration of BC_{FF} and BC_{BB} in indoor air was found to vary between 0.09 and 0.21 µg m^{-3} and between 0.02 and 0.09 µg m^{-3}, respectively. As illustrated in Figure 32, BC_{BB} was found to contribute approximately 20% to the total concentration of BC in indoor and outdoor air. The fraction of BC_{FF} was found to be significantly higher (80%) than that of BC_{BB}, indicating that during the heating season, fossil fuel combustion is the primary contributor to BC mass concentration in Vilnius. The measured outdoor BC concentrations in Vilnius were comparable or lower than those observed in other European sites (Table 1, Table 2).
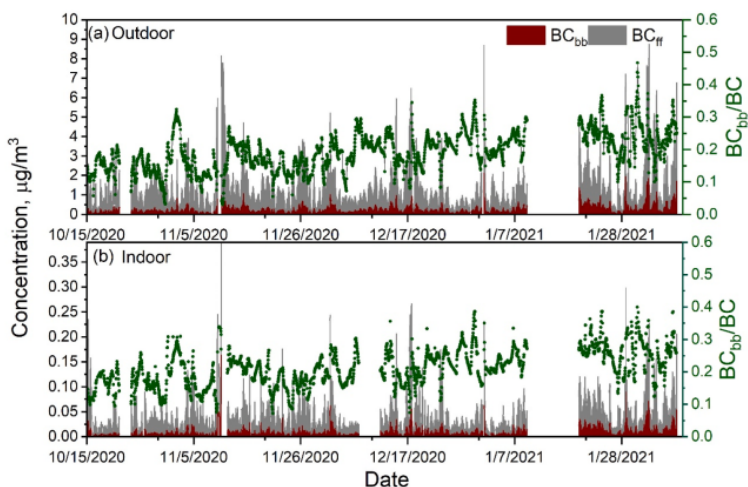
Figure 32. BC_{FF} and BC_{BB} concentration and BC_{BB}/BC ratios in outdoor (a) and indoor (b) samples.

Figure 33 presents the daily profiles of source-specific BC components (BC_{FF} and BC_{BB}) for hourly averaged indoor-outdoor pollutant concentrations. The traffic-related bimodal diurnal profile of BC_{FF} was characterised by concentrations peaking during the morning (1.12 µg m^{-3}) and evening rush hours (1.50 µg m^{-3}) (Figure 32a). In contrast, the diurnal variability of BC_{FF} concentration on weekends was not very pronounced and exhibited a unimodal pattern. The concentration of BC_{FF} increased during the day on weekends, reaching slightly higher concentrations of 0.98–1.50 µg m^{-3} from 10:00 a.m. to 8:00 p.m.
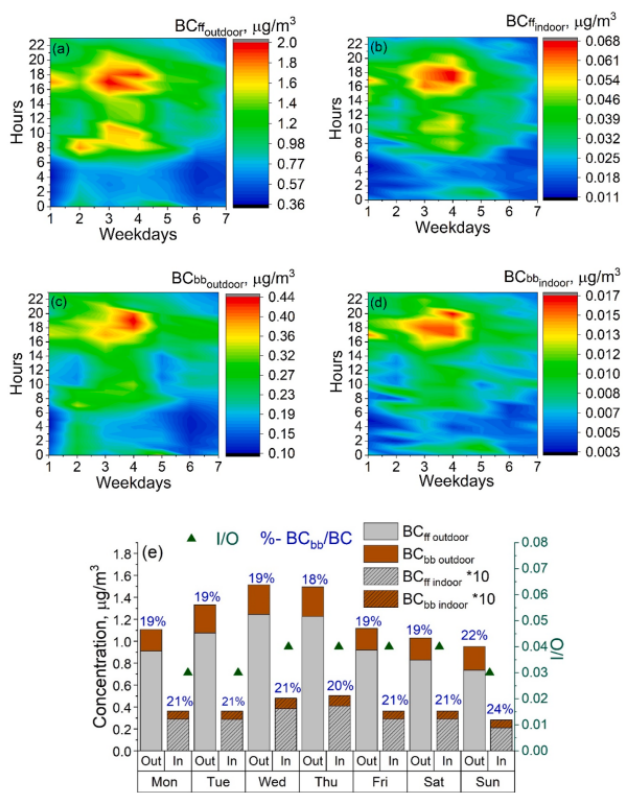
Figure 33. Daily profiles of BC_{FF} (a,b) and BC_{BB} (c,d) indoors and outdoors during the week. Weekly profile of indoor and outdoor BC_{FF} and BC_{BB} concentrations and I/O ratios (e). The green triangles represent the I/O ratios, and the BC_{BB} / BC ratios (%) are indicated in blue.

A comparable weekly BC_{FF} diurnal profile was observed indoors, with morning rush hour peaks being less pronounced than those observed outdoors (Figure 32b). In contrast, the diurnal variability of BC_{BB} exhibited a unimodal pattern, with increasing concentrations up to 0.44 µg m^{-3} after 4:00 p.m., which illustrates the impact of residential wood burning emissions. The concentration of BC_{FF} exhibited a discernible weekly pattern (Figure 33e), with a maximum (1.24 µg m^{-3}) observed on Wednesdays and a minimum (0.74 µg m^{-3}) on Sundays. The BC_{FF} concentrations were approximately 27% higher on weekdays (Figure 33e). The contribution of biomass burning sources remained stable throughout the week, with a mean of 19% (outdoors) and 21% (indoors). However, there was a 3% increase in the BC_{BB} fraction for both environments on Sundays. The BC_{BB} concentration on Sundays was either the same or lower than on weekdays (0.21-0.29 µg m^{-3}). Consequently,

the biomass burning source on Sundays was releasing the same amount of BC_{BB} emissions, although its contribution was higher due to lower emissions of BC_{FF}. The I/O ratio of BC was almost unchanged during the week (variation from 0.03 to 0.04), due to the absence of indoor sources under non-occupied conditions.

3.3 Black carbon deposition on tree foliage

On high pollution days, the ability of trees to capture BC becomes particularly relevant. Urban areas are often subject to traffic-induced and biomass burning related poor air quality. Variability in air quality improvement in urban areas leads to different solutions including green infrastructure, where these locations are also sites of pedestrian activity, exposure to pollution is increased. This study demonstrates the ability of trees to capture BC.

During this measurement period for BC deposition analysis, the BC mass concentration was typical for Vilnius in the non-heating season period at 0.85 (0.91) µg m^{-3}. The values of BC_{FF} and BC_{BB} were 0.42 ± 0.54 µg m^{-3} and 0.39 ± 0.32 µg m^{-3}, respectively (Figure 34).
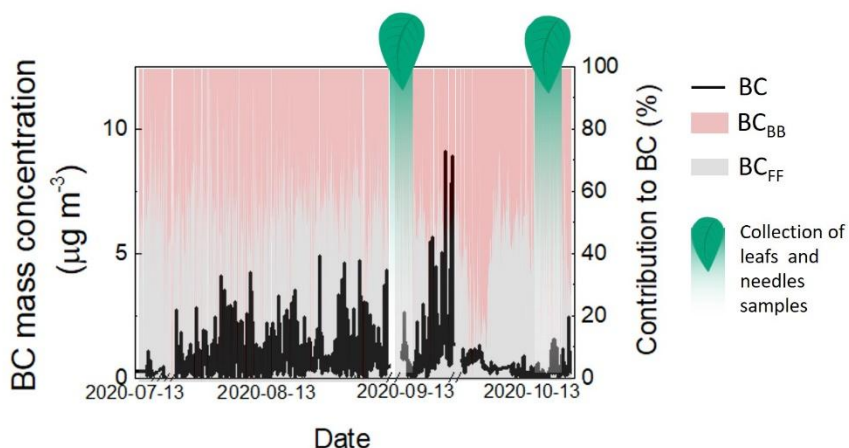
Figure 34. BC mass concentration and contribution (%) of BC_{BB} and BC_{FF} during the leaf and needle sampling periods.

The leaf and needle samples were collected in September - October 2020, before the heating season period in the residential sector. This was the time when all the leaves of Betula pendula Roth were fully developed, but before the defoliation. Hiroshi et al. (2022) investigated the deposition of BC on konara oak (Quercus serrata) leaves and found that the specific mass of BC

deposited on the leaves fluctuated considerably over time [18]. During the bud stage, BC deposition increased rapidly with time, then reached a plateau and began to decrease as defoliation progressed. The plateau was a result of simple accumulation over time and occasional removal due to rainfall and strong winds. The highest mass of BC deposited on the leaves of Quercus serrata was observed in June. All leaf and needle samples collected during the measurement period showed the presence of BC aerosol particles, which are formed by condensing combustion processes. Small amounts of silicon (Si), calcium (Ca) and iron (Fe) were found in aerosol particles (Figure 35). These specific elements can help identify their possible sources. Particles containing Si and Ca may originate from vehicle exhaust, as Si is widely used in fuels and Ca is a common additive for oil. Based on the EDX data obtained, particles containing silicon were identified as quartz and could have been formed by fossil fuel combustion [88]. The trace amounts of Fe may be an indicator of coal burning [60]. The morphology of some particles was altered, most likely due to ageing in the atmosphere [89]. Organic coatings form on BC through coagulation or condensation of primary or secondary organic aerosol. The thickness of the coating increases the light absorption of BC due to a lensing effect, which depends on the degree of aging [89].

A typical BC agglomerate consists of spherical particles fused into a chain. The diameter of the primary particles found ranged from 24.23 nm to 30.02 nm on leaves and from 32.45 nm to 44.13 nm on needles (Table 9). The largest BC particle agglomerates found were 288.52 nm long and 220.39 nm wide. The larger agglomerates were found on needles of coniferous trees. Previous studies have shown that conifers are effective at removing air pollution due to their high tree density and long leaf life, as well as their thicker epicuticular wax layer compared to leaves of deciduous species, making them more efficient at accumulating BC [90,91].
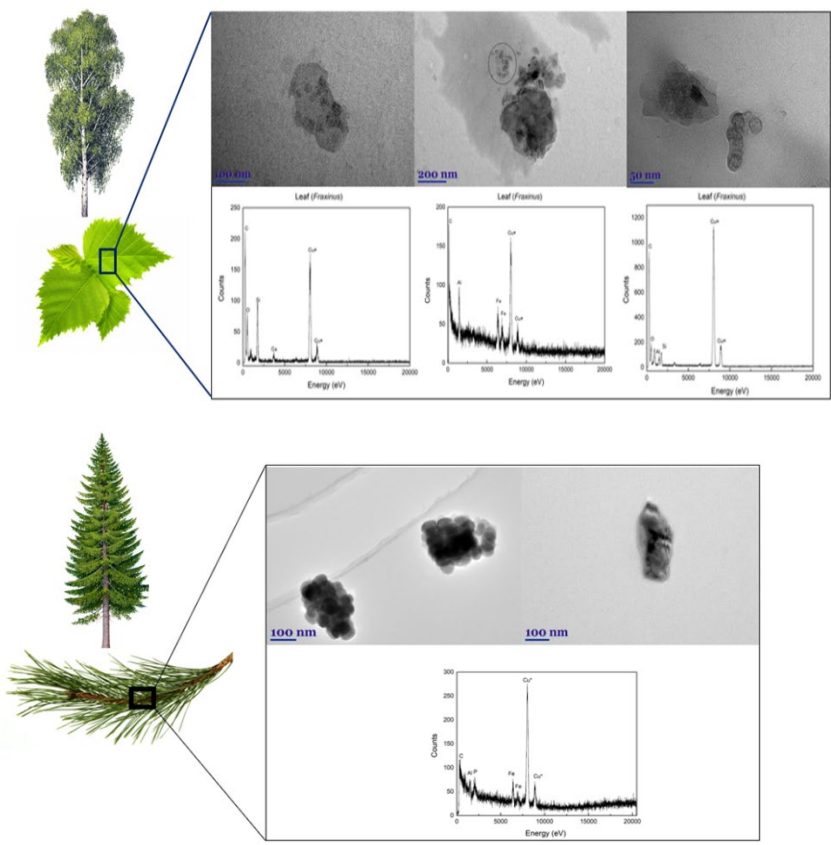
Figure 35. TEM images and EDX spectra of BC containing particles found on leaves and needles.

Table 9. Diameter of primary particle, length and width of BC agglomerate.

Characteristics	Particle code				
	Leaf-1	Leaf-2	Leaf-3	Needle-1	Needle-2
⌀, nm	24.23	23.08	30.02	32.45	41.30
L, nm	234.14	129.74	97.01	175.52	273.30
W, nm	132.29	132.29	68.83	176.65	200.61
⌀ - diameter of primary particle, L and W is the maximum length and width of agglomerate.					

Chapter 3 conclusions

The complex interplay of local emissions, meteorological factors, and seasonal practices such as heating and biomass burning in influencing BC concentrations in Vilnius showed notable seasonal and monthly variations in

BC mass concentrations. BC concentrations were notably higher during the heating season period than the non-heating season period, showing the impact of both traffic and heating emissions. NO_x followed similar daily patterns across both periods, with higher levels during the heating season period. Grass burning in March from neighboring regions, particularly non-European Union countries, can also contribute to higher BC levels. So, March exhibited the highest concentrations for all BC components, with a mean monthly concentration of 1.96 µg m^{-3}. Biomass burning related BC contributed 0.68 µg m^{-3}, while fossil fuel combustion-related BC - 1.28 µg m^{-3}. In September recorded the lowest BC and BC_{BB} levels, while BC_{FF} reached its lowest in July, likely due to decreased vehicular emissions and a higher atmospheric mixing layer during the summer.

The correlation coefficients between source apportioned BC, PM_{10}, NO_x and meteorological parameters were analyzed for different seasons. BC, BC_{FF}, BC_{BB}, and NO_x were consistently clustered together, showing moderate to strong correlations. However, PM_{10} in summer had a weak correlation (0.13) with BC. Interestingly, meteorological parameters were generally grouped together, with pressure being an exception. BC showed strong correlations with wind speed in summer, wind direction and temperature in autumn, and all meteorological parameters in winter, and pressure, wind speed, and temperature in spring. Temperature had a stronger correlation with BC_{BB}, while wind speed had a stronger correlation with BC and BC_{FF}.

The highest BC concentrations were found to be influenced by one dominant local source, with additional sources in autumn at specific wind speeds and directions. The probability of low concentrations and multiple sources in all directions were observed at the 25th percentile. Conversely, it was found that the 75th percentile BC concentration in autumn demonstrated one additional source in the S direction at wind speeds of between 1 and 3 m s^{-1}. The pollution rose plot showed that northwest consistently had the highest pollution concentrations in all seasons, with northeast prominent in summer and south/southeast dominant in autumn and winter.

The dendrogram indicates that all meteorological parameters, except for atmospheric pressure, tend to cluster together. Pressure is often isolated, merging with other meteorological variables only in the autumn season. Temperature shows a particularly strong correlation with BC_{BB}, while wind speed demonstrates a stronger correlation with both BC and BC_{FF}, highlighting the role of meteorological factors in influencing BC concentrations.

The comparison of correlation matrix and dendrogram for relatively non-polluted and polluted days shows significant changes in correlation strength

and structure and varies significantly across seasons. Increased negative correlation between BC, wind speed and temperature were observed across all seasons. Spring exhibited unique patterns with stable BC- NO_x correlation but weakened BC-PM_{10} relationship. Influence of meteorological conditions on BC concentration dynamics is prominent, especially during high pollution periods.

A study found that a mechanical ventilation system without improved filtration had capture efficiencies of 70-80% for certain particles. Biomass burning-related BC contributed around 20% of total BC indoors and outdoors, while fossil fuel-related BC dominated at 80%, highlighting fossil fuel combustion as the main BC source during Vilnius' heating season period. Indoors, BC_{FF} ranged from 0.09 to 0.21 $\mu g\ m^{-3}$, and BC_{BB} from 0.02 to 0.09 $\mu g\ m^{-3}$. On high pollution days ($PM_1 > 25\ \mu g\ m^{-3}$), outdoor BC concentrations increasing by 3–4 times, while indoor levels saw only a twofold increase. The indoor/outdoor infiltration factor of 0.8 indicated no significant indoor BC sources. Indoors, BC_{BB} showed a unimodal rise to 0.44 $\mu g\ m^{-3}$ after 4:00 p.m., reflecting residential wood burning. BC_{FF} had a weekly peak at 1.24 $\mu g\ m^{-3}$ on Wednesdays and a low of 0.74 µg/m³ on Sundays, with weekday levels 27% higher than weekends. BC_{BB} remained stable (19% outdoors, 21% indoors), though Sundays saw a 3% rise in BC_{BB} fraction, despite BC_{BB} concentrations staying within 0.21–0.29 $\mu g\ m^{-3}$. The I/O BC ratio stayed between 0.03 and 0.04 throughout the week due to no indoor sources.

The results demonstrated the presence of BC aerosol particles produced by the condensation mechanism during combustion processes in all samples obtained from the leaf surface. Furthermore, needle-like trees demonstrate greater efficiency than broad-leaved trees in capturing BC. The largest agglomerates of BC particles were observed to measure 288.52 nm in length and 220.39 nm in width. The larger agglomerates were found on the needles of coniferous trees. This is due to a number of factors, including the high tree density and long leaf life of coniferous species, as well as the thicker epicuticular wax layer found on their leaves, which allows them to accumulate BC more efficiently than deciduous species. Potentially, urban trees can contribute to improved air quality by reducing BC levels through dry deposition on foliage

CONCLUSIONS

1. Black carbon concentrations in Vilnius exhibit seasonal variations, with significantly higher levels during the heating season period (1.17 µg m⁻³) compared to the non-heating season period (0.61 µg m⁻³). This difference is further emphasized by the substantially higher BC mass concentration mode during the heating season period (0.26 µg m⁻³) compared to the non-heating (0.16 µg m⁻³). While biomass burning exhibits a pronounced seasonal peak in summer, contributing 41% to the total BC mass concentration, fossil fuel combustion emerges as a dominant and consistent source throughout the year, accounting for 71% of BC emissions.

2. The homogeneous distribution of BC_{FF} and BC_{BB}, alongside NO_x and PM_{10}, at calm wind speeds (up to 0.5 m s⁻¹) suggests the dominance of local emission sources, particularly during the heating season period. However, the non-heating season period reveals a shift in source contributions, with the additional sources from the southwest-southeast direction, highlighting the influence of regional transport. Furthermore, low BC concentrations (25ᵗʰ percentile) are associated with multiple source directions, suggesting a mixture of local and transported pollutants. Conversely, elevated BC levels (75ᵗʰ percentile) observed in autumn, particularly at wind speeds of 1-2 m s⁻¹, point to a distinct source contribution from the south.

3. In spring, the dynamics of air pollution in Vilnius reveal a unique interplay between emission sources and meteorological factors. While the north-west wind direction is typically responsible for the highest pollutant concentrations throughout the year, it shows a distinct shift in spring, with the south-east and south-south-east wind directions emerging as dominant source regions. This seasonal shift is further corroborated by the weakening correlation between BC and PM_{10} suggesting a change in emission sources compared to other seasons. The weaker correlation between BC and pressure on high pollution days in spring (r = 0.18) compared to usual days (r = 0.40) underscores the complex interplay of factors influencing springtime air quality.

4. Black carbon, originating from fossil fuel combustion, contributed a significantly higher fraction (80%) to total BC compared to biomass burning-related BC (20%) both indoors and outdoors. Fossil fuel-related BC exhibited a clear bimodal diurnal profile outdoors, peaking during morning and evening rush hours, reflecting the influence of traffic patterns. While a similar trend was observed indoors, the peaks were less

pronounced, indicating the effectiveness of building filtration in mitigating peak outdoor pollution.

5. Despite its lower overall contribution, BC_{BB} displayed an unimodal diurnal pattern, peaking in the evening. This suggests a potential influence of residential wood burning for heating, particularly during colder evening hours. Even with a mechanical ventilation system, indoor BC concentrations still increased on days with high outdoor PM_1 levels ($> 25\ \mu g\ m^{-3}$). While outdoor BC concentrations rose by 3-4 times, indoor levels doubled, a significant influence of outdoor air infiltration

6. Analysis of leaf and needle samples collected in Vilnius during the non-heating season revealed the presence of BC particles, confirming their deposition and accumulation on tree foliage. Notably larger BC agglomerates were found on coniferous needles (with diameter 32.45 – 41.30 nm) compared to deciduous leaves (24.23 – 30.02 nm). This difference suggests that conifers may be more efficient at capturing air pollutants presumably due to their unique needle structure, thicker wax layers, and year-round foliage.

SANTRAUKA

Įvadas

Atmosferos juodoji anglis (angl., black carbon, BC), dar vadinama suodžiais, yra kietųjų dalelių (toliau KD) sudedamoji dalis, kuri, neigiamai veikia oro kokybę, klimato kaitą ir žmonių sveikatą. Juodoji anglis yra siejama su kvėpavimo takų, širdies ir kraujagyslių ligomis taip pat su pažinimo funkcijų sutrikimais tiek lokaliai, tiek globaliai [12,13]. Ilgalaikis poveikis gali sukelti lėtines sveikatos problemas ir didesnę priešlaikinio mirtingumo riziką [14]. Moksliniai tyrimai rodo, kad BC masės koncentracijos lygiai pasižymi dideliu laikinu ir erdviniu kintamumu, kurį daugiausia lemia matavimo vieta, sezoniškumas, meteorologinės sąlygos ir paros laikas [15,17,29]. Šis kintamumas išryškina kompleksinę BC patekimo į aplinką prigimtį ir iššūkius, su kuriais susiduriama vertinant jos poveikį aplinkai ir sveikatai. Šaltinių kilmės nustatymas yra esminis analitinis metodas, leidžiantis kiekybiškai įvertinti skirtingų šaltinių indėlį BC masės koncentracijai. Ši metodika ypač svarbi siekiant geriau suprasti sudėtingas oro kokybės problemas, susijusias su BC ir KD [23,36,37].

Svarbu pabrėžti, kad lauko oro tarša gali turėti įtaką patalpų oro kokybei. Santykį tarp patalpų ir lauko oro kokybės lemia įvairūs veiksniai, įskaitant teršalo tipą, pastato charakteristikas, nuotolį iki gatvės, vėdinimo sistemas, vidinių taršos šaltinių buvimą ir žmonių skaičių patalpoje [44–46]. Pagrindiniai veiksniai yra artumas prie gatvių, pastato charakteristikos ir žmonių patalpoje kiekis. Didelės taršos epizodai, kai teršalų masės koncentracija viršija 95-ąjį procentilį, rodo veiksmingo reguliavimo ir visuomenės sveikatos apsaugos strategijų poreikį. Šių epizodų priežasčių ir pasekmių analizė yra labai svarbi kuriant priemones, skirtas visuomenės sveikatai apsaugoti bei pagerinti miestų oro kokybę. Juodosios anglies koegzistavimas su azoto oksidais (NO_x) ir KD ore miestuose rodo galimą šių teršalų sinergetinę sąveiką. Bendri taršos šaltiniai, ypač susiję su biomasės deginimu ir transporto veikla, pabrėžia būtinybę tirti BC ir NO_x dinamiką atliekant šaltinių kilmės nustatymo tyrimus [22,36, 54,55].

Siekiant sumažinti transporto ir biomasės deginimo sukeliamą juodosios anglies taršą, ypatingai svarbu įvertinti žaliąją infrastruktūrą. Miesto apželdinimas gali pagerinti oro kokybę, nes sumažina BC koncentraciją dėl sauso nusėdimo ant medžių lajos [56,58]. Svarbu pažymėti, kad apželdinimo įvairiomis rūšimis efektyvumas filtruojant ore esančias daleles labai skiriasi, tai lemia tokie veiksniai kaip lajos struktūra, augimo stadija ir lapų/spyglių šiurkštumas [62,63,65].

Lietuvoje paprastoji eglė (*Picea abies (L.) H.Karst*) ir sidabrinis beržas (*Betula pendula Roth*) yra vienos dažniausiai pasitaikančių medžių rūšių, suteikiančių galimybę ištirti jų potencialą žaliojo miesto koncepcijoje [67]. Šių rūšių specifinių savybių ir naudos mažinant oro taršą supratimas gali padėti formuoti miestų planavimo strategijas, kuriomis siekiama optimizuoti su miestų žalinimo iniciatyvomis susijusius aplinkos ir sveikatos rezultatus.

Pagrindinis tikslas

Šio tyrimo tikslas – ištirti skirtingos kilmės juodosios anglies masės koncentracijos aerozolio dalelėse dinamiką miesto aplinkoje ir nustatyti pagrindinius veiksnius, lemiančius šią koncentraciją.

Darbo uždaviniai

1. Nustatyti paros, savaitės dienų ir sezoninius skirtingos kilmės BC masės koncentracijos dėsningumus bei įvertinti kiekvieno šaltinio indėlį BC masės koncentracijai.
2. Ištirti pagrindinius veiksnius, lemiančius BC masės koncentracijos padidėjimą didelės taršos epizodų metu kiekvieno sezono laikotarpiu.
3. Įvertinti ryšį tarp lauko ir patalpų BC masės koncentracijos lygių, siekiant suprasti, kaip lauko tarša veikia patalpų oro kokybę.
4. Atlikti juodosios anglies nusėdimo ant medžių lapų, kaip oro taršos mažinimo potencialo, vertinimą.

Naujumas

Šiame darbe pateikiamos naujos holistinės įžvalgos apie juodosios anglies taršos šaltinius ir pagrindinius veiksnius Vilniuje, detaliai analizuojant iškastinio kuro ir biomasės deginimo įtaką juodosios anglies masės koncentracijai visais metų laikais. Taip pat įvertinamas BC indėlis patalpų oro kokybei ir nusėdimas ant medžių lajos mieste. Iki šiol Baltijos šalių sostinėse išsamūs BC masės koncentracijos tyrimai nebuvo atlikti.

Ginamieji teiginiai

1. Šildymo sezono metu juodosios anglies masės koncentracija yra didesnė dėl iškastinio kuro deginimo, ir, nepaisant pastebimo biomasės kuro deginimo indėlio padidėjimo birželio–rugpjūčio mėnesiais, išlieka pagrindiniu veiksniu, lemiančiu aukštesnę juodosios anglies masės koncentraciją, kai šildymas nėra naudojamas.

2. Aukštesnę BC masės koncentraciją lemia vyraujantis vietinis šaltinis, o rudenį, esant tam tikram vėjo greičiui, prisideda papildomas šaltinis pietų kryptimi. Tuo tarpu mažesnius BC lygius lemia keli šaltiniai.
3. Pavasarį, ekstremalių taršos epizodų metu, žolės deginimas turi didesnį poveikį BC koncentracijos padidėjimui nei meteorologinės sąlygos.
4. Juodoji anglis, susiformuojanti deginant iškastinį kurą, sudaro apie 80% visos BC masės koncentracijos tiek patalpų, tiek lauko ore. Didelio užterštumo dienomis BC koncentracija lauke padidėja 3–4 kartus, o patalpose – tik du kartus.
5. Sidabrinio beržo lapai ir paprastosios eglės spygliai gali pagerinti oro kokybę mieste, nes padeda efektyviau pašalinti juodąją anglį iš aplinkos oro.

Autoriaus indėlis

Darbo autorė aktyviai dalyvavo atliekant BC masės koncentracijos laiko eilučių analizę ir interpretuojant rezultatus. Taip pat kūrė grafines iliustracijas, buvo vienas iš rankraščių autorių ir pristatė rezultatus mokslinėse konferencijose.

Metodai

Matavimų vietos

Matavimai atlikti VMTI Fizinių mokslų ir technologijų centre (FTMC), esančiame 54,72° šiaurės platumos ir 25,32° rytų ilgumos, Lietuvos sostinėje ir didžiausiame mieste Vilniuje. Iš viso buvo atlikti trys BC masės koncentracijos dinamikos tyrimai, kurių rezultatai padėjo geriau suprasti taršos šaltinius bei jų įtaką įvairiais sezonais (5 paveikslas):
1. Juodosios anglies masės koncentracijos nenutrūkstami matavimai nuo 2021 m. birželio 1 d. iki 2022 m. gegužės 31 d.
2. Juodosios anglies masės koncentracijos ir šaltinių kilmės nustatymas bei lauko ir patalpų oro kokybės tyrimai atlikti 2020 m. spalio – 2021 m. vasario mėnesiais, šildymo sezono metu.
3. Tyrimas, skirtas ištirti BC nusėdimą ant miesto medžių (paprastųjų eglių ir sidabrinių beržų) lajos, atliktas 2020 m. rugsėjo – spalio mėnesiais, prieš prasidedant gyvenamųjų namų šildymo sezonui.

Juodosios anglies matavimų vietovė apibūdinama kaip gyvenamoji teritorija, esanti maždaug 8 km į šiaurės rytus nuo miesto centro ir apie 600 m

nuo judraus kelio bei besiribojanti su mišku. Ši vieta atspindi foninę aplinką platesnei Vilniaus teritorijai, leidžiančią įvertinti oro kokybę, kurią veikia tiek vietiniai, tiek regioniniai veiksniai.

Siekiant įvertinti lauko BC masės koncentracijos indėlį patalpų oro kokybei, matavimai buvo atlikti mechaniškai vėdinamoje FTMC erdvėje, kurią galima apibūdinti kaip tipišką biuro aplinką, kurios oro tiekimo sistemoje įrengtas trijų pakopų filtravimas (G4-F7-F9). Svarbu pažymėti, kad matavimo kampanijos metu patalpoje nebuvo aerozolio dalelių šaltinių, veikla patalpose buvo apribota, išskyrus retus mėginių ėmimo laikotarpius. Pastate nėra teikiamos maitinimo paslaugos, langai ir durys buvo uždaryti. Todėl visi patalpų KD koncentracijos pokyčiai buvo siejami su lauko KD koncentracijos lygiu ir oro filtravimo sistemos veikimo pokyčiais.

Aethalometras (žr. 2.2. Prietaisai ir metodai) buvo patalpintas antrame pastato aukšte. Mėginių ėmimas tarp vidaus ir lauko įvadų buvo perjungiamas naudojant automatinį vožtuvo valdymą, kurio laiko skiriamoji geba yra 30 minučių..

Matavimų įranga ir metodai

Juodoji anglis ir šaltinių kilmės nustatymas

Juodosios anglies masės koncentracijos nenutrūkstami matavimui realiuoju laiku buvo vykdomi naudojant septynių bangos ilgių Aetalometrą (Magee Scientific Aethalometer, modeliai AE-31 ir AE-33). Anglies aerozolio dalelių optinis pralaidumas buvo matuojamas septyniais bangos ilgiais (λ= 370, 470, 520, 590, 660, 880 ir 950 nm). Standartinis BC matavimų kanalas yra 880 nm, nes jis laikomas vyraujančiu absorberiu.

Šaltinių kilmės nustatymo metodika, naudojama matuojant BC masės koncentraciją Aethalometru, yra pagrįsta Sandradewi ir kt. pasiūlytu Aethalometro modeliu. (2008 m.) [70]. Analizei buvo naudojamos vidutinės valandinės BC masės koncentracijos vertės. Darbe nagrinėjami BC masės koncentracijos duomenys pateikiami kaip vidutinė vertė ir standartinis nuokrypis (SD), naudojant UTC+2:00 laiko juostą.

Juodosios anglies nusėdimo ant medžių lajos analizė

Siekiant įvertinti miesto medžių lajos įtaką BC pašalinimui, lapų ir spyglių mėginiai buvo renkami tipiškoje vietovėje, kurioje auga tiek spygliuočiai (paprastosios eglės (*Picea abies H.Karst*)), tiek lapuočiai (sidabriniai beržai (*Betula pendula Roth*)). Ši vietovė yra netoli gyvenamojo rajono, daugiau nei

350 m nuo judrių gatvių ir 3 km atstumu nuo pramonės objektų, apsupta miškingos teritorijos. Lapų ir spyglių mėginiai buvo renkami trijose vietose, išsidėsčiusiose maždaug 500 m nuo BC koncentracijos matavimų vietos.

Pavienės aerozolio dalelių, nusėdusių ant sidabrinio beržo lapo ir paprastosios eglės spyglio ir turinčių sudėtyje juodosios anglies, morfologijai, dydžiui ir elementinei sudėčiai nustatyti buvo naudojama transmisinė elektronų mikroskopija (Tecnai G2 F20 X-TWIN, skiriamoji geba 0,25-0,102 nm) kartu su energijos sklaidos rentgeno spindulių spektroskopija (EDX).

Oro masių pernašos atgalinės trajektorijos ir MODIS palydovo duomenys

Siekiant įvertinti tolimosios oro masių pernašos poveikį BC masės koncentracijai, buvo atlikta 72 valandų atgalinių trajektorijų, slenkančių virš Vilniaus 500 m, 1000 m ir 1500 m aukštyje virš žemės paviršiaus analizė naudojant HYSPLIT4 (angl., Hybrid Single-Particle Lagrangian Integrated Trajectory) modelį.

Gaisrų duomenys buvo gauti iš NASA/GSFC Žemės mokslo duomenų informacinės sistemos ESDIS (angl. Earth Science Data Information System) ir išteklių valdymo sistemos FIRMS (https://firms.modaps.eosdis.nasa.gov/map). Gaisrų vietoms visoje Lietuvoje pavaizduoti buvo panaudoti MODIS duomenys ir karinio jūrų laivyno aerozolio analizės ir prognozavimo sistemos NAAPS (angl. Navy Aerosol Analysis and Prediction System) modelio duomenys. Dūmų sluoksniui virš Vilniaus nustatyti buvo naudojamas NAAPS modelio duomenų ir juodosios anglies (BC) stebėjimų derinys.

Meteorologija

Temperatūros, santykinės drėgmės, vėjo greičio (WS), vėjo krypties (WD), taip pat azotų oksidų (NO_x) ir kietųjų dalelių (KD_{10}) masės koncentracijos duomenis pateikė Lietuvos aplinkos apsaugos agentūra (www.gamta.lt).

Pirmasis tyrimo etapas apėmė tiek šildymo periodą, tiek laikotarpį kai šildymas nebuvo naudojamas. Šildymo laikotarpis, trunkantis nuo spalio iki kovo mėnesio, pasižymi žemesne aplinkos temperatūra ir patalpų šildymo poreikiu. Priešingai, laikotarpis be šildymo, trunka nuo balandžio iki rugsėjo mėnesio ir pasižymi šiltomis oro sąlygomis ir nereikalauja patalpų šildymo (3 lentelė).

Išsamesnei analizei metų laikai buvo suskirstyti į mėnesių grupes: vasara (2021 m. birželis-rugpjūtis), ruduo (2021 m. rugsėjis-lapkritis), žiema (2021 m. gruodžio mėn., sausis-vasaris) ir pavasaris (2022 m. kovo-gegužės mėn.).

Ši klasifikacija leido geriau suprasti sezoninius oro kokybės parametrų pokyčius ir su jais susijusią įtaką visus metus. 4 lentelėje pateikiama aprašomoji keturių metų sezonų statistinė meteorologinių kintamųjų apžvalga.

Statistinė analizė ir sąlyginės tikimybės funkcijos analizė

Sąlyginės tikimybės funkcijai (angl., conditional prpbability function, CPF) apskaičiuoti oro teršalų (įskaitant BC, PM_{10} ir NO_x) bei meteorologinių parametrų, tokių kaip vėjo greitis ir kryptis, duomenys buvo analizuojami naudojant statistinę programinę įrangą Openair (R paketo 4.3.1 versija). Šis paketas suteikia daugybę įrankių, skirtų duomenims importuoti ir tvarkyti, įvairioms analizėms atlikti ir kurti aukštos kokybės grafikus bei vizualizacijas siekiant įvertinti tendencijas bei dinamiką [74]. CPF metodas yra veiksmingas būdas nustatyti pagrindinius oro teršalų šaltinius, apskaičiuojant teršalo slenkstinės vertės tikimybę konkrečiame vėjo krypties sektoriuje. Ši vertė paprastai išreiškiama procentiliu. Šiame tyrime buvo naudojami 25, 75 ir 95 procentiliai tiek sąlyginai aukštoms koncentracijoms (75-asis), tiek foninei (25-asis) vertei įvertinti.

Rezultatai

BC masės koncentracijos dinamika miesto aplinkoje

Juodosios anglies masės koncentracijos analizė apima laiko eilučių tyrimą šildymo periodu ir laikotarpiu be šildymo, taip pat sezonų, paros ir didelės taršos dienomis. Siekiant geriau suprasti BC sąsajas ir elgseną per visą metinį matavimo laikotarpį, papildomai analizuotos KD_{10} ir NO_x koncentracijos bei meteorologiniai duomenys.

Nustatyta, kad vidutinė metinė BC koncentracija siekia 0,89 µg m⁻³ (standartinis nuokrypis – 0,99 µg m⁻³). Tyrimas atskleidė ryškius sezoninius ir mėnesinius BC masės koncentracijos svyravimus. Didžiausia visų teršalų, įskaitant ir BC, koncentracija buvo stebima kovo mėnesį (6 paveikslas). Vidutinė kovo mėnesio koncentracija siekė 1,96 µg m⁻³, iš kurių 0,68 µg m⁻³ sudarė biomasės deginimo kilmės BC, o 1,28 µg m⁻³ – iškastinio kuro deginimo kilmės BC. Ir atvirkščiai, žemiausia BC masės koncentracija (0,5 µg m⁻³) ir biomasės deginimo kilmės BC_{BB} (0,05 µg m⁻³) nustatyta rugsėjo mėnesį. Iškastinio kuro deginimo kilmės BC_{FF} vidutinė mėnesio koncentracija buvo stebėta liepos mėnesį ir siekė 0,31 µg m⁻³, tikėtina, dėl sumažėjos transporto priemonių taršos ir padidėjusio maišymosi sluoksnio. Rezultatai rodo, kad BC masės koncentracija Vilniuje yra panaši į daugelio Europos

miestų koncentraciją įvairiais laikotarpiais. Vilniuje nustatytų BC verčių palyginimas su kitomis šalimis pateikiamas 2 lentelėje.

Atlikus BC šaltinių paskirstymą nustatyta, kad iškastinio kuro ir biomasės deginimas turi skirtingą indėlį masės koncentracijai. Vidutinė metinė BC_{FF} ir BC_{BB} koncentracija buvo atitinkamai 0,63 µg m⁻³ (0,67) µg m⁻³ ir 0,27 µg m⁻³ (0,35) µg m⁻³. Biomasės deginimo kilmės BC_{BB} dalis sudarė 29,0% (11%) (7 paveikslas). Tai rodo, kad nemaža dalis BC išmetama deginant biomasę, ypač šaltesniais mėnesiais, kai šildomi gyvenamieji namai, tokiu būdu didžiausia vidutinė BC masės koncentracija (1,14 µg m⁻³) buvo nustatyta žiemos sezonu. Tai galima paaiškinti ir tuo, kad žiemos sezono metu sumažėja maišymosi sluoksnis ir padidėja gyvenamųjų namų šildymo ir biomasės deginimo poreikis [36]. Tuo tarpu liepos mėnesį buvo nustatyta mažiausia vidutinė mėnesio vertė (0,50 µg m⁻³), o tai siejama su dviem pagrindiniais veiksniais: pirma, vasarą stebimu aukštesniu ribiniu sluoksniu [36] ir, antra, atostogų laikotarpiu, dėl kurio sumažėjo eismo aktyvumas mieste.

Nustatyta, kad darbo dienomis BC masės koncentracija didėja, o savaitgaliais mažėja, tai galima paaiškinti sumažėjusiu eismo intensyvumu. Ryškūs teršalų išmetimo pikai stebimi rytais (nuo 7:00 iki 9:00) ir vakarais (nuo 18:00 iki 23:00). Metinė vidutinė BC, BC_{FF} ir BC_{BB} koncentracijos vertė rytais atitinkamai siekė 1,21 µg m⁻³, 0,87 µg m-3 ir 0,34 µg m⁻³, o vakarais – atitinkamai 1,25 µg m⁻³, 0,85 µg m⁻³ ir 0,41 µg m⁻³. Didžiausios BC koncentracijos vertės buvo fiksuotos kovo mėnesį pučiant vėjui iš pietryčių, pietų ir pietvakarių krypčių, o savaitės viduryje – iš pietryčių, su mažiausiomis fiksuojamomis koncentracijomis pučiant iš šiaurės vakarų krypties. Nuo 7:00 iki 11:00 val buvo stebimi du koncentracijos maksimumai, stipriausiai susiję su pietvakarių krypties vėjais. Didžiausia BC koncentracija fiksuota ryte, kai vyrauja pietryčių, pietų ir pietvakarių krypties vėjai (nuo 7:00 iki 11:00), o vakare – pučiant vėjui iš šiaurės rytų krypties (nuo 19:00 iki 23:00).

Atlikta tyrimo analizė parodė, kad miesto teršalų koncentracijos labai skiriasi priklausomai nuo mėnesio, laiko ir eismo intensyvumo. Nustatyta, kad vidutinė metinė KD_{10} masės koncentracija yra 19,68 µg m⁻³ (standartinis nuokrypis – 11,36 µg m⁻³), o vidutinė metinė NO_x koncentracija yra 21,62 µg m⁻³ (standartinis nuokrypis – 23,10 µg m⁻³). Didžiausios KD_{10} ir NO_x koncentracijos buvo stebimos kovo mėnesį, o mažiausios – sausio ir birželio–liepos mėnesiais. Tyrimas taip pat rodo, kad vidutinės savaitės dienų koncentracijos buvo didesnės savaitės viduryje, ypač trečiadienį ir ketvirtadienį, tai gali būti susiję su padidėjusiu eismu šiomis dienomis. Savaitgaliais (šeštadienį ir sekmadienį) koncentracijos buvo mažesnės, tikėtina dėl mažesnio eismo intensyvumo. Be to, pirmadieniais koncentracijos

buvo šiek tiek žemesnės, kas gali būti susiję su mažesniu eismo intensyvumu savaitgaliais. Šie rezultatai rodo, kad teršalų koncentracijos mieste yra labai kintančios ir priklauso nuo daugelio išorinių veiksnių.

Tai patvirtina faktas kad mažiausia NO_x ir KD_{10} koncentracija buvo stebima ankstyvą rytą (nuo 00:00 iki 06:00 val. NO_x atveju ir nuo 00:00 iki 07:00 val. KD_{10} atveju). Tai siejama su tuo, kad naktį eismo nėra, todėl teršalai išsisklaido dienos metu. Vėliau NO_x koncentracija laipsniškai didėja nuo 07:00 iki 10:00 val. ir nuo 08:00 iki 11:00 val. Be to, nuo 14:00 iki 18:00 val. pastebėta NO_x didėjimo tendencija, tačiau nuo 19:00 iki 22:00 val. ji stabilizuojasi, kas gali būti susiję su vakarinio eismo piko valandomis. Kietųjų dalelių KD_{10} mažėjimo tendencija stebima po 12:00 val.

Kovo mėnesį stebėtas didžiausias NO_x ir KD_{10} koncentracijos lygis siejamas su vėju pietryčių kryptimi. Tuo tarpu didžiausia KD_{10} koncentracija stebėta darbo dienomis nuo 8:00 iki 17:00 val. pietryčių ir rytų kryptimis, o didžiausia NO_x koncentracija − savaitės viduryje nuo 8:00 iki 12:00 val. vakarų ir pietvakarių kryptimis. Tai galima paaiškinti žolės deginimu ir oro masių pernašomis iš kaimyninių regionų, ypač ne Europos sąjungai priklausančių šalių, kuriose tai laikoma nelegalia veikla. Ši hipotezė yra patvirtinta naudojant FIRMS MODIS sistemą, kurioje buvo aptikti aktyvūs gaisro židiniai ir NAAPS modelio rezultatus, kuriuose pastebima didesnė dūmų koncentracija kovo mėnesį. Ši informacija išsamiai aptariama skyriuje "Didelės taršos epizodų analizė".

Skirtingos kilmės juodosios anglies tyrimai šildymo periodu ir laikotarpiu be šildymo

Rezultatai parodė, kad BC, BC_{FF} ir BC_{BB} bei NO_x masės koncentracijos šildymo sezonu ir laikotarpiu be šildymo reikšmingai skyrėsi. Vidutinė BC, BC_{FF} ir BC_{BB} koncentracija šildymo laikotarpiu buvo maždaug 2 kartus aukštesnė nei laikotarpiu be šildymo. Teršalų vidutinės koncentracijos vertės laikotarpiais be šildymo ir šildymo sezono metu siekė: BC 0.61 (0.56) ir 1.17 (1.22) µg m^{-3}, BC_{FF} − 0.43 (0.44) ir 0. 81 (0.80), BC_{BB} − 0.17 (0.17) ir 0.36 (0.44) µg m^{-3}, KD_{10} − 20.02 (10.89) ir 19.37 (11.78) µg m^{-3}, NO_x 18.27 (16.47) ir 24.92 (27.76) µg m^{-3}. Pažymėtina, kad Vilniuje nebuvo pastebėta reikšmingų KD_{10} koncentracijos skirtumų laikotarpiais be šildymo ir šildymo sezono metu.

Kaip parodyta 10 paveiksle, šildymo sezono laikotarpiu BC, BC_{FF}, BC_{BB} ir NO_x masės koncentracijos vertės buvo aukštesnės. Be to, nustatyta, kad šios koncentracijos buvo aukštesnės savaitės darbo dienomis, palyginti su savaitgaliais. Tikėtina, kad šį reiškinį lemia mažesnis eismo intensyvumas

savaitgaliais. Tiek šildymo sezonu, tiek laikotarpiu be šildymo stebėta koncentracijos eiga buvo panaši, tačiau BC, BC_{FF} ir BC_{BB} vidutinės valandinės vertės svyravimai abiem sezonais labai skyrėsi. Šį skirtumą galima paaiškinti šildymo metu išmetamų teršalų kiekio ir oro sąlygų svyravimais. Šildymo laikotarpiu BC, BC_{FF} ir BC_{BB} paros vidutinės vertės svyravimų intervalas buvo didelis ir siekė atitinkamai 0,76 µg m^{-3}, 0,52 µg m^{-3} ir 0,27 µg m^{-3}. Juodosios anglies, BC_{FF} ir BC_{BB} koncentracijų paros svyravimai atskleidžia ryškią miesto oro taršos dinamiką, kuriai būdingi ryto ir vakaro taršos pikai. Šildymo laikotarpiu didžiausia juodosios anglies koncentracija siekė 1,44 µg m^{-3}, iš kurios 1,05 µg m^{-3} sudarė iškastinio kuro deginimo kilmės juodosios anglies komponentė, o 0,39 µg m^{-3} – biomasės deginimo kilmės.

Papildomai palyginus abiejų sezonų KD_{10} ir NO_x duomenis, matyti, kad nuo 00:00 iki 16:00 val. jų paros koncentracijos eiga yra labai panaši, tačiau šildymo laikotarpiu koncentracijos yra didesnės. Nors NO_x koncentracijos eiga abiem sezonais yra beveik identiška, NO_x vidutinės koncentracijos paros svyravimai šildymo laikotarpiu yra gerokai didesni nei laikotarpiu be šildymo. Taip yra dėl transporto išmetamų teršalų kintamumo ir vyraujančių Šis skirtumas sietinas su transporto išmetamųjų teršalų kintamumu ir vyraujančiomis meteorologinėmis sąlygomis, pavyzdžiui, mažesniu maišymosi sluoksnio aukščiu [84].

Meteorologinių veiksnių įtaka juodosios anglies koncentracijai buvo vertinama tiek šildymo sezono metu, tiek laikotarpiu be šildymo. Šildymo sezono metu nustatyta stipri teigiama koreliacija tarp BC ir NO_x bei neigiama koreliacija tarp BC, BC_{FF}, BC_{BB}, NO_x ir vėjo greičio. Šie rezultatai rodo, kad mažesnis vėjo greitis skatina didesnį teršalų koncentracijos kaupimąsi, o transporto ir šildymo išmetamosios dujos reikšmingai prisideda prie padidėjusios BC ir NO_x koncentracijos. Laikotarpiu be šildymo koreliacija yra silpnesnė, tačiau išliko teigiama tarp BC, BC_{FF}, BC_{BB} ir KD_{10} bei BC, BC_{FF}, BC_{BB} ir NO_x. Be to, susilpnėjo neigiama koreliacija tarp BC, BC_{FF}, BC_{BB}, NO_x, KD_{10} ir vėjo greičio. Nors BC masės koncentracija tiesiogiai nepriklauso nuo vėjo krypties, poliarinis grafikas leido įžvelgti oro taršos erdvinės ir laikinės kaitos ypatumus. 17 paveiksle pateikta vidutinė BC, BC_{FF}, BC_{BB}, NO_x ir KD_{10} masės koncentracija, atsižvelgiant į vėjo greitį ir kryptį, suteikiant galimybę įvertinti erdvinį teršalų pasiskirstymą. Polinis grafikas atskleidžia, kad šildymo laikotarpiu teršalų šaltiniai yra tolygiai pasiskirstę aplink mėginių ėmimo vietą, nepriklausomai nuo vėjo krypties ir greičio iki 0,5 m s^{-1}. Toks vienodas šaltinių pasiskirstymas rodo, kad vietiniai taršos šaltiniai, tokie kaip gyvenamieji namai su decentralizuotu šildymu, stipriai prisideda prie BC ir NO_x emisijų, o vėjo greitis turi tik ribotą poveikį teršalų pernašai šioje teritorijoje. Vis dėl to galima pastebėti, kad KD_{10} teršalai atkeliauja iš

papildomų šaltinių pietvakarių ir vakarų kryptimis, kai vėjo greitis siekia apie 3 m s^{-1}, bei šiaurės vakarų kryptimi, kai vėjo greitis yra nuo 2,5 iki 3 m s^{-1}. Tuo tarpu BC, BC$_{FF}$, BC$_{BB}$ ir NO$_x$ polinės diagramos laikotarpiu be šildymo atskleidžia, kad teršalų sklaidai didžiausią įtaką daro du pagrindiniai šaltiniai. Šiuo laikotarpiu pagrindinis BC šaltinis išlieka vietinės kilmės, panašus į stebėtąjį šildymo sezono metu, tačiau nustatyta papildoma tarša iš pietvakarių ir pietryčių krypčių. Didžiausia BC koncentracija, viršijanti 0,70 µg m^{-3}, buvo stebėta esant mažam vėjo greičiui ramiomis dienomis, kai vietiniai išmetamieji teršalai buvo tolygiai pasiskirstę po visą teritoriją, taip pat esant didesniam nei 2,5 m s^{-1} vėjo greičiui.

<center>BC masės koncentracijos sezoniškumas ir paros laiko dinamika</center>

BC masės koncentracijos kintamumas rodo sudėtingą sąveiką tarp išmetamųjų teršalų šaltinių, meteorologinių sąlygų ir žmonių veiklos miestuose. Žiemos mėnesiais BC koncentracija buvo aukštesnė (1,14 µg m^{-3}), palyginti su vasaros mėnesiais (0,55 µg m^{-3}). Šį reiškinį galima paaiškinti padidėjusiu biomasės deginimu gyvenamųjų namų šildymui ir žemesne temperatūra (4 lentelė, 6 paveikslas). Didžiausios biomasės deginimo kilmės BC$_{BB}$ koncentracijos buvo stebimos žiemą (0,35 µg m^{-3}), o mažiausios – rudenį (0,23 µg m^{-3}). Panaši tendencija pastebima ir su BC$_{FF}$ koncentracija, kuri taip pat aukštesnė žiemą (0,78 µg m^{-3}), palyginti su kitais metų laikais. Be to, pavasarį, ypač kovo mėnesį, žolės deginimas reikšmingai prisideda prie padidėjusios oro taršos, įskaitant BC koncentraciją dėl oro masių tolimosios pernašos iš kaimyninių regionų, ypač ne Europos Sąjungos šalių [81-83]. Vidutinė biomasės deginimo kilmės BC$_{BB}$ dalis bendroje BC masės koncentracijoje skirtingais metų laikais taip pat reikšmingai kito: didžiausia BC$_{BB}$ dalis (41,0%) buvo stebėta vasarą, o mažiausia – rudenį (23%). Šie rezultatai atspindi sezoninius taršos šaltinių įtakos skirtumus ir jų poveikį BC koncentracijai.

Savaitės dienų BC masės koncentracijos tendencijos rodo, kad savaitės darbo dienomis koncentracijos buvo didesnės, o tai gali būti siejama su intensyvesne miesto veikla ir padidėjusiais transporto srautais. Panašūs dėsningumai pastebimi ir kituose tyrimuose [30,41]. 5 paveiksle pateikiama skirtingos kilmės BC masės koncentracijos, paros eiga ir dažnių pasiskirstymas. Visų keturių sezonų BC$_{FF}$ ir BC$_{BB}$ paros eiga pasižymėjo panašiomis kitimo tendencijomis. Pavasario ir vasaros sezonais ryškiausi rytiniai koncentracijos maksimumai buvo nuosekliai stebimi tarp 07:00 ir 09:00 val., o žiemos ir rudens sezonais jie buvo registruojami šiek tiek vėliau, tarp 08:00 ir 11:00 val. Be to, visais keturiais metų laikais buvo stebimas

vakarinis BC koncentracijos pikas. Pažymėtina, kad perėjimas iš žiemos į vasaros laiką turi įtakos piko pasireiškimo laikui perkeldamas jį vėlesniam paros laikui. Siekiant kiekybiškai įvertinti BC masės koncentracijos verčių kintamumą skirtingais metų laikais ir geriau suprasti su biomasės deginimu bei transporto išmetamaisiais teršalais susijusius svyravimus, buvo sudaryti dažninio skirstinio (histogramos) grafikai. Vasarą BC_{FF} masės koncentracijos dažnio skirstinys buvo palyginti siauras, neviršijantis 0,4 µg m^{-3}. Tuo tarpu rudenį ir žiemą BC_{FF} dažnio skirstinio diapazonas buvo platesnis, tačiau neviršijo 1 µg m^{-3}.

Vėjo krypties ir poliarinės sąlyginės tikimybės funkcijos (CPF) analizės derinys suteikia vertingų įžvalgų apie teršalų šaltinio vietą ir jų charakteristikas. Šis metodas leidžia nustatyti, ar teršalai kyla iš tolimųjų regionų ar formuojasi vietoje. Pastebėta, kad BC masės koncentracija yra aukštesnė rudens ir žiemos sezonais, ypač esant silpnam vėjo greičiu (0,5 m s^{-1}). Norint įvertinti šalia esančių taršos šaltinių poveikį, buvo atlikta duomenų vizualizacija procentilių rožės grafiku, kuris atskleidė didelių koncentracijų kryptis skirtingais metų laikais. Diagramos analizė rodo, kad teršalų šaltiniai skiriasi priklausomai nuo sezono. Rudenį, pavasarį ir vasarą didelės koncentracijos kyla iš kelių krypčių, tuo tarpu žiemą didžiausios koncentracijos koncentruojasi šiaurės vakarų, vakarų ir šiaurės rytų kryptimis.

Kompleksinė juodosios anglies masės koncentracijos analizė taikant sąlygines tikimybės funkcijas

Atmosferos teršalų šaltinių nustatymui buvo taikoma plačiai naudojama sąlyginės tikimybės funkcijos (CPF) analizė. Šis metodas suteikia informaciją apie teršalų šaltinių kryptis, nurodydamas, kurios vėjo kryptys ir greičiai yra susiję su didžiausiomis teršalų koncentracijomis. Rudenį BC koncentracijos 75-ojo procentilio CPF analizė atskleidė papildomą taršos šaltinį pietų kryptimi, kai vėjo greitis svyruoja nuo 1 iki 3 m s^{-1} (21c paveikslas). Tuo tarpu, BC koncentracijos 25-ojo procentilio CPF analizė rodo nedidelę vietinės taršos indėlio tikimybę ir nurodo kelių taršos šaltinių buvimą visomis kryptimis (20-23d paveikslai). Rudens ir žiemos sezonu CPF pasižymi panašiais bruožais, o didžiausia tikimybė stebima šiaurės vakarų, vakarų, šiaurės rytų, pietų ir pietryčių kryptimis. Analizuojant 24-25 paveikslus, pastebima, kad NO_x tarša visais metų laikais sąlygojama vietinių šaltinių, t.y. rodo pastovų emisijos šaltinį, nesusijusį su tolimųjų pernašų poveikiu. Tuo tarpu KD_{10} tarša, ypač pavasarį gali kilti iš šiaurės rytų ir šiaurės vakarų krypčių, kai vėjo greitis siekia 2,5 m s^{-1}. Be to, identifikuotas taršos šaltinis pietų kryptimi, kai vėjo greitis siekia 1-1,5 m s^{-1}. Šie duomenys pabrėžia

skirtingą teršalų šaltinių pobūdį ir sklaidos mechanizmus. Teršalų koncentracijos rožių diagramose pavaizduota vėjo krypčių įtaka bendrai teršalų koncentracijai, taip pat pateikti skirtingi koncentracijos lygiai. Analizuojant duomenis, matyti, kad visais keturiais metų laikais šiaurės vakarų krypties vėjai nuolat lemia didžiausią teršalų – BC, NO_x ir KD_{10} koncentraciją (20-25 pav.). Tačiau sezoniškumas išryškina krypties ir šaltinių skirtumus: vasaros mėnesiais vyrauja šiaurės rytų krypties vėjai, rodantys kitokius šaltinius ar sklaidos mechanizmus, tuo tarpu rudens ir žiemos sezonais didžiausią įtaką turi pietų ir pietryčių kryptys.

Pearsono koreliacijos koeficientų matricos ir dendrogramos, pateiktos 24 paveiksle, leidžia įvertinti tarpusavio sąsajas tarp oro teršalų (BC, KD_{10} ir NO_x) ir meteorologinių parametrų (vėjo greitis (WS), vėjo kryptis (WD), santykinė drėgmė (RH), temperatūra (T) ir atmosferos slėgis (P)) skirtingais metų laikais – vasarą, rudenį, žiemą ir pavasarį. Analizė atskleidė, kad koreliacijos koeficientas tarp BC ir kitų parametrų kinta priklausomai nuo sezono, Rezultatai patvirtina, kad BC, BC_{FF}, BC_{BB} ir NO_x nuolat formuoja tą patį klasterį, pasižymintį vidutiniu arba stipriu koreliacijos laipsniu (nuo r=0,48 iki r=0,65). Pavyzdžiui, vasaros sezono metu KD_{10} išsiskiria į atskirą klasterį, turintį labai silpną koreliaciją su BC ir jo sudedamosiomis dalimis. Tačiau kitais sezoniniais laikotarpiais koreliacija svyruoja nuo silpnos iki vidutinės (nuo r=0,38 iki r=0,53). Dendrograma rodo, kad visi meteorologiniai parametrai, išskyrus slėgį, yra nuosekliai sugrupuoti, tačiau slėgis paprastai yra atskirtas ir tik rudens mėnesiais patenka į tą patį klasterį kaip ir kiti meteorologiniai parametrai. Koreliacinė matrica atskleidžia, kad vasarą BC labiausiai koreliuoja su vėjo greičiu; rudenį su temperatūra, ypač BC_{BB}; žiemą pastebima koreliacija su visais meteorologiniais parametrais, tačiau stipriausia yra tarp vėjo greičio ir BC bei BC_{FF}; pavasarį didžiausia koreliacija siejama su slėgiu, vėjo greičiu ir temperatūra. Be to, temperatūra turi stipresnę koreliaciją su biomasės deginimo kilmės BC_{BB}, o vėjo greitis rodo stipresnę koreliaciją su BC ir iškastinio kuro deginimo kilmės $BC_{FF.}$

Didelės taršos epizodų BC masės koncentracijos įvykių analizė

Kaip aptarta ankstesniuose šio tyrimo skyriuose, BC koncentracijos kaita atspindi ne tik meteorologinių sąlygų, bet ir šaltinio kilmės įtaką, todėl pastebimi ryškūs sezoniniai svyravimai. Atsižvelgiant į šias aplinkybes, siekiant tiksliau įvertinti kiekvieno sezono specifinius veiksnius ir sąlygas, duomenys buvo analizuojami atskirai kiekvienam sezonui. Tyrimo metu buvo identifikuota 18 dienų, kai BC masės koncentracija viršijo 95-ąjį atitinkamo sezono užregistruotų koncentracijų procentilį (27 paveikslas). Šie atvejai

pasiskirstė tarp sezonų: vasarą užfiksuoti penki atvejai (birželio 12 d., birželio 23 d., birželio 30 d., liepos 16 d. ir rugpjūčio 23 d.), rudenį – keturi (spalio 8-10 d. ir lapkričio 11 d.), žiemą – penki (gruodžio 23 d., gruodžio 31 d., sausio 10 d., sausio 12 d. ir sausio 23 d.) ir pavasarį – keturi (kovo 14-15 d. ir kovo 22-23 d., kai kurios dienos laikytinos dviem atvejais dėl jų trukmės dvi paras iš eilės. Analizė taip pat atskleidė, pastebėta, kad šiomis dienomis dažnai buvo padidėjusi KD_{10} ir NO_x koncentracija. Lyginant šių dienų poveikį vidutinei metinei koncentracijai su dienomis, kai tarša buvo įprasta, nustatyta, kad BC, BC_{FF} ir BC_{BB} koncentracijos padidėjo atitinkamai 9,9%, 10,5% ir 12,5%, o KD_{10} ir NO_x – 3,5% ir 6,9%. Kaip parodyta 28 paveiksle, didelės taršos dienomis BC, KD_{10} ir NO_x koncentracijos buvo maždaug dvigubai didesnės nei įprastomis dienomis, t.y. sąlyginai neužterštomis dienomis. Šiomis dienomis vidutinė BC, KD_{10} ir NO_x koncentracija atitinkamai siekė 0,81, 19,02 ir 20,21 $\mu g\ m^{-3}$. Tuo tarpu didelės taršos dienomis šios vertės padidėjo iki 2,38, 32,17 ir 48,56 $\mu g\ m^{-3}$, t. y. BC koncentracija padidėjo tris kartus, o NO_x – 2,4 karto.

Pagrindiniai veiksniai, lemiantys padidėjusias koncentracijas ir didelio užterštumo epizodus, yra glaudžiai susiję su sezoniniais skirtumais. Analizuojant didelės taršos epizodus, nustatyta neigiama koreliacija (nuo – 0,43 iki – 0,54) tarp vėjo greičio ir BC koncentracijos visais sezonais, išskyrus žiemą. Tai rodo, kad didesni vėjo greičiai yra susiję su žemesnėmis BC koncentracijomis dėl teršalų išsklaidymo. Tačiau žiemos sezonu pastebėtas aiškus ryšys tarp ramių pietinių vėjų ir didesnių BC koncentracijų (r = 0,56), pabrėžiantis vietinių šaltinių svarbą šiuo laikotarpiu. Be to, net 80% didelės taršos epizodų žiemą stebėta teigiama koreliacija tarp BC ir KD_{10} (nuo 0,26 iki 0,57) bei NO_x (nuo 0,60 iki 0,87). Šie duomenys rodo, kad šių teršalų kilmė gali būti glaudžiai susijusi, greičiausiai atsirandanti iš bendrų taršos šaltinių, tokių kaip šildymo sistemos ar transportas. Priešingai, likusiems 20% didelės taršos epizodų buvo būdinga neigiama koreliacija (nuo -0,11) tarp KD_{10} ir NO_x (nuo -0,29), kas leidžia daryti prielaidą apie skirtingus šių teršalų šaltinius arba sklaidos sąlygas. Šiais atvejais koreliacija su vėjo kryptimi taip pat buvo nevienareikšmė: ji kito nuo neigiamos koreliacijos su vėjo greičiu (nuo -0,39 iki -0,82) iki teigiamos (nuo 0,51 iki 0,81). Šie rezultatai pabrėžia skirtingų šaltinių vietos ir meteorologinių sąlygų poveikį teršalų koncentracijų dinamikai žiemą. Vasaros sezono metu 60 % atvejų nustatyta silpna teigiama koreliacija tarp BC ir KD_{10} (nuo 0,09 iki 0,18), o likusiais 40% atvejų – stipri teigiama koreliacija (nuo 0,45 iki 0,57). Šie rezultatai gali rodyti labiau koncentruotus taršos šaltinius arba specifines meteorologines sąlygas, darančias įtaką taršos pasiskirstymui. Be to, vasaros sezono metu pastebėtas

kintantis ryšys su vėjo greičiu: 80% atvejų nustatyta neigiama koreliacija (nuo -0,21 iki -0,39), o 20% – teigiama (0,38), kas rodo krypties priklausomybę nuo specifinių taršos šaltinių.

Vienas ryškiausių epizodų, kai vasaros mėnesiais fiksuota didžiausia oro tarša, yra birželio 23-24 d., sutampantis su Joninių šventės laikotarpiu. Šiomis dienomis pastebimas reikšmingas oro užterštumo padidėjimas, kurį lemia intensyvus malkų deginimas atviruose laužuose, tradiciškai siejamas su šventės apeigomis. Padidėjusios teršalų koncentracijos atmosferoje šiuo laikotarpiu yra būdingas sezoninis reiškinys, kurį lemia plataus masto laužų deginimas. Šis poveikis gali apimti ne tik Lietuvą, bet ir kai kurias kaimynines šalis, reikšmingai blogindamas oro kokybę. Palyginti su ankstesnėmis ir vėlesnėmis dienomis, birželio 23-24 d. buvo stebimas dvigubai didesnis tiek BC, tiek biomasės deginimo kilmės BC_{BB} koncentracijos lygis. Santykinės oro drėgmės ir temperatūros poveikis buvo reikšmingas tik vasaros ir pavasario sezonais, o didelės taršos dienomis šių meteorologinių veiksnių įtaka padidėjo daugiau nei dvigubai Šie rezultatai atskleidžia, kad šiltuoju metų laiku meteorologinės sąlygos gali ženkliai prisidėti prie teršalų kaupimosi atmosferoje, ypač esant intensyviems vietiniams taršos šaltiniams. Rudens sezonu 50% atvejų nustatyta stipri teigiama koreliacija tarp BC ir KD_{10} (r = 0,64) bei neigiama su vėjo kryptimi (r = -0,53). Likusiais 50% atvejų ryšys tarp BC ir KD_{10} buvo labai silpnas (r = 0,12), kaip ir su vėjo kryptimi (-0,19). Pavasarį didelės taršos epizodai dažnai siejami su nelegaliu žolės deginimu žemės ūkyje Kaliningrado srityje, Ukrainoje ir Baltarusijoje [82,83]. Šią prielaidą patvirtina smogo formavimosi ir aktyvių gaisrų duomenys. Tai patvirtina 29 paveiksle pateiktas tipiškas pavasarinio žolės deginimo pavyzdys, stebėtas 2022 m. kovo 22 dienomis.

Palyginus įprastų dienų (24 paveikslas) bei didelės taršos epizodų (30 paveikslas) dendrogramą, pastebimas koreliacijų sustiprėjimas ir duomenų klasterizacijos pokytis. Aptiktas stipresnis neigiamas ryšys tarp BC ir meteorologinių parametrų, ypač vėjo greičio ir oro temperatūros, visais metų laikais. Šie rezultatai atskleidžia atvirkštinį ryšį, kai didesnis vėjo greitis susijęs su mažesniu BC lygiu, o žemesnė oro temperatūra – su aukštesniu BC lygiu. Tarp BC ir vėjo krypties taip pat fiksuotas stipresnis ryšys tam tikromis žiemos ir pavasario sezonų dienomis. Pastarasis pavasario sezonas išsiskyrė kaip netipiškas ir reikalauja atskiros analizės. Pavasarį koreliacija tarp BC ir NO_x išliko nepakitusi, tačiau ryšys su KD_{10} susilpnėjo. Tai taip pat vienintelis sezonas, kai BC koreliacija su atmosferos slėgiu didelės taršos epizodais buvo žymiai silpnesnė nei įprastomis dienomis. Žiemos sezonu stebėtas unikalus drėgmės poveikis, kuomet koreliacija su santykine drėgme pasikeitė iš silpnai teigiamos į silpnai neigiamą, kas išskiria šį laikotarpį nuo kitų metų sezonų.

BC koncentracijos santykis tarp vidaus ir išorės aplinkos

Tyrimo tikslas buvo įvertinti lauko taršos kietosiomis dalelėmis poveikį patalpų oro kokybei. Rezultatai parodė, kad trijų pakopų filtro sistema patalpose užtikrina veiksmingą apsaugą nuo taršos kietosiomis dalelėmis iš įvairių šaltinių, taip žymiai sumažindama šios taršos poveikį patalpose. Vidutinė kietųjų dalelių ir BC koncentracija buvo reikšmingai didesnė (1.20 ± 0.97 µg m^{-3}) lauke nei patalpose (0.04 ± 0.03 µg m^{-3}). Be to, stebint taršos pikus, nustatyta, kad didelės taršos dienomis BC koncentracija lauke didėjo 3-4 kartus, tuo tarpu patalpose ji išliko maža. Nepaisant to, smulkių aerozolio dalelių (<1 µm) koncentracija patalpose padidėjo tik nežymiai, ypač BC atveju. Šie rezultatai leido geriau suprasti ryšį tarp BC ir didelės taršos epizodų.

Vėdinimo sistemos filtravimo efektyvumas buvo įvertintas naudojant patalpų ir lauko koncentracijos (I/O) santykį kaip aerozolio dalelių infiltracijos rodiklį, ypač kai patalpoje nėra jokių vietinių taršos šaltinių. Infiltracijos koeficientas (F_{inf}) rodo, kokia dalis aerozolio dalelių lauko ore patenka į patalpas, todėl jis yra svarbus rodiklis vertinant vidinės oro kokybės pokyčius ir lauko taršos poveikį. F_{inf} vertės buvo apskaičiuotos taikant tiesinės regresijos metodą, kurio nuolydis atitinka infiltracijos koeficientą, o intercepcija interpretuojama kaip patalpose išmetamų teršalų šaltinio rodiklis [85]. Tiriamuoju laikotarpiu F_{inf} reikšmės vertinant BC lygiu lauko ore ir patalpose siekė 0,8, o tai atitinka ankstesnio tyrimo rezultatus [86].

Lauko ore BC$_{FF}$ ir BC$_{BB}$ masės koncentracija svyravo nuo 0,03 iki 7,25 µg m^{-3} (vidutinė vertė siekė $0,97 \pm 0,79$ µg m^{-3}) ir nuo 0,03 iki 2,13 µg m^{-3} (vidutinė vertė siekė $0,23 \pm 0,20$ µg m^{-3}), o patalpų ore svyruoja atitinkamai nuo 0,09 iki 0,21 µg m^{-3} ir nuo 0,02 iki 0,09 µg m^{-3}. Tyrimo rezultatai rodo, kad BC$_{BB}$ sudaro apie 20% visos BC koncentracijos tiek patalpose, tiek lauko ore (32 paveikslas). Nustatyta, kad BC$_{FF}$ dalis yra žymiai didesnė (80%) nei BC$_{BB}$ dalis, o tai rodo, kad šildymo sezono metu iškastinio kuro deginimas yra pagrindinis BC masės koncentracijos Vilniuje šaltinis. 32 paveiksle pateikti biomasės deginimo ir iškastinio kuro deginimo BC (BC$_{FF}$ ir BC$_{BB}$) valandinių vidutinių koncentracijų paros eigos patalpų ir lauko ore. Iškastinio kuro deginimo kilmės BC$_{FF}$ koncentracijai būdingas bimodalinis dienos eigos profilis, susijęs su srautais, kurio aukščiausios koncentracijos stebimos rytinio (1,12 µg m^{-3}) ir vakarinio piko valandomis (1,50 µg m^{-3}) (33a paveikslas). Priešingai, savaitgaliais BC$_{FF}$ koncentracijos paros kaita buvo mažiau ryški ir pasižymėjo vienmodaliniu pasiskirstymu. Savaitgaliais BC$_{FF}$ koncentracija didėjo dienos metu ir nuo 10 iki 20 val. siekė – 0,98-1,50 µg m^{-3}.

Patalpose buvo stebimas panašus BC_{FF} koncentracijos savaitės eigos profilis, tačiau rytinio piko valandomis padidėjimas nebuvo toks ryškus kaip lauke (32b paveikslas). Kita vertus, BC_{BB} paros koncentracijos eiga pasižymėjo vienmodaliniu pasiskirstymu, kuomet po 16:00 val. koncentracija stabiliai kilo ir pasiekė 0,44 µg m⁻³. Šis skirtumas tarp BC komponentų rodo skirtingus teršalų šaltinius ir veiklos ypatumus, lemiančius specifinę paros eigą patalpų ir lauko ore. Šie rezultatai rodo reikšmingą gyvenamųjų namų medienos deginimo poveikį oro kokybei, ypač per šildymo sezoną. Kaip pavaizduota 33e paveiksle, BC_{FF} koncentracija lauke pasižymėjo ryškia savaitės eiga (33e paveikslas): didžiausia koncentracija (1,24 µg m⁻³) buvo stebima trečiadieniais, o mažiausia (0,74 µg m⁻³) – sekmadieniais. Darbo dienomis BC_{FF} koncentracija buvo vidutiniškai 27% didesnė nei savaitgaliais, atspindėdama padidėjusią su transportu ir gyvenamųjų patalpų šildymu susijusią veiklą. Ši tendencija leidžia geriau suprasti darbo savaitės metu vyraujančius teršalų šaltinius bei šildymo poreikių skirtumus. Tyrimo rezultatai parodė, kad biomasės deginimo šaltinių indėlis BC masės koncentracijai išliko stabilus visą savaitę, sudarydamas apie 19% lauke ir 21% patalpose. Sekmadieniais BC_{BB} koncentracija buvo panaši į darbo dienų lygį (0,21-0,29 µg m⁻³) arba net žemesnė, o tai leidžia daryti prielaidą, kad biomasės deginimo intensyvumas šiuo metu nekinta. Vis dėlto, dėl sumažėjusios BC_{FF} koncentracijos sekmadieniais, BC_{BB} indėlis atrodo santykinai didesnis. Savaitės juodosios anglies koncentracijų I/O santykio vertės per savaitę išliko pastovios, svyruodamos tarp 0,03 ir 0,04, kas rodė, jog patalpose emisijos šaltinių nebuvo.

Juodosios anglies nusėdimas ant medžių lajos

Šio tyrimo metu nustatyta, kad medžių gebėjimas sulaikyti taršą turi potencialą ir yra svarbus ypač didelio užterštumo dienomis, kai miesto teritorijose, dėl transporto eismo ir biomasės deginimo šildymo reikmėms, pablogėja oro kokybė.

Juodosios anglies nusėdimo analizė, atlikta Vilniuje ne šildymo sezono metu, parodė tipišką šio miesto sąlygas atitinkančią BC masės koncentraciją – 0,85 (0,91) µg m⁻³. Tuo tarpu, atskiros BC frakcijų (BC_{FF} ir BC_{BB}) vertės siekė $0,42 \pm 0,54$ µg m⁻³ ir $0,39 \pm 0,32$ µg m⁻³, atitinkamai (34 paveikslas).

Tyrimo metu nustatyta, kad lapų ir spyglių mėginiuose randama su kuro ir biomasės deginimu susijusių aerozolio dalelių. Be to, šiose dalelėse aptikta nedidelės koncentracijos Si, Ca ir Fe elementų, kurie padeda identifikuoti teršalų šaltinius. Silicio ir kalcio dalelės gali atsirasti iš transporto priemonių išmetamųjų dujų, kadangi Si naudojamas degaluose, o Ca – kaip alyvos

priedas [88]. Silicio turinčios dalelės taip pat buvo identifikuotos kaip kvarcas, kuris gali atsirasti deginant iškastinį kurą o geležies pėdsakai gali būti siejami su deginimu [60]. Taip pat buvo pastebėta, kad kai kurios dalelės buvo paveiktos atmosferos sąlygų ir senėjimo procesų [89]. Juodosios anglies apvalkalas ant dalelių susidaro, kai pirminis arba antrinis organinis aerozolis koaguliuojasi arba kondensuojasi. Šis apvalkalas padidina šviesos sugertį dėl lęšio efekto, kuris priklauso nuo dalelių senėjimo laipsnio, taip prisidedant prie didesnės oro taršos poveikio.

Tipišką BC aglomeratą sudaro į grandinę susijungusios sferinės dalelės. Nustatyta, kad pirminių dalelių skersmuo svyravo nuo 24,23 nm iki 30,02 nm ant lapų ir nuo 32,45 nm iki 44,13 nm ant spyglių (9 lentelė). Didžiausi BC dalelių aglomeratai buvo 288,52 nm ilgio ir 220,39 nm pločio, o didesnių aglomeratų aptikta ant paprastųjų eglių spyglių. Ankstesni tyrimai taip pat parodė, kad spygliuočiai veiksmingiau i šalina oro taršą dėl didelio medžių tankumo, ilgesnės spyglių gyvavimo trukmės ir storesnio epicuticularinio vaško sluoksnio, palyginti su lapuočių rūšių lapais [90,91]. Šie veiksniai lemia didesnį BC kaupimąsi spygliuose, sustiprindami oro valymo efektyvumą.

Išvados

1. Juodosios anglies koncentracija Vilniuje pasižymi sezoniškumu. Šildymo sezono metu BC koncentracija yra žymiai aukštesnė (1,17 µg m^{-3}), palyginus su laikotarpiu, kai šildymo veikla nevykdoma (0,61 µg m^{-3}). Šį skirtumą dar labiau išryškina didesnė BC masės koncentracijos moda šildymo sezono metu (0,26 µg m^{-3}), palyginus su 0,16 µg m^{-3}, kai šildymas nebuvo vykdomas. Nors biomasės deginimo kilmės BC$_{BB}$ indėlis pasižymi ryškiu sezoniniu maksimumu vasarą, sudarydamas 41% visos BC masės koncentracijos, iškastinio kuro deginimas išlieka dominuojančiu ir pastoviu šaltiniu ištisus metus, sudarydamas 71% bendros BC masės koncentracijos.

2. Sąlyginės tikimybės funkcijos analizė atskleidė homogenišką BC$_{FF}$ ir BC$_{BB}$ pasiskirstymą (kaip ir NO$_x$ ir KD$_{10}$ atveju) esant ramiam vėjo greičiui (iki 0,5 m s^{-1}), kas rodo, kad šildymo sezono metu vyrauja vietiniai taršos šaltiniai. Tačiau laikotarpiu, kai šildymo veikla nevykdoma, pastebimas šaltinių indėlio pokytis, atsirandantis dėl papildomų nutolusių šaltinių pietvakarių ir pietryčių kryptimis, kas rodo regioninės pernašos poveikio įtaką. Be to, sąlyginai žemos BC koncentracijos, išreikštos 25-uoju procentiliu, yra susijusios su keliomis šaltinių kryptimis, kas rodo tiek vietinių, tiek pernešamų teršalų mišinį. Atvirkščiai, rudenį, esant 1–2 m s^{-1} vėjo greičiui, stebimos padidėjusios BC koncentracijos (75-asis procentilis), susijusios su šaltiniu pietų kryptimi.

3. Pavasarį Vilniaus oro taršos dinamika atskleidžia unikalią taršos šaltinių ir meteorologinių veiksnių sąveiką. Nors ištisus metus didžiausią BC masės koncentraciją paprastai lemia šiaurės vakarų vėjo kryptis, pavasarį dominuojančiais taršos šaltiniais tampa pietryčių ir pietų-pietryčių krypčių vėjai. Šį sezoninį pokytį patvirtina ir silpnėjanti koreliacija tarp BC ir PM_{10}, rodanti, kad, palyginti su kitais sezonais, pasikeitė taršos šaltiniai. Silpnesnė koreliacija (r =0,18) tarp BC ir slėgio didelio užterštumo dienomis pavasarį, palyginti su įprastomis dienomis (r =0,40), atskleidžia sudėtingą pavasario oro kokybę lemiančių veiksnių tarpusavio sąveiką.

4. Iškastinio kuro deginimo kilmės juodoji anglis sudarė žymiai didesnę dalį (80%) bendros BC masės koncentracijos, palyginti su biomasės deginimu susijusios BC dalimi (20%) tiek patalpose, tiek lauke. Iškastinio kuro kilmės BC masės koncentracija lauke pasižymėjo aiškiu bimodaliniu paros profiliu, pasiekdama aukščiausius lygius rytinio ir vakarinio piko valandomis, kas atspindi eismo intensyvumo įtaką. Nors panaši tendencija buvo stebima ir patalpose, maksimumai buvo mažiau ryškūs, kas rodo pastatų filtravimo efektyvumą.

5. Nepaisant mažesnio BC_{BB} indėlio bendrai BC koncentracijai, paros eiga pasižymėjo vienmodaliniu profiliu, su aukščiausiomis vertėmis vakare, kurios susijusios su gyvenamųjų namų šildymu biomase. Nustatyta, kad BC taršai lauke didėjant 3–4 kartus, BC koncentracija patalpose dvigubėja, kas rodo didelę lauko oro infiltracijos įtaką ekstremalios taršos epizodais.

6. Vilniuje surinktų paprastosios eglės spyglių ir sidabrinio beržo lapų mėginių analizė atskleidė, kad didesni BC aglomeratai nusėda ant spyglių (skersmuo 32,45–41,30 nm), palyginti su lapais (24,23–30,02 nm). Šis skirtumas leidžia daryti prielaidą, kad spygliuočiai geba efektyviau sulaikyti oro teršalus dėl unikalios spyglių struktūros, storesnių vaško sluoksnių ir ištisus metus esančios lajos.

REFERENCES

[1]   V. A. Lanz et al., *Characterization of Aerosol Chemical Composition with Aerosol Mass Spectrometry in Central Europe: An Overview*, Atmos. Chem. Phys. **10**, 10453 (2010).

[2]   S. K. Friedlander~ and W M Keck, "THE CHARACTERIZATION OF AEROSOLS DISTRIBUTED WITH RESPECT TO SIZE AND CHEMICAL COMPOSITION", Pergamon Press, 1970.

[3]   U.S. EPA, *Report to Congress on Black Carbon*, Dep. Inter. Environ. Relat. Agencies Appropriations Act, 2010 388 (2012).

[4]   European Environment, *European Environment Agency, Air Quality in Europe – 2019 Report* (2019).

[5]   B. M. Steensen, M. Schulz, N. Theys, and H. Fagerli, *A Model Study of the Pollution Effects of the First Three Months of the Holuhraun Volcanic Fissure*, Atmos. Chem. Phys. Discuss. **2016**, 1 (2016).

[6]   O. Ramírez, A. M. Sánchez de la Campa, D. Sánchez-Rodas, and J. D. de la Rosa, *Hazardous Trace Elements in Thoracic Fraction of Airborne Particulate Matter: Assessment of Temporal Variations, Sources, and Health Risks in a Megacity*, Sci. Total Environ. **710**, 136344 (2020).

[7]   S. M. Almeida, M. Manousakas, E. Diapouli, Z. Kertesz, L. Samek, E. Hristova, K. Šega, R. P. Alvarez, C. A. Belis, and K. Eleftheriadis, *Ambient Particulate Matter Source Apportionment Using Receptor Modelling in European and Central Asia Urban Areas*, Environ. Pollut. **266**, 115199 (2020).

[8]   F. Karagulian, C. A. Belis, C. F. C. Dora, A. M. Prüss-Ustün, S. Bonjour, H. Adair-Rohani, and M. Amann, *Contributions to Cities' Ambient Particulate Matter (PM): A Systematic Review of Local Source Contributions at Global Level*, Atmos. Environ. **120**, 475 (2015).

[9]   S. Chansuebsri, P. Kolar, P. Kraisitnitikul, N. Kantarawilawan, N. Yabueng, W. Wiriya, D. Thepnuan, and S. Chantara, *Chemical Composition and Origins of PM2.5 in Chiang Mai (Thailand) by Integrated Source Apportionment and Potential Source Areas*, Atmos. Environ. **327**, 120517 (2024).

[10]   F. Pini, G. Piras, D. Astiaso Garcia, and P. Di Girolamo, *Impact of the Different Vehicle Fleets on PM10 Pollution: Comparison between the Ten Most Populous Italian Metropolitan Cities for the Year 2018*, Sci. Total Environ. **773**, (2021).

[11]   L. Drudi, M. Giardino, M. Tedone, A. Tiano, D. Janner, F. Pognant, F. Matera, M. Sacco, L. Bardi, and R. Bellopede, *An Analysis of the PM10 Chemical Composition and Its Spatial and Seasonal Variation in Piedmont (Italy) Using Raman Spectroscopy*, Sci. Total Environ. **951**, 175427 (2024).

[12]   H. Rosen and T. Novakov, *Optical Transmission through Aerosol*

Deposits on Diffusely Reflective Filters: A Method for Measuring the Absorbing Component of Aerosol Particles, Appl. Opt. **22**, 1265 (1983).

[13] European Environment Agency, *Air Quality in Europe 2021, EEA Report No 15/2021, Publications Office of the European Union* (2021).

[14] O. Gruzieva, A. Georgelis, N. Andersson, T. Bellander, C. Johansson, and A. S. Merritt, *Comparison of Measured Residential Black Carbon Levels Outdoors and Indoors with Fixed-Site Monitoring Data and with Dispersion Modelling*, Environ. Sci. Pollut. Res. (2020).

[15] M. Becerril-Valle, E. Coz, A. S. H. Prévôt, G. Močnik, S. N. Pandis, A. M. Sánchez de la Campa, A. Alastuey, E. Díaz, R. M. Pérez, and B. Artíñano, *Characterization of Atmospheric Black Carbon and Co-Pollutants in Urban and Rural Areas of Spain*, Atmos. Environ. **169**, 36 (2017).

[16] S. Mbengue, N. Serfozo, J. Schwarz, N. Ziková, A. H. Šmejkalová, and I. Holoubek, *Characterization of Equivalent Black Carbon at a Regional Background Site in Central Europe: Variability and Source Apportionment ✰*, Environ. Pollut. **260**, (2020).

[17] N. Zioła, B. Błaszczak, and K. Klejnowski, *Temporal Variability of Equivalent Black Carbon Components in Atmospheric Air in Southern Poland*, Atmosphere (Basel). **12**, (2021).

[18] J. O. Klompmaker, D. R. Montagne, K. Meliefste, G. Hoek, and B. Brunekreef, *Spatial Variation of Ultrafine Particles and Black Carbon in Two Cities: Results from a Short-Term Measurement Campaign*, Sci. Total Environ. **508**, 266 (2015).

[19] Y. Zhou et al., *Personal Black Carbon and Ultrafine Particles Exposures among High School Students in Urban China*, Environ. Pollut. **265**, (2020).

[20] Y. Huang, L. Zhang, Y. Qiu, Y. Chen, G. Shi, T. Li, L. Zhang, and F. Yang, *Five-Year Record of Black Carbon Concentrations in Urban Wanzhou, Sichuan Basin, China*, Aerosol Air Qual. Res. **20**, 1282 (2020).

[21] E. Hristova, E. Georgieva, B. Veleva, N. Neykova, S. Naydenova, L. Gonsalvesh-Musakova, R. Neykova, and A. Petrov, *Black Carbon in Bulgaria—Observed and Modelled Concentrations in Two Cities for Two Months*, Atmosphere (Basel). **13**, (2022).

[22] A. Helin et al., *Characteristics and Source Apportionment of Black Carbon in the Helsinki Metropolitan Area, Finland*, Atmos. Environ. **190**, 87 (2018).

[23] A. Farah, P. Villani, C. Rose, S. Conil, L. Langrene, P. Laj, and K. Sellegri, *Characterization of Aerosol Physical and Optical Properties at the Observatoire Pérenne de l'Environnement (OPE) Site*, Atmosphere (Basel). **11**, 172 (2020).

[24] S. Gani, S. E. Chambliss, K. P. Messier, M. M. Lunden, and J. S. Apte, *Spatiotemporal Profiles of Ultrafine Particles Differ from Other*

Traffic-Related Air Pollutants: Lessons from Long-Term Measurements at Fixed Sites and Mobile Monitoring, Environ. Sci. Atmos. **1**, 558 (2021).

[25] L. Kirago, M. J. Gatari, Ö. Gustafsson, and A. Andersson, *Black Carbon Emissions from Traffic Contribute Substantially to Air Pollution in Nairobi, Kenya*, Commun. Earth Environ. **3**, 1 (2022).

[26] L. K. Tran, T. N. Quang, N. T. Hue, M. Van Dat, L. Morawska, M. Nieuwenhuijsen, and P. K. Thai, *Exploratory Assessment of Outdoor and Indoor Airborne Black Carbon in Different Locations of Hanoi, Vietnam*, Sci. Total Environ. **642**, 1233 (2018).

[27] G. R. Begam, C. V. Vachaspati, Y. N. Ahammed, K. R. Kumar, S. S. Babu, and R. R. Reddy, *Measurement and Analysis of Black Carbon Aerosols over a Tropical Semi-Arid Station in Kadapa, India*, Atmos. Res. **171**, 77 (2016).

[28] M. Piñeiro-Iglesias, J. Andrade-Garda, S. Suárez-Garaboa, S. Muniategui-Lorenzo, P. López-Mahía, and D. Prada-Rodríguez, *Study of Temporal Variations of Equivalent Black Carbon in a Coastal City in Northwest Spain Using an Atmospheric Aerosol Data Management Software*, Appl. Sci. **11**, 1 (2021).

[29] E. Diapouli, A. C. Kalogridis, C. Markantonaki, S. Vratolis, P. Fetfatzis, C. Colombi, and K. Eleftheriadis, *Annual Variability of Black Carbon Concentrations Originating from Biomass and Fossil Fuel Combustion for the Suburban Aerosol in Athens, Greece*, Atmosphere (Basel). **8**, (2017).

[30] E. Ezani, S. Dhandapani, M. R. Heal, S. M. Praveena, M. F. Khan, and Z. T. A. Ramly, *Characteristics and Source Apportionment of Black Carbon (Bc) in a Suburban Area of Klang Valley, Malaysia*, Atmosphere (Basel). **12**, 1 (2021).

[31] M. P. Raju, P. D. Safai, S. M. Sonbawne, P. S. Buchunde, G. Pandithurai, and K. K. Dani, *Black Carbon Aerosols over a High Altitude Station, Mahabaleshwar: Radiative Forcing and Source Apportionment*, Atmos. Pollut. Res. **11**, 1408 (2020).

[32] A. Ryś and L. Samek, *Yearly Variations of Equivalent Black Carbon Concentrations Observed in Krakow, Poland*, Atmosphere (Basel). **13**, (2022).

[33] K. N. Fossum, J. Ovadnevaite, D. Liu, M. Flynn, C. O'Dowd, and D. Ceburnis, *Background Levels of Black Carbon over Remote Marine Locations*, Atmos. Res. **271**, 106119 (2022).

[34] J. Deng, H. Guo, H. Zhang, J. Zhu, X. Wang, and P. Fu, *Source Apportionment of Black Carbon Aerosols from Light Absorption Observation and Source-Oriented Modeling: An Implication in a Coastal City in China*, Atmos. Chem. Phys. **20**, 14419 (2020).

[35] A. Rana, S. Dey, P. Rawat, A. Mukherjee, J. Mao, S. Jia, P. S. Khillare, A. K. Yadav, and S. Sarkar, *Optical Properties of Aerosol Brown Carbon (BrC) in the Eastern Indo-Gangetic Plain*, Sci. Total Environ.

716, (2020).

[36] B. Liu, Y. Ma, W. Gong, M. Zhang, and Y. Shi, *The Relationship between Black Carbon and Atmospheric Boundary Layer Height*, Atmos. Pollut. Res. **10**, 65 (2019).

[37] X. Liu, Y. Wei, X. Liu, L. Zu, B. Wang, S. Wang, R. Zhang, and R. Zhu, *Effects of Winter Heating on Urban Black Carbon: Characteristics, Sources and Its Correlation with Meteorological Factors*, Atmosphere (Basel). **13**, (2022).

[38] M. Kucbel, A. Corsaro, B. Švédová, H. Raclavská, K. Raclavský, and D. Juchelková, *Temporal and Seasonal Variations of Black Carbon in a Highly Polluted European City: Apportionment of Potential Sources and the Effect of Meteorological Conditions*, J. Environ. Manage. **203**, 1178 (2017).

[39] S. K. Pani, S. H. Wang, N. H. Lin, S. Chantara, C. Te Lee, and D. Thepnuan, *Black Carbon over an Urban Atmosphere in Northern Peninsular Southeast Asia: Characteristics, Source Apportionment, and Associated Health Risks*, Environ. Pollut. **259**, (2020).

[40] E. Liakakou et al., *Long-Term Variability, Source Apportionment and Spectral Properties of Black Carbon at an Urban Background Site in Athens, Greece*, Atmos. Environ. **222**, 117137 (2020).

[41] R. Tang, X. Zhang, Y. Li, and Y. Tan, *Distinct Black Carbon at Two Roadside Sites in Yantai: Temporal Variations and Influencing Factors*, Urban Clim. **44**, 101182 (2022).

[42] M. M. Lunden, T. W. Kirchstetter, T. L. Thatcher, S. V. Hering, and N. J. Brown, *Factors Affecting the Indoor Concentrations of Carbonaceous Aerosols of Outdoor Origin*, Atmos. Environ. **42**, 5660 (2008).

[43] E. Cheek, V. Guercio, C. Shrubsole, and S. Dimitroulopoulou, *Portable Air Purification: Review of Impacts on Indoor Air Quality and Health*, Sci. Total Environ. 142585 (2020).

[44] C.-H. Jeong, S. Salehi, J. Wu, M. L. North, J. S. Kim, C.-W. Chow, and G. J. Evans, *Indoor Measurements of Air Pollutants in Residential Houses in Urban and Suburban Areas: Indoor versus Ambient Concentrations*, Sci. Total Environ. **693**, 133446 (2019).

[45] L. Ferguson, J. Taylor, M. Davies, C. Shrubsole, P. Symonds, and S. Dimitroulopoulou, *Exposure to Indoor Air Pollution across Socio-Economic Groups in High-Income Countries: A Scoping Review of the Literature and a Modelling Methodology*, Environment International.

[46] I. Nezis, G. Biskos, K. Eleftheriadis, P. Fetfatzis, O. Popovicheva, N. Sitnikov, and O.-I. Kalantzi, *Linking Indoor Particulate Matter and Black Carbon with Sick Building Syndrome Symptoms in a Public Office Building*, Atmos. Pollut. Res. **13**, 101292 (2022).

[47] X. Yue et al., *Mitigation of Indoor Air Pollution: A Review of Recent Advances in Adsorption Materials and Catalytic Oxidation*, Journal of Hazardous Materials.

[48] V. Kauneliene, E. Krugly, L. Kliucininkas, I. Stasiulaitiene, T. Prasauskas, A. Auzbikaviciute, P.-A. Bergqvist, T. Tomsej, and D. Martuzevicius, *PAHs in Indoor and Outdoor Air from Decentralized Heating Energy Production: Comparison of Active and Passive Sampling*, Polycycl. Aromat. Compd. **36**, 410 (2016).

[49] L. Kliucininkas, E. Krugly, I. Stasiulaitiene, I. Radziuniene, T. Prasauskas, A. Jonusas, V. Kauneliene, and D. Martuzevicius, *Indoor–Outdoor Levels of Size Segregated Particulate Matter and Mono/Polycyclic Aromatic Hydrocarbons among Urban Areas Using Solid Fuels for Heating*, Atmos. Environ. **97**, 83 (2014).

[50] V. Martins, T. Faria, E. Diapouli, M. I. Manousakas, K. Eleftheriadis, M. Viana, and S. M. Almeida, *Relationship between Indoor and Outdoor Size-Fractionated Particulate Matter in Urban Microenvironments: Levels, Chemical Composition and Sources*, Environ. Res. **183**, 109203 (2020).

[51] J. L. Parker, R. R. Larson, E. Eskelson, E. M. Wood, and J. M. Veranth, *Particle Size Distribution and Composition in a Mechanically Ventilated School Building during Air Pollution Episodes*, Indoor Air **18**, 386 (2008).

[52] B. Stephens and J. A. Siegel, *Penetration of Ambient Submicron Particles into Single-Family Residences and Associations with Building Characteristics*, Indoor Air **22**, 501 (2012).

[53] S. C. Zee, M. Strak, M. B. A. Dijkema, B. Brunekreef, and N. A. H. Janssen, *The Impact of Particle Filtration on Indoor Air Quality in a Classroom near a Highway*, Indoor Air **27**, 291 (2017).

[54] B. Alfoldy, M. M. Mahfouz, A. Gregorič, M. Ivančič, I. Ježek, and M. Rigler, *Atmospheric Concentrations and Emission Ratios of Black Carbon and Nitrogen Oxides in the Arabian/Persian Gulf Region*, Atmospheric Environment.

[55] M. Arif, R. Kumar, R. Kumar, Z. Eric, and P. Gourav, *Ambient Black Carbon, PM2.5 and PM10 at Patna: Influence of Anthropogenic Emissions and Brick Kilns*, Sci. Total Environ. **624**, 1387 (2018).

[56] S. Janhäll, *Review on Urban Vegetation and Particle Air Pollution – Deposition and Dispersion*, Atmos. Environ. **105**, 130 (2015).

[57] Y. Barwise, *Designing Vegetation Barriers for Urban Air Pollution Abatement : A Practical Review for Appropriate Plant Species Selection*, Npj Clim. Atmos. Sci. 1 (2014).

[58] S. Yin, Z. Shen, P. Zhou, X. Zou, S. Che, and W. Wang, *Quantifying Air Pollution Attenuation within Urban Parks: An Experimental Approach in Shanghai, China*, Environ. Pollut. **159**, 2155 (2011).

[59] X. Lan, Y. Jin, and L. Zhu, *High Exposure of Ultrafine Particles at Guangzhou Bus Stops and the Impact of Urban Layout*, Urban Clim. **53**, 101777 (2024).

[60] L. Chen, C. Liu, L. Zhang, R. Zou, and Z. Zhang, *Variation in Tree Species Ability to Capture and Retain Airborne Fine Particulate*

Matter (PM2.5), Sci. Rep. **7**, 3206 (2017).

[61] A. G. Ponette-González, D. Chen, E. Elderbrock, J. E. Rindy, T. E. Barrett, B. W. Luce, J. H. Lee, Y. Ko, and K. C. Weathers, *Urban Edge Trees: Urban Form and Meteorology Drive Elemental Carbon Deposition to Canopies and Soils*, Environ. Pollut. **314**, (2022).

[62] J. Yao, S. Wu, Y. Cao, J. Wei, X. Tang, L. Hu, J. Wu, H. Yang, J. Yang, and X. Ji, *Dry Deposition Effect of Urban Green Spaces on Ambient Particulate Matter Pollution in China*, Sci. Total Environ. **900**, 165830 (2023).

[63] E. Elderbrock, A. G. Ponette-González, J. E. Rindy, J.-H. Lee, K. C. Weathers, and Y. Ko, *Modeling Black Carbon Removal by City Trees: Implications for Urban Forest Planning*, Urban For. Urban Green. **86**, 128013 (2023).

[64] M. Gaglio, R. Pace, A. N. Muresan, R. Grote, G. Castaldelli, C. Calfapietra, and E. A. Fano, *Species-Specific Efficiency in PM2.5 Removal by Urban Trees: From Leaf Measurements to Improved Modeling Estimates*, Sci. Total Environ. **844**, (2022).

[65] E. J. Jin, J. H. Yoon, E. J. Bae, B. R. Jeong, S. H. Yong, and M. S. Choi, *Particulate Matter Removal Ability of Ten Evergreen Trees Planted in Korea Urban Greening*, Forests **12**, 438 (2021).

[66] M. C. Cho, Y. G. Jo, J. A. Son, I. Kim, C. Oh, and S. J. Yook, *Deposition Characteristics of Soot and Tire-Wear Particles on Urban Tree Leaves*, J. Aerosol Sci. **155**, 105768 (2021).

[67] K. Jõgiste et al., *Imprints of Management History on Hemiboreal Forest Ecosystems in the Baltic States*, Ecosphere **9**, (2018).

[68] L. Davulienė et al., *Synergic Use of In-Situ and Remote Sensing Techniques for Comprehensive Characterization of Aerosol Optical and Microphysical Properties*, Sci. Total Environ. **906**, 167585 (2024).

[69] P. Zotter, H. Herich, M. Gysel, I. El-Haddad, Y. Zhang, G. Mocnik, C. Hüglin, U. Baltensperger, S. Szidat, and A. S. H. Prévôt, *Evaluation of the Absorption Ångström Exponents for Traffic and Wood Burning in the Aethalometer-Based Source Apportionment Using Radiocarbon Measurements of Ambient Aerosol*, Atmos. Chem. Phys. **17**, 4229 (2017).

[70] J. Sandradewi, A. S. H. Prévôt, S. Szidat, N. Perron, M. R. Alfarra, V. A. Lanz, E. Weingartner, and U. Baltensperger, *Using Aerosol Light Absorption Measurements for the Quantitative Determination of Wood Burning and Traffic Emission Contributions to Particulate Matter*, Environ. Sci. Technol. **42**, 3316 (2008).

[71] L. Drinovec et al., *The "Dual-Spot" Aethalometer: An Improved Measurement of Aerosol Black Carbon with Real-Time Loading Compensation*, Atmos. Meas. Tech. **8**, 1965 (2015).

[72] A. Minderytė, J. Pauraite, V. Dudoitis, K. Plauškaitė, A. Kilikevičius, J. Matijošius, A. Rimkus, K. Kilikevičienė, D. Vainorius, and S.

Byčenkienė, *Carbonaceous Aerosol Source Apportionment and Assessment of Transport-Related Pollution*, Atmos. Environ. **279**, 119043 (2022).

[73] A. Minderytė, E. A. Ugboma, F. F. Mirza Montoro, I. S. Stachlewska, and S. Byčenkienė, *Impact of Long-Range Transport on Black Carbon Source Contribution and Optical Aerosol Properties in Two Urban Environments*, Heliyon **9**, (2023).

[74] D. C. Carslaw and K. Ropkins, *Openair — An R Package for Air Quality Data Analysis*, Environ. Model. Softw. **27**–**28**, 52 (2012).

[75] L. L. Ashbaugh, W. C. Malm, and W. Z. Sadeh, *A Residence Time Probability Analysis of Sulfur Concentrations at Grand Canyon National Park*, Atmospheric Environment (1967).

[76] J. A. Kamińska, T. Turek, M. Van Poppel, J. Peters, J. Hofman, and J. K. Kazak, *Whether Cycling around the City Is in Fact Healthy in the Light of Air Quality – Results of Black Carbon*, J. Environ. Manage. **337**, (2023).

[77] P. Krecl, Y. A. Cipoli, A. C. Targino, M. de O. Toloto, D. Segersson, Á. Parra, G. Polezer, R. H. M. Godoi, and L. Gidhagen, *Modelling Urban Cyclists' Exposure to Black Carbon Particles Using High Spatiotemporal Data: A Statistical Approach*, Sci. Total Environ. **679**, 115 (2019).

[78] M. Renzi, F. Forastiere, J. Schwartz, M. Davoli, P. Michelozzi, and M. Stafoggia, *Long-Term PM10 Exposure and Cause-Specific Mortality in the Latium Region (Italy): A Difference-in-Differences Approach*, Environ. Health Perspect. **127**, (2019).

[79] K. Bodor, M. M. Micheu, Á. Keresztesi, M. V. Birsan, I. A. Nita, Z. Bodor, S. Petres, A. Korodi, and R. Szép, *Effects of PM10 and Weather on Respiratory and Cardiovascular Diseases in the Ciuc Basin (Romanian Carpathians)*, Atmosphere.

[80] X. Liu, H. Hadiatullah, P. Tai, Y. Xu, X. Zhang, J. Schnelle-Kreis, B. Schloter-Hai, and R. Zimmermann, *Air Pollution in Germany: Spatio-Temporal Variations and Their Driving Factors Based on Continuous Data from 2008 to 2018*, Environ. Pollut. **276**, 116732 (2021).

[81] S. Byčenkienė, V. Ulevicius, V. Dudoitis, and J. Pauraitė, *Identification and Characterization of Black Carbon Aerosol Sources in the East Baltic Region*, Adv. Meteorol. **2013**, 1 (2013).

[82] V. Ulevicius et al., *Fossil and Non-Fossil Source Contributions to Atmospheric Carbonaceous Aerosols during Extreme Spring Grassland Fires in Eastern Europe*, Atmos. Chem. Phys. **16**, 5513 (2016).

[83] J. Pauraitė, I. Garbarienė, A. Minderytė, V. Dudoitis, G. Mainelis, L. Davulienė, I. Uogintė, K. Plauškaitė, and S. Byčenkienė, *Effect of Spring Grass Fires on Indoor Air Quality in Air-Conditioned Office Building*, Lith. J. Phys. **61**, (2021).

[84] M. S. Al Rashidi, *Assessment of the Atmospheric Mixing Layer Height*

and Its Effects on Pollutant Dispersion, (2018).

[85] G. Hoek, G. Kos, R. Harrison, J. de Hartog, K. Meliefste, H. ten Brink, K. Katsouyanni, A. Karakatsani, M. Lianou, and A. Kotronarou, *Indoor–Outdoor Relationships of Particle Number and Mass in Four European Cities*, Atmos. Environ. **42**, 156 (2008).

[86] B. C. Singer, W. W. Delp, D. R. Black, and I. S. Walker, *Measured Performance of Filtration and Ventilation Systems for Fine and Ultrafine Particles and Ozone in an Unoccupied Modern California House*, Indoor Air **27**, 780 (2017).

[87] A. M. Avery, M. S. Waring, and P. F. Decarlo, *Seasonal Variation in Aerosol Composition and Concentration upon Transport from the Outdoor to Indoor Environment*, Environ. Sci. Process. Impacts **21**, 528 (2019).

[88] W. J. Li and L. Y. Shao, *Observation of Nitrate Coatings on Atmospheric Mineral Dust Particles*, Atmos. Chem. Phys. **9**, 1863 (2009).

[89] D. Liu et al., *Black-Carbon Absorption Enhancement in the Atmosphere Determined by Particle Mixing State*, Nat. Geosci. **10**, 184 (2017).

[90] K. Dzierżanowski, R. Popek, H. Gawrońska, A. Sæbø, and S. W. Gawroński, *Deposition of Particulate Matter of Different Size Fractions on Leaf Surfaces and in Waxes of Urban Forest Species*, Int. J. Phytoremediation **13**, 1037 (2011).

[91] Huixia Wang, Hui Shi, and Yangyang Li, *Leaf Dust Capturing Capacity of Urban Greening Plant Species in Relation to Leaf Micromorphology*, in *2011 International Symposium on Water Resource and Environmental Protection*, Vol. 3 (IEEE, 2011), pp. 2198–2201.

PRIEDAI

ACKNOWLEDGMENTS/PADĖKA

PUBLIKACIJŲ SĄRAŠAS /LIST OF PUBLICATIONS

1. **D. Pashneva**, A. Minderytė, L. Davulienė, V. Dudoitis, S. Byčenkienė (2024) Understanding the Dynamics of Source-Apportioned Black Carbon in an Urban Background Environment, Atmosphere; Volume 15; https://doi.org/10.3390/atmos15070832

2. **D. Pashneva**, A. Minderytė, L. Davulienė, V. Dudoitis, S. Byčenkienė (2024) Variations of black carbon, particulate matter and nitrogen oxides mass concentrations in urban environment with respect to winter heating period and meteorological conditions; Lithuanian Journal of Physics; Volume 60; https://doi.org/10.3952/physics.2024.64.3.4

3. I.Garbarienė; J.Pauraitė; **D. Pashneva**; A.Minderytė; K.Sarka; V.Dudoitis; L.Davulienė; M.Gaspariūnas; V.Kovalevskij; D.Lingis (2022) Indoor-outdoor relationship of submicron particulate matter in mechanically ventilated building: Chemical composition, sources and infiltration factor, Building and Environment, Volume 222;

4. S.Byčenkienė, **D. Pashneva**, I.Uogintė, J.Pauraitė, A.Minderytė, L.Davulienė, K.Plauškaitė, M. Skapas, V.Dudoitis, G. Touqeer, J.Andriejauskiene, V.Araminienė, E. F. Dzenajavičienė, P. Sicard, V. Gudynaitė-Franckevičienė, I.Varnagirytė-Kabašinskienė, N.Pedišius, E. Lemanas, T. Vonžodas (2021) Black Carbon emissions and deposition on tree foliage, Environmental Research; Volume 207; https://doi.org/10.1016/j.envres.2021.112218

Not related to thesis:

5. L. Davulienė, L. Janicka, A. Minderytė, A. Kalinauskaitė, P. Poczta, M. Karasewicz, A. Hafiz, **D. Pashneva**, V. Dudoitis, K. Kandrotaitė, D. Valiulis, C. Böckmann, D. Schüettemeyer, I. S. Stachlewska, S.Byčenkienė (2023) Synergetic use of in-situ and remote sensing techniques for comprehensive characterization of aerosol optical and microphysical properties, Science of the Total Environment; Volume 906; https://doi.org/10.1016/j.scitotenv.2023.167585

6. Mašalaitė, I. Garbarienė, A. Garbaras, J. Šapolaitė, Ž. Ežerinskis, L. Bučinskas, V. Dudoitis, A. Kalinauskaitė, **D. Pashneva**, A. Minderytė, V. Remeikis, S. Byčenkienė, (2024) Dual-isotope ratios of carbonaceous aerosols for seasonal observation and their assessment as source

indicators, Science of the Total Environment; Volume 949; https://doi.org/10.1016/j.scitotenv.2024.175094

LIST OF CONFERENCES

1. D. Pashneva et al., SOURCE APPORTIONMENT OF BLACK CARBON AEROSOL IN BACKGROUND ENVIRONMENT (PREILA, LITHUANIA), Conference of Doctoral Students and Young Researchers FizTech (FizTech2020), 22 – 23 October 2020, Vilnius, Lithuania, poster
2. D. Pashneva et al., OUTDOOR AND INDOOR LEVELS OF BLACK CARBON IN AN URBAN ENVIRONMENT, 64th International Conference for Students of Physics and Natural Sciences „OpenReadings 2021", 16-19th of March, 2021, Vilnius, Lithuania, oral presentation
3. D. Pashneva et al., IMPACT OF OUTDOOR BLACK CARBON LEVEL TO INDOOR AIR QUALITY, CESENY 2021 17th international conference of young scientists on energy and natural sciences issues (CYSENY 2021), May 24-28, 2021, Vilnius, Lithuania, oral presentation
4. D. Pashneva et al., IMPACT OF A LONG-RANGE SMOKE TRANSPORT EVENT FOR OUTDOOR AND INDOOR AIR QUALITY, 24th ETH-Conference on Combustion Generated Nanoparticles - June 22-24, Zürich, Switzerland (Online Conference)
5. D. Pashneva et al., LEVELS OF BLACK CARBON IN OUTDOOR AND INDOOR AIR IN AN URBAN ENVIRONMENT, XXIth International Multidisciplinary Scientific GeoConference Surveying, Geology and Mining, Ecology and Management – SGEM 2021 14 -22 august, 2021 in Bulgaria
6. D. Pashneva et al., OFFICE INDOOR AIR QUALITY IN LITHUANIA: THE ROLE OF A LONG-RANGE SMOKE TRANSPORT EVENT, European Aerosol Conference (EAC 2021), EAC 2021, 30 August - 3 September 2021.
7. D. Pashneva et al., BLACK CARBON DEPOSITION ON TREE FOLIAGE AN URBAN BACKGROUND IN VILNIUS, 22nd INTERNATIONAL SCIENTIFIC CONFERENCE "EcoBalt 2021", (EcoBalt 2021), Riga, Latvia, 21–23 October 2021, poster
8. D. Pashneva et al., SOURCE APPORTIONMENT OF BLACK CARBON AEROSOL AND ITS DEPOSITION ON TREE FOLIAGE, Conference of Doctoral Students and Young Researchers FizTech (FizTech2021), 20-21 October 2021, Vilnius, Lithuania, oral

9. D. Pashneva et al., RELATIONSHIP INDOOR AIR QUALITY FROM URBAN BLACK CARBON LEVEL, 44 Lietuvos nacionalinė fizikos konferencija, (44 LNFK), 6-8 October 2021, Vilnius, Lithuania, poster

10. D. Pashneva et al., EFFECTS OF WILDFIRES ON OUTDOOR BLACK CARBON LEVEL TO INDOOR AIR QUALITY, American Association for Aerosol Research 39th Annual Conference, (AAAR 39th), 18-22 October 2021, New Mexico, poster

11. D. Pashneva et al., COMPARISON OF THE ANTHROPOGENIC BLACK CARBON EMISSIONS FROM DIFFERENT TYPES OF FUEL USED FOR RESIDENTIAL HEATING IN THE VILNIUS, CESENY 2022 18th international conference of young scientists on energy and natural sciences issues (CYSENY 2022), May 24-27, 2022, Kaunas, Lithuania, oral presentation

12. D. Pashneva et al., IMPACT OF AMBIENT SUBMICRON PARTICULATE POLLUTION ON AIR QUALITY IN MECHANICALLY VENTILATED OFFICE BUILDINGS, Nordic Aerosol Symposium NOSA 2022, (NOSA), March 14-16, 2022, poster

13. D. Pashneva et al., THE ROLE OF TREE FOLIAGE ON BLACK CARBON DEPOSITION AN URBAN BACKGROUND IN VILNIUS, 65th International Conference for Students of Physics and Natural Sciences „OpenReadings 2022", (OpenReadings 2022) 15-18th of March, 2022, Vilnius, Lithuania, poster

14. D. Pashneva al., INDOOR-OUTDOOR INFILTRATION OF SUBMICRON PARTICULATE MATTER IN THE MECHANICALLY VENTILATED BUILDING, Conference of Doctoral Students and Young Researchers FizTech (FizTech2021), 20-21 October 2022, Vilnius, Lithuania, oral presentation

15. D. Pashneva et al., YEARLY VARIATIONS OF EQUIVALENT BLACK CARBON COMPONENTS OBSERVED IN VILNIUS, LITHUANIA, Nordic Aerosol Symposium NOSA 2023, (NOSA), 13-15 March, 2023, Oslo, poster

16. D. Pashneva et al., Seasonal variations of aerosol black carbon concentration in Vilnius, Conference of Doctoral Students and Young Researchers FizTech (FizTech2023), 18-19 October 2023, Vilnius, Lithuania, oral presentation

CURRICULUM VITAE

Daria Pashneva
1991-09-02, St.Petersburg, Russia.

Education:

2020-2024	SRI Center for Physical Sciences and Technology (FTMC) *Ph.D. studies*
2013-2015	St. Petersburg State National Research University of Information Technologies, Mechanics and Optics Faculty of Technological Management and Innovation *Master's degree, Cum laude*
2013-2008	Saint Petersburg State National Research University of Information Technologies, Mechanics and Optics, Institute of Biotechnology and Cold Environmental engineering *Specialist 's degree, Cum laude*

Work experience:

2022 - present	Center for Physical Sciences and Technology (FTMC) *Junior researcher*
2020 - 2022	Center for Physical Sciences and Technology (FTMC) *Engineer*
2015 - 2020	St. Petersburg university *Deputy director of the Department of Ecology*
2013 - 2015	St. Petersburg university *Environmental engineer*

APIE AUTORIŲ

Daria Pashneva

1991-09-02 m. Sankt Peterburgas, Rusija.

Išsilavinimas:

2020-2024	Fizinių ir technologijos mokslų centras
	Doktorantūros studijos
2013-2015	Sankt Peterburgo valstybinis nacionalinis mokslinių tyrimų, informacinių technologijų, mechanikos ir optikos universitetas
	Technologijų vadybos ir inovacijų fakultetas
	Magistro kvalifikacinis laipsnis, Cum laude
2013-2008	Sankt Peterburgo valstybinis nacionalinis mokslinių tyrimų, informacinių technologijų, mechanikos ir optikos universitetas, Biotechnologijų ir šalčio institutas
	Aplinkos inžinerija
	Specialisto laipsnis, Cum laude

Profesinė veikla:

2022 - present	VMTI Fizinių ir technologijos mokslų centras
	Jaunesnioji mokslo darbuotoja
2020 - 2022	VMTI Fizinių ir technologijos mokslų centras
	Inžinierius
2015 - 2020	Sankt Peterburgo universitetas
	Ekologijos departamento direktoriaus pavaduotojas
2013 - 2015	Sankt Peterburgo universitetas
	Aplinkos apsaugos inžinierius

NOTES

NOTES